

# Exact WKB analysis of inverted triple-well: resonance, PT-symmetry breaking, and resurgence

---

Syo Kamata,<sup>1</sup> Tatsuhiro Misumi,<sup>2</sup> Cihan Pazarbaşı,<sup>3</sup> Hidetoshi Taya<sup>4,5</sup>

<sup>1</sup>*Department of Physics, The University of Tokyo, Tokyo 113-0033, Japan*

<sup>2</sup>*Department of Physics, Kindai University, Osaka 577-8502, Japan*

<sup>3</sup>*Okinawa Institute of Science and Technology, Okinawa 904-0495, Japan*

<sup>4</sup>*Hiyoshi Department of Physics, Keio University, Hiyoshi, Kanagawa 223-8521, Japan*

<sup>5</sup>*iTHEMS, TRIP Headquarters, RIKEN, Wako, Saitama 351-0198, Japan*

*E-mail:* [skamata1phys@gmail.com](mailto:skamata1phys@gmail.com), [misumi@phys.kindai.ac.jp](mailto:misumi@phys.kindai.ac.jp),  
[cihan.pazarbasi@gmail.com](mailto:cihan.pazarbasi@gmail.com), [h\\_taya@keio.jp](mailto:h_taya@keio.jp)

**ABSTRACT:** We study non-Hermitian quantum mechanics of an inverted triple-well potential within the exact WKB framework. For a single classical potential, different Siegert boundary conditions define three distinct quantum problems: the PT-symmetric, resonance, and anti-resonance systems. For each case, we derive the exact quantization condition and construct the associated trans-series solution. By identifying the resurgent structures and cancellations in these non-Hermitian setups, we obtain the median-summed series, clarifying when the spectra are real or complex in accordance with the physical properties of each system. Establishing explicit links to the semi-classical path integral formalism, we elucidate the roles of bounce and bion configurations in these non-Hermitian systems. This analysis predicts PT-symmetry breaking, which we also verify numerically. Using the median quantization conditions, we prove the existence of this symmetry breaking and establish an exact equation for the exceptional point, which emerges as a remarkably simple algebraic relation between the bounce and bion actions. We further show that the median-summed non-perturbative correction to the spectrum vanishes at the exceptional point, while the resurgent structure survives through a universal minimal trans-series. For the resonance and anti-resonance systems, we find that the exact median-summed spectra are related by complex conjugation, representing time reversal in this setting, are necessarily complex, and do not exhibit an exceptional point. Although their spectra differ significantly from the PT-symmetric case, they share the same minimal trans-series. By maintaining explicit links with the path integral saddles and the formal theory of resurgence, our analysis provides a unified and general perspective on the quantization of non-Hermitian theories.

---

## Contents

<b>1</b>	<b>Introduction</b>	<b>1</b>
<b>2</b>	<b>Review of exact WKB and resurgence theory</b>	<b>5</b>
2.1	A brief introduction to exact WKB	5
2.2	A brief review of the resurgence theory	12
2.3	Resurgent spectrum in exact WKB	15
<b>3</b>	<b>Quantum mechanics of inverted triple-well</b>	<b>20</b>
3.1	Setup and numerical solutions	20
3.2	Semi-classical picture	21
3.3	Exact WKB of inverted triple-well	28
<b>4</b>	<b>Trans-series from exact WKB</b>	<b>31</b>
4.1	PT-symmetric case	31
4.2	Resonance and anti-resonance cases	39
<b>5</b>	<b>Exact solutions from median quantization conditions</b>	<b>45</b>
5.1	PT-symmetric case	46
5.2	Resonance and anti-resonance cases	56
<b>6</b>	<b>Discussion and outlook</b>	<b>59</b>

---

## 1 Introduction

Non-Hermitian quantum mechanics [1, 2] provides a natural framework for describing quantum systems with gain, loss, decay, and/or external driving; namely, situations that cannot in general be captured within ordinary Hermitian quantum mechanics. In this sense, non-Hermitian quantum mechanics can serve as an effective description of open quantum systems interacting with an environment and can encode intrinsically non-equilibrium phenomena. One of its most well-known characteristics is the appearance of the complex spectrum<sup>1</sup>, in contrast to the real spectra of standard Hermitian systems. The presence of complex eigenvalues indicates the nonequilibrium nature of the system, as the corresponding quantum states, also called *resonance* states, dissipate in time, leading to a non-zero probability

---

<sup>1</sup>Technically, the price to pay to include the complex spectrum is extending the space of solutions to rigged-Hilbert space [3, 4] and allowing the oscillating solutions, for which the normalizability is ensured by the Zel'dovich regularization [5]. Provided by this established structure, the quantization procedure can be performed as in the Hermitian quantum mechanics by solving the Schrödinger equation with appropriate boundary conditions. Since we will not need the normalization throughout this paper, we will not discuss this mathematical construction.

flux through the boundaries of the system. Although the lack of probability conservation leads to a non-unitary time evolution, it is known that overall characteristics<sup>2</sup> of a resonance system can be captured by the tools of Hermitian quantum mechanics, such as the Wentzel-Kramers-Brillouin (WKB) approximation for which the  $\alpha$  decay stands as the most famous example [6].

The non-Hermitian character of a Hamiltonian, however, does not necessarily imply a complex spectrum [7, 8]. The appearance or absence of complex eigenvalues is determined by genuinely quantum properties of the system, rather than by the classical Hamiltonian alone. A celebrated class of non-Hermitian systems with real spectra is provided by PT-symmetric quantum mechanics, which can admit a consistent unitary formulation in the PT-unbroken phase, similarly to Hermitian quantum mechanics [9, 10]. Originally developed as a mathematical extension of quantum theory, PT-symmetric quantum mechanics has grown into an active research field on the experimental side as well; see [11, 12] for recent comprehensive reviews.

Heuristically, the reality of the spectrum, or the lack of complex eigenvalues in a PT-symmetric system, can be understood in terms of the balance between gain and loss. More specifically, real spectrum can be understood as the conservation of probability in a finite region, leading to unitary behaviors. This balance can break down at a critical point, known as an *exceptional point*, beyond which the PT-symmetric system develops complex eigenvalues. This transition, referred to as *PT-symmetry breaking*, signals the onset of genuinely non-Hermitian behaviors, or the breakdown of the equilibrium character of the system.

In one-dimensional quantum mechanics with a Hermitian Hamiltonian, the gain and loss due to the probability flux and the corresponding quantum states can be formulated clearly in terms of the Siegert boundary condition [13]. In this setting, a boundary condition on the real axis is specified by choosing, at each spatial infinity, whether the surviving asymptotic wave is incoming or outgoing. This choice determines the pattern of the probability flux, thereby distinguishing resonance, anti-resonance, and PT-symmetric systems. Choosing outgoing waves on both sides of the spatial infinity defines a resonance system, while choosing incoming ones yields the time reversal of the resonance, called an anti-resonance system. By contrast, choosing one incoming and one outgoing wave leads to a PT-symmetric system, which can lead to zero total probability flux.

Recently, similar spectral problems have also been studied by imposing boundary conditions in the complexified coordinate plane rather than on the real axis [14–18]. In this approach, the relevant complex boundary conditions are typically selected by the analytic continuation of an associated Hermitian problem, so that the two descriptions remain closely related to each other. In the present paper, in contrast, we focus on boundary conditions imposed on the real axis and on the corresponding probability-flow interpretation mentioned above. From this viewpoint, the PT-symmetric, resonant, and anti-resonant characters of the system are determined by the choice of incoming and outgoing waves at the spatial

---

<sup>2</sup>Although it describes an open system that interacts with the environment, non-Hermitian quantum mechanics does not include the effects of backreaction from the environment, which would lead to a constant change in the quantum system itself.

infinity. This suggests the possibility of analyzing these different non-Hermitian quantum problems in one WKB-type connection problem, which is one of the main motivations of the present work.

Although the choice of boundary conditions determines whether the system is PT-symmetric or (anti-)resonant, this does not quantitatively determine the spectral properties. In general, a proper treatment of a non-Hermitian system with a real potential requires non-perturbative inputs. For example, it is well known that the complex eigenvalues of resonance systems are tied to quantum tunneling and are therefore intrinsically non-perturbative. In the PT-symmetric case, in contrast, there is no *a priori* criterion that determines whether the exact spectrum is real or complex, and one must instead analyze the eigenvalue problem explicitly. Moreover, for real potentials, perturbation theory alone is not directly informative in this respect, since it typically yields real formal series only.

Recent developments in a wide range of physical systems have shown that a consistent non-perturbative quantization often requires a proper resurgent framework [19–61]. In Hermitian quantum mechanics, resurgence explains how non-perturbative sectors cancel the ambiguities of non-Borel-summable perturbative expansions, thereby restoring a single-valued, real spectrum. In a non-Hermitian system, in contrast, the exact spectrum may well be complex, but the same resurgent interplay remains essential in order to keep it single-valued and physically meaningful. One must therefore distinguish carefully between imaginary parts that arise as artifacts of Borel resummation and those that represent genuine physical features of the quantum system.

In one-dimensional quantum theories, the exact WKB (EWKB) formalism [62–76] provides a powerful unifying framework for spectral problems and resurgence theory. Within this framework, physical observables are encoded in the geometry of Stokes graphs, monodromies, and Voros multipliers through a rigorous synthesis of resurgence theory and the global connection problem for the Schrödinger equation [77–81]. It has been widely used in the analysis of various theoretical and physical setups: 4d  $\mathcal{N} = 2$  gauge theories [82–87], wall-crossing phenomena [88, 89], ODE/IM correspondence [90–95], TBA equations [96–98], topological string theory [99–106], PT-symmetric quantum mechanics [16, 17, 107], time-dependent quantum systems [108–112], black hole quasi-normal modes [113, 114], and resonance states [115, 116]; see also other applications [117–121].

Despite its technical sophistication, EWKB remains, at its core, a refined version of the familiar WKB connection problem. In this sense, it provides a natural framework for analyzing PT-symmetric, resonance, and anti-resonance systems within a unified picture. As we will show, the exact quantization conditions (QCs) associated with different boundary conditions can be organized into a single two-by-two transition matrix relating the asymptotic regions on the real axis. Together with its close connection to resurgence theory, this makes EWKB particularly suited to a detailed analysis of one-dimensional non-Hermitian quantum systems.

In this paper, we consider an inverted triple-well (ITW) potential with parity symmetry and study its quantization within the EWKB formalism. The ITW potential consists of two perturbatively degenerate wells and three barriers, giving rise to non-perturbative WKB cycles associated with instanton configurations. Owing to the parity symmetry, there

are only two independent non-perturbative configurations; namely, a bion and a bounce. Their interplay in the exact QCs leads to remarkably rich structure, making this system interesting from both physical and mathematical perspectives. By deriving and solving the exact QCs for the PT-symmetric, resonance, and anti-resonance cases on an equal footing, we uncover the structure of the corresponding trans-series solutions and non-perturbative spectra, and clarify their similarities and differences. We also compare our analytical results with numerical computations whenever feasible.

Recently, related EWKB analyses have been presented for the inverted quartic double-well (IDW) and for inverted oscillators without a quadratic (mass) term. These studies were carried out in connection to the Ai-Bender-Sarkar (ABS) conjecture [122]<sup>3</sup> in [16], with the zeta-function sum rules in [17], and with a non-perturbative version of the Gutzwiller trace formula in [107]. By contrast, the ITW potential has a much richer semi-classical structure than IDW, and this allows us to obtain a more intricate and more general picture of resurgence in non-Hermitian systems. In particular, we provide a more detailed analysis of the resurgent structure and the associated cancellations, which further clarifies the contrast with the better-understood Hermitian cases.

Before turning to the detailed analysis, let us summarize our main results and outline the organization of the paper:

- At the level of the exact QCs, we show that the resonance and anti-resonance systems are not invariant under time reversal, reflecting their intrinsically irreversible and non-equilibrium characters. Rather, their QCs are related to each other by complex conjugation, so that the two systems are mapped into one another as time-reversed partners. In the PT-symmetric case, in contrast, the time-reversal operation maps the QC to itself, up to an irrelevant overall constant.

We also identify the distinct roles played by the complex conjugation (time-reversal) operator and the Stokes automorphism. Although these operations appear closely related in Hermitian settings, they are conceptually different in the present problem. Our analysis explicitly demonstrates that complex conjugation relates QCs corresponding to opposite directions of time flow, whereas the Stokes automorphism connects different analytic continuations of a given QC without changing the direction of time.

- In the PT-symmetric case, the exact QCs admit two distinct trans-series solutions, governing the physical spectra in different parameter regimes. One of these solutions yields a complex spectrum, thereby signaling a PT-symmetry breaking. We show moreover that the trans-series structure undergoes a drastic reorganization across the exceptional point, offering a new perspective on the origin of the PT-symmetry breaking.

- In all cases, by identifying the relevant resurgent structures and the associated cancellations, we obtain the median-summed trans-series contributions to the physical spectra.

---

<sup>3</sup>The ABS conjecture relates the (logarithm of the) partition functions of a resonance theory and an associated PT-symmetric theory through analytic continuation. According to the conjecture, this continuation ensures the reality of the PT-symmetric spectrum. We do not study the ABS conjecture here, since it requires a different theoretical setup. We note, however, that our analysis reveals no direct link between the resonance and PT-symmetric systems.

This analysis differs from the more familiar Hermitian cases, since in non-Hermitian systems one must allow genuinely complex spectra. Accordingly, in addition to the resurgence cancellations themselves, the signs of the resulting imaginary contributions become essential in the analysis of the resonance, anti-resonance, and broken PT-symmetric cases. We show that these signs are fully consistent with the physical character of each system. To our knowledge, a detailed resurgence analysis of a non-Hermitian theory from this perspective has not been carried out before.

- Utilizing the Stokes automorphism, we obtain the *exact* median-summed non-perturbative spectra from the median QCs for each system. Along with recovering the corresponding trans-series solutions, this approach allows us to analyze the exceptional point directly in the PT-symmetric case. In this way, we derive an explicit equation for the exact locations of the exceptional points and establish exact bounds separating the broken and unbroken PT-symmetric phases. We also prove the reality of the spectrum in the corresponding phases without invoking any trans-series construction or numerical computation. Moreover, we show that the exact median-summed non-perturbative correction to the spectrum vanishes at the exceptional point. We further demonstrate that the non-perturbative splitting exhibits a characteristic square-root behavior near the exceptional point. These results illuminate both the non-perturbative nature of the transition and its continuity.

- We uncover a universal minimal trans-series that participates in the resurgence cancellations in the same way for every system and in every parameter regime, including at the exceptional point, where the remaining non-perturbative corrections cancel exactly. By applying Alien calculus to the median QCs, we show that this minimal series is generated from the perturbative sector and thus captures the universal part of the resurgent structure that is forced solely by the non-Borel-summability of perturbation theory. The remaining, sector-dependent non-perturbative contributions then encode the genuine physical distinctions between PT-symmetric and (anti-)resonant boundary conditions.

The organization of this paper is as follows. In Section 2, we review the EWKB formalism, Stokes automorphisms, the median summation, and Alien calculus that are needed in the later analysis. In Section 3, we introduce the ITW system, discuss its boundary conditions and numerical solutions, and formulate the EWKB connection problem. In Section 4, we derive the trans-series solutions for the PT-symmetric, resonance, and anti-resonance cases and discuss the associated resurgence cancellations, leading to the median-summed spectra. In Section 5, we solve the median QCs exactly, determine the PT-symmetry breaking and exceptional-point conditions exactly, and analyze the associated resurgent structures, including the minimal trans-series, by using Alien calculus. Section 6 is devoted to discussion and outlook.

## 2 Review of exact WKB and resurgence theory

### 2.1 A brief introduction to exact WKB

The main mathematical framework in this paper is the exact-WKB (EWKB) formalism. Therefore, in this subsection, focusing on the time-independent Schrödinger equation of

form,

$$\left[ -\frac{\hbar^2}{2} \frac{d^2}{dx^2} + Q(x) \right] \phi(x) = 0, \quad (2.1)$$

where  $Q(x) = V(x) - E$  is assumed to be a polynomial, we briefly discuss the EWKB formalism and present formulas that will be used in the upcoming sections. Rather than providing a thorough explanation of the mathematical construction of the EWKB framework, we concentrate on the general aspects and the necessary details, which we will utilize in the following sections. More detailed explanations can be found in the literature; see e.g., [71, 77, 78, 80, 81].

The WKB approach to (2.1) starts with the ansatz,

$$\phi^\pm(x) = \exp \left\{ \pm \int_{x_0}^x dx' s(x', \hbar) \right\}, \quad s(x, \hbar) = \sum_{n=-1}^{\infty} s_n \hbar^n. \quad (2.2)$$

Using it in (2.1) leads to the Riccati equation, which can be solved recursively to get an asymptotic series solution,

$$\phi^{(\pm)}(x) = \frac{e^{\pm\sigma(x)}}{\sqrt{\sigma(x)}} \sum_{n=0}^{\infty} \phi_n^{(\pm)} \hbar^n, \quad (2.3)$$

where

$$\sigma(x) = \int_{x_0}^x dz \sqrt{Q(z)}. \quad (2.4)$$

Note that the lower bound  $x_0$  is called the normalization point. In general,  $x_0$  could be chosen arbitrarily, however for our purpose, it is chosen as a point satisfying  $Q(x_0) = 0$  throughout this paper.

It is known that the series (2.3) is factorially divergent [65], and, therefore, it should be treated via the Borel-summation procedure. In general, the Borel summation of  $\phi^{(\pm)}(x)$  is expressed as an integral of the form,

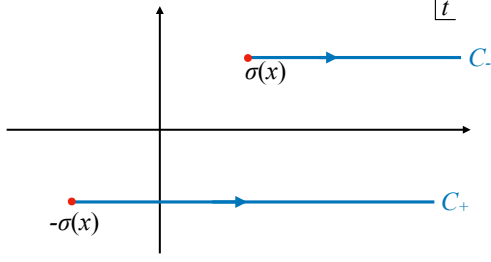
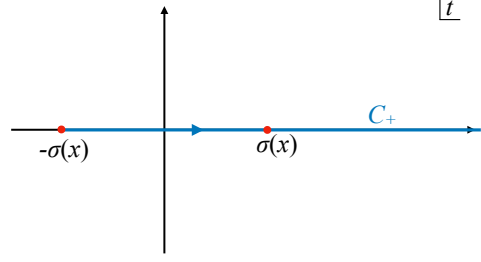
$$\psi^{(\pm)}(x) = \frac{1}{\sqrt{\sigma(x)}} \int_{\mp\sigma(x)}^{\infty + \text{Im}[\mp\sigma(x)]} dt e^{-t} \mathfrak{B} [\phi^\pm] (t \pm \sigma(x)), \quad (2.5)$$

where  $\mathfrak{B} [\phi^{(\pm)}]$  (called Borel transformation) has singularities at  $t = \pm\sigma(x)$ . Then, when  $\text{Im} \sigma = 0$ , for one of the solutions  $\psi^{(\pm)}$ , the Borel contour  $C_\pm = [\mp\sigma(x), \infty)$  hits the singularity at  $\pm\sigma(x)$ , making the corresponding solution  $\psi^{(\pm)}$  become discontinuous. See Fig. 1 for an illustration of the Borel summable and discontinuous cases.

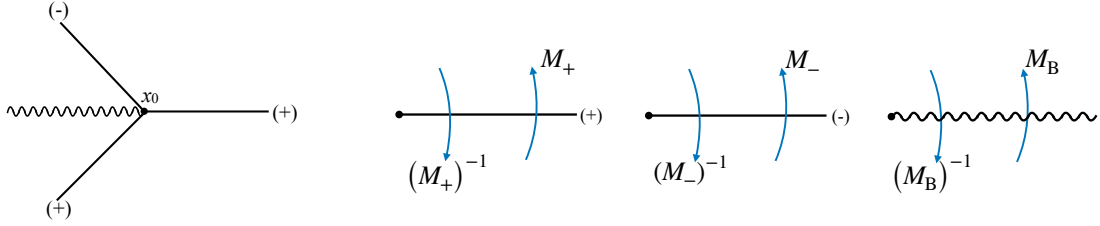
On the  $x$ -plane, the singularity corresponds to a *Stokes curve*, which is given by

$$\text{Im} \sigma(x) = \text{Im} \int_{x_0}^x dz \sqrt{Q(z)} = 0. \quad (2.6)$$

For each curve satisfying (2.6), the particular singular solution is determined by the sign of  $\text{Re} \sigma(x)$ : If  $\text{Re} \sigma(x) > 0$ ,  $\psi^{(+)}$  is singular, while if  $\text{Re} \sigma(x) < 0$ , the singular solution is  $\psi^{(-)}$ . Note that this can easily be deduced from the Borel contours in (2.5) and the locations of the singularities of  $\mathfrak{B} [\phi^{(\pm)}]$ .

(a)  $\text{Im } \sigma(x) \neq 0$ : Borel summable case(b)  $\text{Im } \sigma(x) = 0$ : Singular case for  $\psi^{(+)}$ 

**Figure 1:** (a) Borel-summable case with  $\text{Im } \sigma(x) \neq 0$ , where the contours  $C_{\pm}$  avoid the singularities at  $t = \pm\sigma(x)$ . (b) Singular case with  $\text{Im } \sigma(x) = 0$  and  $\text{Re } \sigma(x) > 0$ , where the contour hits a Borel singularity and  $\psi^{(+)}$  becomes discontinuous. It is straightforward to deduce that when  $\text{Re } \sigma(x) < 0$ , the locations of the singularities exchange and  $\psi^{(-)}(x)$  becomes singular.

(a) Stokes diagram for Airy equation(b) Monodromies for Airy-type EWKB

**Figure 2:** (a) Stokes diagram for the Airy potential around a simple turning point  $x_0$ . The labels  $(\pm)$  indicate which WKB solution is non-Borel summable across each Stokes line. (b) Airy-type monodromies  $M_{\pm}$  and  $M_B$  acting on the Borel-resummed solutions across the Stokes lines (solid lines) and the branch cut (wavy line).

**Airy-type approach:** For one-dimensional smooth curves, the points  $x_0 \in \mathbb{C}$  such that  $Q(x_0) = 0$  are special for the WKB analysis because they correspond to branch points of  $\sqrt{Q(x)}$ , which defines the Stokes curve (2.6). From the physical perspective, they are turning points of the potential  $V(x)$  at the classical energy level  $E$ .

It is well-known that around simple turning points such that  $Q'(x_0) \neq 0$ , the Schrödinger equation (2.1) is approximated to the Airy equation,

$$\left[ -\frac{\hbar^2}{2} \frac{d^2}{dx^2} + x - E \right] \phi(x) = 0, \quad (2.7)$$

for which the EWKB analysis can be performed exactly. In Fig. 2a, we illustrated the Stokes diagram for the Airy equation where the labels  $(+)$  and  $(-)$  for the individual curves indicate that the corresponding solutions,  $\psi^{(+)}$  and  $\psi^{(-)}$ , respectively, are non-Borel



summable. The discontinuities across the Stokes curves are represented by the monodromy matrices, which are defined as

$$M_+ = \begin{pmatrix} 1 & i \\ 0 & 1 \end{pmatrix}, \quad M_- = \begin{pmatrix} 1 & 0 \\ i & 1 \end{pmatrix}, \quad M_B = \begin{pmatrix} 0 & -i \\ -i & 0 \end{pmatrix}, \quad (2.8)$$

and their action is described in Fig. 2b. Note that the last matrix  $M_B$  encodes the discontinuity of the branch cut emanating from  $x_0 = E$ . Other than these discontinuities at the Stokes curves, both asymptotic series are Borel summable. On the  $x$ -plane, these regions separated by the Stokes curves are called the *Stokes sectors*.

A very important theorem by Aoki, Kawai, and Takei states that when  $V(x)$  is a polynomial, the approximate mapping between (2.1) and (2.7) can be made exact in the EWKB framework [65]. More specifically, this map holds for the Borel-summable solutions in each Stokes sector. This means that when  $x_0$  is chosen as one of the simple turning points of a generic polynomial  $V(x)$ , the geometry of the Stokes diagram emanating from  $x_0$  becomes the same as the one in Fig. 2a up to details of the exact form of the curves and the sign choice that determines the discontinuous solution.

As a consequence of this theorem, the entire Stokes diagram for any polynomial  $V(x)$  is given by a collection of Airy-type diagrams emanating from the simple turning points defined by  $E = V(x)$ . Since these diagrams are of Airy type, the monodromy matrices in (2.8) determine the discontinuities for general  $V(x)$ . This underlies the power of the EWKB analysis, which allows complicated problems to be treated in terms of simple Airy-type formulas.

For generic polynomials  $V(x)$ , the only additional ingredient is to connect the Stokes diagrams associated with different turning points. This requires changing the normalization point and, accordingly, the solutions  $\psi^{(\pm)}$  are additionally modified by the so-called *Voros matrix*,

$$N_{x_0, x_1} = \begin{pmatrix} e^{\mathcal{V}_{x_0, x_1}} & 0 \\ 0 & e^{-\mathcal{V}_{x_0, x_1}} \end{pmatrix}, \quad (2.9)$$

for the change of the normalization point from  $x_0$  to  $x_1$ . The quantity  $\mathcal{V}$  is given by the integral between the turning points  $x_0$  and  $x_1$ ,

$$\mathcal{V}_{x_0, x_1} = \int_{x_0}^{x_1} dx \tilde{s}(x, \hbar), \quad (2.10)$$

which can easily be deduced from the WKB ansatz (2.2).

Having the monodromy matrices (2.8) and the Voros matrix (2.9), any connection problem for a polynomial  $V(x)$  is encoded in the corresponding Stokes diagram. Let us briefly illustrate the connection problem in the case of a simple harmonic oscillator,

$$\left[ -\frac{\hbar^2}{2} \frac{d^2}{dx^2} + \frac{x^2}{2} - E \right] \phi(x) = 0. \quad (2.11)$$

The corresponding Stokes diagram is depicted in Fig. 3. Connecting the regions I and III requires incorporating the monodromy matrices. In addition to that, since the natural

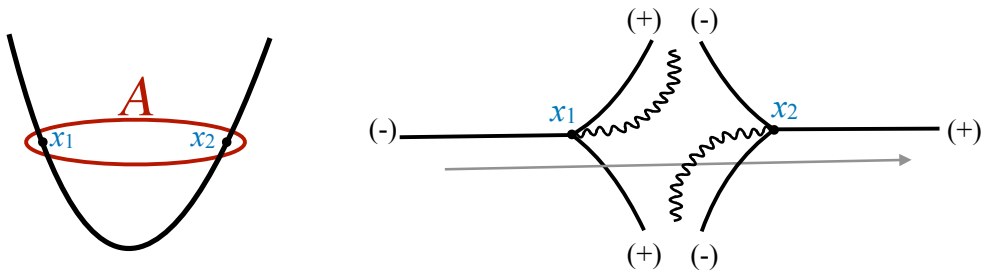


**Figure 3:** Potential (left) and Stokes diagram (right) for the harmonic oscillator (2.11). The  $A$ -cycle, enclosing the two turning points  $x_1$  and  $x_2$ , encodes the connection problem between the left and right asymptotic regions.

normalization points for  $\psi_{\text{I}}$  and  $\psi_{\text{III}}$  are  $x = \mp\sqrt{2E}$ , respectively, we need to change the normalization points to relate these  $\psi_{\text{I}}$  and  $\psi_{\text{III}}$  by using (2.9).

The connection problem between the regions I and III is formulated as

$$\Psi_{\text{III}} = M_- M_{\text{B}} N_{x_1, x_2} M_+, \quad (2.12)$$

where  $\Psi_i = \begin{pmatrix} \psi_i^{(+)} \\ \psi_i^{(-)} \end{pmatrix}$  and the integral in the Voros matrix is

$$\mathcal{V}_{x_1, x_2} = \frac{1}{2} \oint dx \tilde{s}(x, \hbar). \quad (2.13)$$

Note that the Voros matrix introduces a very important object to the picture: The WKB cycle associated with the curve  $Q(x) = E - V(x)$ . In Fig. 3, it is labeled as  $A$ -cycle and in this case, it contains all information about the quantized theory.

At this point, we stress that the quantization scheme in the Schrödinger setting requires additional information, stemming from the boundary condition. For example, in the harmonic oscillator problem, the natural boundary conditions are  $\psi^{(+)}(+\infty) = 0$  and  $\psi^{(-)}(-\infty) = 0$ , which would keep the system normalizable. Imposing this in (2.12), we obtain the Bohr-Sommerfeld QC, which we write as

$$1 + \Pi_A = 0, \quad (2.14)$$

where

$$\Pi_A = \exp \left\{ \oint_A dx \tilde{s}(x, \hbar) \right\}, \quad (2.15)$$

is the exponentiated action corresponding to the  $A$ -cycle.

For a higher-order polynomial  $V(x)$ , even though the connection problem becomes more complicated and the physical information is encoded by more WKB cycles, at its core, it stays the same. The main addition to the harmonic oscillators is the tunneling cycles, which we call  $B$ -cycles. In Fig. 4, we illustrate two cases with different types of  $B$ -cycles, which we consider in this paper. In Fig. 4a, there is one minimum and one simple turning point at  $E = E_{\text{cr}}$ , but in Fig. 4b, two minima of  $V(x)$  are at the same critical level  $E = E_{\text{cr}}$ . It turns

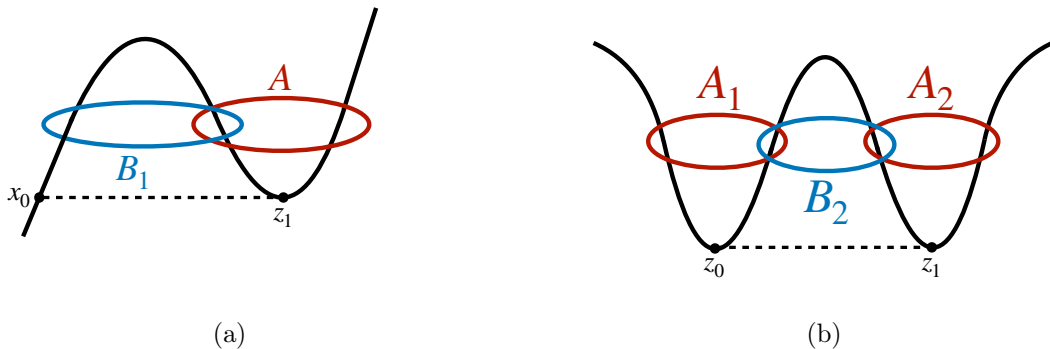


**Figure 4:** Two representative WKB-cycle configurations which have different expressions in the Weber-type EWKB approach. **(a)** A configuration with one saddle point  $z_1$  and one simple turning point  $x_0$  at  $E = E_{\text{cr}}$ , involving an  $A$ -cycle and a tunneling  $B_1$ -cycle. **(b)** A symmetric double-well configuration with two minima at the same critical level  $E = E_{\text{cr}}$ , involving  $A_{1,2}$  and the tunneling cycle  $B_2$ .

out that the  $B$ -cycles have slightly different characters in these two cases. To understand this difference, we turn our focus to a slightly different setup in the EWKB framework, which we call the *Weber-type* EWKB.

**Weber-type approach:** As the name suggests, the Weber-type EWKB utilizes the Weber equation, which we write in the following form:

$$\left[ -\hbar^2 \frac{d^2}{dy^2} + \frac{y^2}{4} - \hbar\tilde{E} \right] \tilde{\phi}(y) = 0. \quad (2.16)$$

Note that this can also be considered as a (rescaled) harmonic oscillator but with an important difference that the energy parameter is now written as a quantum term rather than a classical one. This means that in (2.16), the classical energy is set to be zero. Then, the Stokes curves (2.6) emanate from the saddle point, i.e., double turning point, at the  $E = 0$  level. For (2.16), we illustrate the potential and the Stokes diagram in Fig. 5.

Note that from a quantum-mechanical perspective, having an energy parameter as  $\hbar\tilde{E}$  is not a problem, as it is well-known that the quantized energy around a locally harmonic well starts with  $O(\hbar)$ . Then, in some sense, the parameter in (2.16) can be considered as a rescaling of  $E = \hbar\tilde{E}$ . Then, in this perspective, the approaches using (2.11) and (2.16) become equivalent to each other.

Similarly to the generalization of the setup for the Airy equation to generic polynomials, the Weber equation (2.16) forms a basis for cases when  $V(x)$  is locally harmonic, i.e.,  $V(x) \sim (x - z_0)^2$  around a saddle point  $x = z_0$ . This is again possible due to another theorem by Aoki, Kawai, and Takei [66] which introduces an exact mapping between (2.16) and the Schrödinger equation (2.1) with the rescaling  $E = \hbar\tilde{E}$ :

$$\left[ -\frac{\hbar}{2} \frac{d^2}{dx^2} + V(x) - \hbar\tilde{E} \right] \tilde{\phi}(x) = 0. \quad (2.17)$$

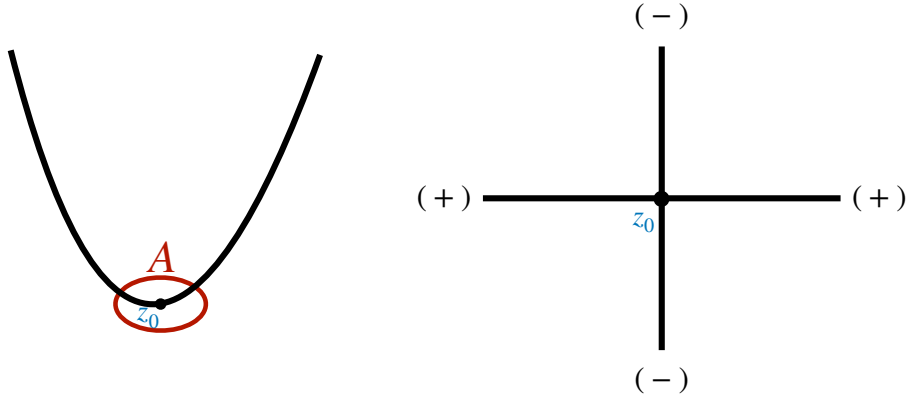


**Figure 5:** (Left) Harmonic potential with a minimum at  $x = z_0$ .  $A$ -cycle represents the limiting case of an Airy-type cycle at classical energy  $E = 0$ . (Right) The Weber-type Stokes diagram emanating from the saddle point at  $x = z_0$ .

Then, when we focus on the classical energy levels corresponding to the saddle points of  $V(x)$ , the Weber-type Stokes diagrams in Fig. 5 become the building blocks for general locally harmonic polynomials  $V(x)$ .

**Dictionary:** Provided by the exact mapping theorems, we infer that for any locally harmonic  $V(x)$ , we can turn an Airy-type setup to a Weber-type one by simply rescaling the energy parameter as  $E = \hbar\tilde{E}$ . It turns out that in the Weber-type analysis, the WKB actions  $\Pi_A$  and  $\Pi_B$  have universal forms [69, 78, 80, 81], which lead to greater computational power than the direct Airy-type approach, especially for higher-order polynomials. The precise link between the expressions for these two setups is given by a dictionary, which was first<sup>4</sup> put forward in [78] and then generalized in [80, 81].

For the two cases illustrated in Fig. 4, the dictionary reads

$$\Pi_A = e^{-2\pi i \mathcal{F}_P(\frac{E}{\hbar}, \hbar)}, \quad (2.18)$$

and

$$\Pi_{B_1} = e^{-\mathcal{G}_1(\frac{E}{\hbar}, \hbar)} \frac{\sqrt{2\pi} \left(\frac{\hbar}{\mathcal{C}_1}\right)^{-\mathcal{F}_P(\frac{E}{\hbar}, \hbar)}}{\Gamma\left(\frac{1}{2} + \mathcal{F}_P\left(\frac{E}{\hbar}, \hbar\right)\right)}, \quad \Pi_{B_2} = e^{-\mathcal{G}_2(\frac{E}{\hbar}, \hbar)} \frac{2\pi \left(\frac{\hbar}{\mathcal{C}_2}\right)^{-2\mathcal{F}_P(\frac{E}{\hbar}, \hbar)}}{\left[\Gamma\left(\frac{1}{2} + \mathcal{F}_P\left(\frac{E}{\hbar}, \hbar\right)\right)\right]^2}. \quad (2.19)$$

<sup>4</sup>In fact, before its utilization in the EWKB framework, an equivalent mapping has been used in the uniform WKB formalism, which turns out to be closely related to the Weber-type EWKB approach, but it lacks the geometric information that Stokes diagrams provide. See e.g. [28] for more discussion about the uniform WKB in this direction.

The constants  $\mathcal{C}_1$  and  $\mathcal{C}_2$  are given by the following integrals:

$$\mathcal{C}_1 = 2\omega_0 (z_1 - x_0)^2 \exp \left\{ 2 \int_{x_0}^{z_1} dx \left[ \frac{\omega_0}{\sqrt{2V(x)}} - \frac{1}{z_1 - x} \right] \right\}, \quad (2.20)$$

$$\mathcal{C}_2 = 2\omega_0 (z_1 - z_0)^2 \exp \left\{ \int_{z_0}^{z_1} dx \left[ \frac{\omega_0}{\sqrt{2V(x)}} - \frac{1}{x - z_0} - \frac{1}{z_1 - x} \right] \right\}, \quad (2.21)$$

where  $\omega_0$  corresponds to the local curvature (harmonic frequency) of the wells located at  $x_0$  and  $x_1$ . Note that the expression for  $\Pi_{B_2}$  in (2.19) and the constant  $\mathcal{C}_2$  in (2.21) assume that the  $B_2$ -cycle lies between two wells with the same curvature. If the curvatures are different, the expressions differ slightly as discussed in [81]. For our purposes in this paper, the general formulas are not needed.

The important objects in (2.18) and (2.19) are the exponents  $\mathcal{F}_P$  and  $\mathcal{G}$ . In general, they are represented by series expansions in  $\hbar$  of the forms,

$$\mathcal{F}_P = \sum_{m=0}^{\infty} \mathcal{F}_{P,k} \hbar^k, \quad \mathcal{G}_i = \frac{S_i}{\hbar} + \sum_{m=1}^{\infty} \mathcal{G}_m \hbar^m, \quad (2.22)$$

where  $S_i$  corresponds to the classical action of the corresponding  $B_i$ -cycle.

In the dictionaries (2.18) and (2.19),  $\mathcal{F}_P$  and  $\mathcal{G}$  represent the perturbative and non-perturbative information, respectively. Note that  $\mathcal{F}_P$  appears in the expression for  $\Pi_{B_i}$ . This means that the non-perturbative action contains the information about the perturbative one, indicating resurgence. A greater manifestation of resurgence is established for genus-one curves via an explicit differential equation between  $\mathcal{F}$  and  $\mathcal{G}$  [28, 35, 61, 80, 81, 123–127].

Finally, the non-perturbative part of the dictionary in (2.19) links the actions  $\Pi_{B_i}$  to the instanton configurations in the path integral picture. We will come back to this relationship in Section 3.2, where we discuss the semi-classical-quantization perspective for the inverted triple-well system.

## 2.2 A brief review of the resurgence theory

The EWKB framework provides a very elegant setup for the analysis of the differential equation by incorporating the resurgence theory. In general, any physical quantity can be dictated from the geometry of  $A$ - and  $B$ -cycles and their expressions of  $\Pi_A$  and  $\Pi_{B_{1,2}}$  in (2.18) and (2.19), respectively. However, these expressions are still formal, and in fact, their  $\hbar$  expansions can be asymptotic. Therefore, when the Schrödinger equation (2.1) is solved in terms of  $\Pi_A$  and  $\Pi_B$ , the solutions should also be handled carefully in view of the resurgence theory.

A convenient way of incorporating the resurgence theory into the solutions of (2.1) is to construct the trans-series solutions for the physical observables, e.g., spectral parameter  $E$ . In this method, the trans-series consists of a collection (infinitely many) divergent series such that

$$E(\hbar) = \sum_{m=0}^{\infty} e^{-m \frac{S}{\hbar}} \sum_{n=0}^{\infty} \mathcal{E}_n^{(m)} \hbar^n. \quad (2.23)$$

To give a proper meaning to  $E(\hbar)$ , each series should be handled by the Borel summation method. When the series are not Borel summable, this leads to *non-perturbatively ambiguous* result for each series and indicates multi-valued character of  $E(\hbar)$  at first sight. This is not acceptable because there should be only one spectrum for the physical system. When the entire trans-series is considered, however, the Borel-summed trans-series  $\mathcal{S}_\pm [E(\hbar)]$  leads to physically appropriate results via cancellation among different ambiguous terms. In the literature, this resurgence cancellation is known as the Bogomolny-Zinn-Justin (BZJ) mechanism [19, 20, 128, 129] and has been tested in various systems [21, 22, 26–42, 44–50, 61, 81].

In the following, we discuss formal aspects of this approach based on the Stokes automorphism and Alien calculus, which we later apply to the EWKB framework. Again, we only keep our discussion brief and focus on what will help our purpose. For thorough discussions, we refer to [16, 69, 130].

**Stokes automorphism  $\mathfrak{S}_\theta$ :** Let us start by introducing the Stokes automorphism. The main function of a Stokes automorphism is to encode the discontinuities of Borel summations. For example, for a trans-series consisting of infinitely many factorially divergent series such that

$$\Phi(\hbar) = \sum_{m=0}^{\infty} e^{-m\frac{A}{\hbar}} \sum_{n=0}^{\infty} f_n^{(m)} \hbar^n \quad f_n^{(m)} \sim \left(|A|e^{i\theta_h}\right)^{-n} n!, \quad (2.24)$$

the Borel summation is defined in general as

$$F(\hbar, \theta) = \mathcal{S}_\theta [\Phi(\hbar)] = \int_0^{\infty e^{i\theta}} dt e^{-\frac{t}{\hbar}} \mathfrak{B} [\Phi(\hbar)] (t), \quad (2.25)$$

where the functional  $\mathfrak{B} [\Phi(\hbar)] (t)$  is the Borel transform of  $\Phi(\hbar)$ . The Stokes automorphism compares the Borel summations along the two sides of a ray  $\theta = \theta_1$ . Then, it is defined as

$$\mathcal{S}_{\theta_1^+} = \mathcal{S}_{\theta_1^-} \circ \mathfrak{S}_{\theta_1} = \mathcal{S}_{\theta_1^-} \circ (\text{Id} - \text{disc}_{\theta_1}), \quad (2.26)$$

where  $\theta_1^\pm = \theta_1 \pm 0^+$  and  $\text{disc}_{\theta_1}$  corresponds to the discontinuity of  $F(\hbar, \theta)$  at  $\theta = \theta_1$ . If the function is continuous at  $\theta = \theta_1$ , it holds that  $\mathcal{S}_{\theta_1} = \text{Id}$  and that the two Borel summations are equal to each other as

$$\mathcal{S}_{\theta_1^+} [\Phi(\hbar)] = \mathcal{S}_{\theta_1^-} [\Phi(\hbar)] = \mathcal{S}_\theta [\Phi(\hbar)]. \quad (2.27)$$

This equality means that the asymptotic series is Borel summable.

Let us now consider a direction  $\theta = \theta_h$  where the Borel summation is discontinuous (or equivalently the asymptotic series is not Borel summable). Then, the directional Borel summations  $\mathcal{S}_{\theta_h^\pm}$  are related to each other via the Stokes automorphism as

$$\mathcal{S}_{\theta_h^+} [\Phi(\hbar)] = \mathcal{S}_{\theta_h^-} [\Phi(\hbar)] \circ \mathfrak{S}_{\theta_h}. \quad (2.28)$$

We call this singular direction  $\theta = \theta_h$  on the Borel plane as a *Stokes ray*. It turns out that in many physical problems, the observables are associated with the Stokes rays and the Borel summation at the limit  $\theta \rightarrow \theta_h^\pm$  should be defined carefully. Using the relationship

in (2.28), we analyze such limiting cases by considering half-Stokes automorphisms and define the Borel summation exactly at  $\theta = \theta_{\hbar}$  as

$$F(\hbar, \theta_{\hbar}) = \mathcal{S}_{\theta_{\hbar}}[\Phi(\hbar)] = \mathcal{S}_{\theta_{\hbar}^-} \circ \mathfrak{S}_{\theta_{\hbar}}^{1/2}[\Phi(\hbar)] = \mathcal{S}_{\theta_{\hbar}^+} \circ \mathfrak{S}_{\theta_{\hbar}}^{-1/2}[\Phi(\hbar)], \quad (2.29)$$

which is the so-called *median summation*. Note that the last equality is simply guaranteed by (2.28).

**Alien Derivative ( $\dot{\Delta}_{\theta}$ ):** The Stokes automorphism  $\mathfrak{S}_{\theta}$  encodes the entire discontinuity along a Stokes ray. It is possible to re-organize this information by introducing Alien derivatives as

$$\mathfrak{S}_{\theta} = \exp \left\{ \sum_{\omega \in \Gamma_{\theta}} e^{-\omega g} \Delta_{\omega} \right\}, \quad (2.30)$$

where  $\Gamma_{\theta}$  is the set of singularities  $\omega$  along the singular ray  $\theta$  and  $\Delta_{\omega}$  are the Alien derivatives along this ray. It is also convenient to define the Alien derivative by recombining the contributions from all singularities and rewrite  $\mathfrak{S}_{\theta}$  as

$$\mathfrak{S}_{\theta} = e^{\dot{\Delta}_{\theta}}. \quad (2.31)$$

We will only use the “pointed” Alien derivative  $\dot{\Delta}$  for our purpose in this paper. Probing each singularity individually stands as an interesting way to uncover “exact” trans-series structure, which was recently discussed in the literature [131].

As the name suggests, the Alien derivative possesses the ordinary derivative properties. A useful one, which we will utilize later, is the Leibniz rule: When there is a functional such that  $\Gamma(\Phi(\hbar))$ , it is possible to introduce an Alien derivative  $\dot{\Delta}_{\Phi}$  by considering  $\Phi$  as a variable. Then, the action of  $\dot{\Delta}_{\theta_{\hbar}}$  is decomposed into two parts via the chain rule as

$$\dot{\Delta}_{\theta_{\hbar}}[\Gamma(\Phi(\hbar))] = \dot{\Delta}_{\Phi}[\Gamma] + \frac{\partial \Gamma}{\partial \Phi} \dot{\Delta}_{\theta_{\hbar}} \Phi. \quad (2.32)$$

To understand the role of the Alien derivative in relation to the trans-series (2.24), let us consider the expansion of the exponential in (2.31)

$$\mathfrak{S}_{\theta_{\hbar}}^{\nu} = \sum_{k=0}^{\infty} \frac{\nu^k}{k!} \dot{\Delta}_{\theta_{\hbar}}^k. \quad (2.33)$$

This is a non-trivial re-arrangement of the entire Stokes discontinuity in a power series  $\nu$  where the order corresponds to the number of Alien derivative acted on a given function. For example, if we consider the median summed function  $F(\hbar, \theta_{\hbar})$  in (2.29), the action of the Stokes automorphism becomes

$$\mathfrak{S}_{\theta_{\hbar}}^{\nu}[F(\hbar, \theta_{\hbar})] = \sum_{k=0}^{\infty} F^{(k)}(\hbar, \theta_{\hbar}) \frac{\nu^k}{k!}, \quad (2.34)$$

where  $F^{(k)}(\hbar, \theta_{\hbar}) = \dot{\Delta}_{\theta_{\hbar}}^k(F(\hbar, \theta_{\hbar}))$ . With this formula, we can return back to the trans-series (2.24). First, we need to remove the directional Borel summations  $\mathcal{S}_{\theta_{\hbar}^{\pm}}$  in (2.29), which is done equivalent to re-expanding  $F(\hbar, \theta_{\hbar})$  for  $\hbar \ll 1$ . Then, (2.34) becomes

$$\Phi^{(\nu)}(\hbar) = \sum_{k=0}^{\infty} \frac{\nu^k}{k!} \sum_{n=0}^{\infty} F_n^{(k)} \hbar^n, \quad (2.35)$$

and setting  $\nu = \pm\frac{1}{2}$  recovers the original trans-series (2.24).

Note that the choice of the sign at the end seems *ambiguous* and problematic. However, this is nothing but the infamous non-perturbative ambiguity that we discussed above. In that sense, by using the Alien-derivative expansion (2.33) and re-expanding  $F(\hbar, \theta_\hbar)$  in  $\hbar$ , we recover the ambiguous trans-series.

Despite its equivalence to (2.24), (2.35) is organized in a different way. The importance of this reorganization reveals itself in (2.34): We first observe that at the leading order in (2.34), i.e.,  $k = 0$ , there is no ambiguity and  $F^{(0)} = F(\hbar, \theta)$  is the median-summed function. The higher-order terms, on the other hand, only appear in the directional Borel summations, i.e.,  $\mathcal{S}_{\theta_\hbar^\pm}$  for  $\nu = \mp\frac{1}{2}$  and canceled out in the median summation. However, they are still important to reveal the resurgence structure of the corresponding function.

This approach stands out as a powerful way to extract the median-summed function along with the resurgence structure. Let us now return back to the EWKB framework to discuss how the Stokes automorphism and the Alien calculus can be implemented to construct exact solutions to (2.1).

### 2.3 Resurgent spectrum in exact WKB

As we discussed in Section 2.1, a Stokes curve normalized at a turning point  $x = x_0$  is a result of Borel singularities of the formal WKB series (2.3), and it represents the discontinuities of the Borel-summed WKB solutions. However, this is different from the discontinuities of physical observables for which we need to address the global structure of a Stokes diagram.

For a generic polynomial  $V(x)$ , let us first consider a part of a Stokes diagram corresponding to a well and barrier region. Treating  $\hbar$  as a complex parameter and defining  $\hbar = |\hbar|e^{i\theta_\hbar}$ , we can draw the corresponding Stokes diagrams for  $\theta_\hbar = 0$ ,  $\theta_\hbar > 0$ , and  $\theta_\hbar < 0$  as in Fig. 6. The diagram at  $\theta_\hbar = 0$  in Fig. 6a stands out as a special case, since the Stokes line in the tunneling region connects two simple points  $x_2$  and  $x_3$ . We call such a Stokes diagram as *degenerate*, for which the standard Airy-type monodromies cannot be applied directly. Instead, one needs to turn on the phase  $\theta_\hbar$ , which leads to either of the diagrams in Fig. 6b or Fig. 6c, depending on the sign of  $\theta_\hbar$ .

It turns out that the connection problem encoded by these two diagrams is related to a Stokes automorphism. In the particular case of Fig. 6, the discontinuity is due to the non-Borel summability of the  $A$ -cycle action  $\Pi_A$ . The associated Stokes discontinuity is [68, 69, 76]

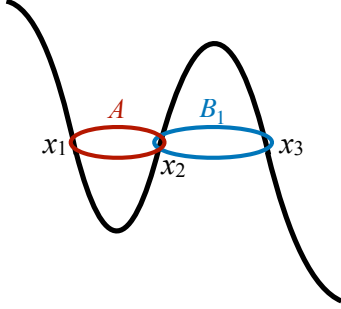
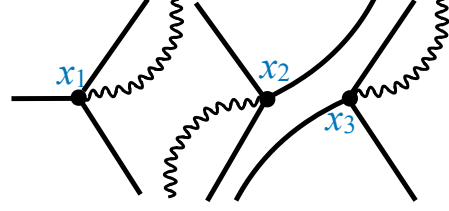
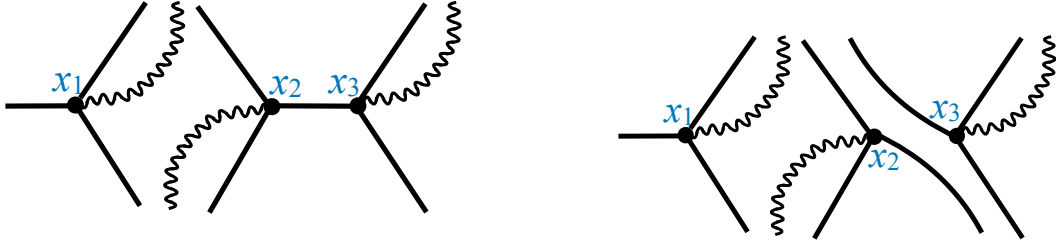
$$\mathfrak{S}_A : \mathcal{S}_{\theta_\hbar^+} [\Pi_A] \mapsto \mathcal{S}_{\theta_\hbar^-} [\Pi_A] (1 + \Pi_B) , \quad (2.36)$$

where the subscript  $A$  indicates that the discontinuity is associated to the  $A$ -cycle. Note that although they are related, the Stokes automorphisms (2.36) and (2.28) are different and probe the discontinuities of different objects, which we elaborate later. Finally, for more general diagrams, the Stokes automorphism (2.36) becomes

$$\mathfrak{S}_{A_i} : \mathcal{S}_{\theta_\hbar^+} [\Pi_{A_i}] \mapsto \mathcal{S}_{\theta_\hbar^-} [\Pi_{A_i}] \prod_{j=1}^n (1 + \Pi_{B_j})^{\nu_j} . \quad (2.37)$$

where  $i$  and  $j$  refer to different  $A$ - and  $B$ -cycles, respectively, and  $\nu_i = \langle A, B_i \rangle$  is the intersection number between  $A$  and  $B_i$  cycles.



(a) Potential and Stokes diagram at  $\theta_{\hbar} = 0$ .(b) Stokes diagram for  $\theta_{\hbar} > 0$ (c) Stokes diagram for  $\theta_{\hbar} < 0$ 

**Figure 6:** Stokes diagrams for a well-barrier system as the phase of  $\hbar = |\hbar|e^{i\theta_{\hbar}}$  is varied. (a) At  $\theta_{\hbar} = 0$  the diagram is degenerate, with a Stokes line connecting the simple turning points  $x_2$  and  $x_3$ . (b)-(c) Turning on  $\theta_{\hbar} \neq 0$  breaks the degeneracy into two analytic continuations related by the Stokes automorphism of the  $A$ -cycle.

This is a very useful formula for the EWKB analysis of spectral problems. For example, let us consider a generic polynomial potential  $V(x)$  with  $n$   $A$ -cycles and  $m$   $B$ -cycles at a given classical energy level  $E$  and denote the exact QCs at  $\theta = \theta_{\hbar} \neq 0$  by

$$D_{\pm\theta_{\hbar}}(\Pi_{A_1}, \Pi_{A_2} \dots \Pi_{A_n}, \Pi_{B_1}, \Pi_{B_2} \dots, \Pi_{B_m}) = 0. \quad (2.38)$$

Then, when there are degenerate Stokes lines, the  $A$ -cycles at  $\theta = \theta_{\hbar}^{\pm}$ , which have non-zero intersection with the corresponding  $B$ -cycles, are related via (2.37). As a result, the Stokes automorphism (2.37) maps the entire QC at  $\theta = \theta_{\hbar}^+$  to the one at  $\theta = \theta_{\hbar}^-$ .

In terms of the QCs, the Stokes automorphism is expressed as

$$\mathfrak{S}_A : D_{\theta_{\hbar}^+} \mapsto D_{\theta_{\hbar}^-}. \quad (2.39)$$

Then, in a similar manner to the median summations, we can consider half-Stokes automorphisms and define *median quantization conditions* (median QC) as

$$D_{\text{med}} = \mathfrak{S}_A^{1/2} D_{\theta_{\hbar}^+} = \mathfrak{S}_A^{-1/2} D_{\theta_{\hbar}^-} = 0. \quad (2.40)$$

Similarly to the median summations, the median QC probes the singular Stokes ray at  $\theta = \theta_{\hbar}$ . Its careful investigation leads to the median summed trans-series in a straightforward manner. This powerful approach prevents us from the hassle of Borel summations of a trans-series representation of the spectrum  $E(\hbar)$ .

**Solving quantization conditions:** We note that in relation to the exact spectrum  $\Delta_{\theta_{\hbar}^{\pm}}$  and  $D_{\text{med}}$  are in fact functional relations because  $\Pi_{A_i}$  and  $\Pi_{B_j}$  are also functions of  $\mathcal{F}_{\text{P}}(\hbar)$  and  $\mathcal{G}(\hbar)$ , which induce the  $\hbar$  expansions forming the trans-series (2.23). Let us briefly review how this trans-series is formed from the exact QCs (2.38).

If we only want to concentrate on the perturbative spectrum, the problem becomes an equivalent of the simple harmonic oscillator, and exact QC reduces to the Bohr-Sommerfeld equation (2.14) for each  $A$ -cycle. Then, in terms of  $\mathcal{F}_{\text{P}} = \frac{i}{2\pi} \log \Pi_A$ , we have

$$\mathcal{F}_{\text{P}}(E_{\text{P}}(\hbar, N), \hbar) = N + \frac{1}{2}. \quad (2.41)$$

Except when  $V(x) \propto x^2$ , this is a series expansion in  $\hbar$  as in (2.22), its inversion yields the perturbative spectrum  $E_{\text{P}}(\hbar, N)$ .

The trans-series (2.23) can be considered as (infinitely many) non-perturbative corrections around this series. Then, it is convenient to promote  $\mathcal{F}_{\text{P}}$  to a non-perturbative object and define

$$\mathcal{F} = \mathcal{F}_{\text{P}} + \delta_{\text{NP}}. \quad (2.42)$$

Then, solving  $D_{\theta_{\hbar}^{\pm}} = 0$  around  $\mathcal{F} = \mathcal{F}_{\text{P}}$  with a  $\delta_{\text{NP}}$  expansion leads to a trans-series solution without the leading perturbative order, which is set by the perturbative QC in (2.41). Finally, to relate this construction with the spectrum (2.23), we consider the energy parameter  $E(\mathcal{F}, \hbar)$  and expand it around  $\mathcal{F}_{\text{P}}$  for  $\delta_{\text{NP}} \ll 1$  as

$$E \simeq E_{\text{P}} + \delta_{\text{NP}} \left[ \frac{\partial E_{\text{P}}}{\partial \mathcal{F}} \right]_{\mathcal{F}=\mathcal{F}_{\text{P}}} + \frac{1}{2} \delta_{\text{NP}}^2 \left[ \frac{\partial^2 E_{\text{P}}}{\partial \mathcal{F}^2} \right]_{\mathcal{F}=\mathcal{F}_{\text{P}}} + O(\delta_{\text{NP}}^3), \quad (2.43)$$

which corresponds to the trans-series expansion of  $E(\hbar, N)$ .

Note that (2.43) contains imaginary ambiguities hidden in  $\delta_{\text{NP}}$  terms. Moreover, additional ambiguities arise when each series associated with  $\frac{\partial^k E_{\text{P}}}{\partial \mathcal{F}^k}$  is Borel summed. As stated above, the physical spectrum, on the other hand, should be obtained via the median summation of the entire trans-series, which should remove all the ambiguities and leads to a single-valued spectrum.

In Section 4, we will consider the reconstruction of the spectrum for PT-symmetric and (anti-)resonance systems using the solution scheme that we described above. A detailed analysis in this way will also reveal the resurgence structure of the physical spectrum. Note that the median-summed spectrum can also be obtained by solving the median QC (2.40) directly. The associated resurgence structure, on the other hand, requires incorporation of the Alien calculus in a similar way to Section 2.2, which we will discuss next, before finishing this section.

**Alien calculus of quantization conditions:** The median QC in (2.40) is obtained by the Stokes automorphism  $\mathfrak{S}_A$  acted on  $D_{\theta_{\hbar}^{\pm}}$ . As we explained above, this relationship stems from the discontinuity of  $\Pi_A$  at  $\theta = \theta_{\hbar}$ , and  $\mathfrak{S}_A$  is a different object from  $\mathfrak{S}_{\theta_{\hbar}}$ , which encodes the Stokes discontinuities of the trans-series of the form (2.23), or equivalently (2.43). Therefore, to probe the resurgence structure of  $E(\mathcal{F}, \hbar)$ , we should consider the action of  $\mathfrak{S}_{\theta_{\hbar}}$  on  $D_{\text{med}}$ .

Motivated by (2.34), we first formally define  $D_{\text{med}}^{(\nu)} = \mathfrak{S}_{\theta_{\hbar}}^{\nu} D_{\text{med}}$  and express the Alien derivative expansion of the exact QC as

$$D_{\text{med}}^{(\nu)} = \sum_{k=0}^{\infty} \frac{\nu^k}{k!} \mathfrak{D}_k, \quad (2.44)$$

where  $\mathfrak{D}_k = \dot{\Delta}_{\theta_{\hbar}}^k [D_{\text{med}}]$ . Note that, since the dependence on  $\hbar$  is via  $\Pi_A(\mathcal{F}(\hbar))$ , to compute the expansion in (2.44) properly, we need to use the chain rule in (2.32) as

$$\dot{\Delta}_{\theta_{\hbar}} [\mathfrak{D}_k(\Pi_A(\mathcal{F}))] = \dot{\Delta}_A [D_{\text{med}}] + \frac{d\mathfrak{D}_k}{d\mathcal{F}} \dot{\Delta}_{\theta_{\hbar}} [\mathcal{F}]. \quad (2.45)$$

The first Alien derivative in (2.45) is defined via  $\dot{\Delta}_A = \log \mathfrak{S}_A$ , from the relation in (2.37), its action on  $\Pi_A$  becomes

$$\dot{\Delta}_A \Pi_A^{\alpha} = \alpha \Pi_A^{\alpha} \sum_{i=1}^n \nu_i \log(1 + \Pi_{B_i}) = \alpha \Pi_A^{\alpha} \log \left[ \prod_{i=1}^n (1 + \Pi_{B_i})^{\nu_i} \right]. \quad (2.46)$$

Then, it is also convenient to define the action of  $\dot{\Delta}_A$  on the median QC as

$$D_k = \dot{\Delta}_A^k [D_{\text{med}}]. \quad (2.47)$$

In addition to that  $\dot{\Delta}_{\theta_{\hbar}} [\mathcal{F}]$  in (2.45) induces another trans-series. We define it as

$$\mathcal{F}^{(\nu)} = \sum_{k=0}^{\infty} \frac{\nu^k}{k!} \mathcal{F}_k, \quad (2.48)$$

where

$$\mathcal{F}^{(0)} = \mathcal{F}_k = \dot{\Delta}_{\theta_{\hbar}}^k [\mathcal{F}]. \quad (2.49)$$

Note that the non-perturbative ansatz (2.42) is linked to  $\mathcal{F}^{(\pm\frac{1}{2})}$ , but the organization of (2.48) is different from (2.42). More specifically,  $\mathcal{F}_0$  corresponds to the median summation of the expression in (2.42), i.e.,

$$\mathcal{F}_0 = \mathcal{S}_{\pm} \left[ \mathfrak{S}_{\theta_{\hbar}}^{\pm 1/2} \mathcal{F} \right], \quad (2.50)$$

and  $\mathcal{F}_{k \geq 1}$  encodes the resurgence structure when  $\nu = \pm\frac{1}{2}$ .

This construction is on an equal footing with (2.34) and reveals the entire resurgence structure of the spectrum in a more abstract way. To understand the precise connection, let us consider a generalized QC:

$$D_{\text{med}}^{(\nu)}(\mathcal{F}_0) = \mathfrak{D}_0(\mathcal{F}_0) + \nu \mathfrak{D}_1(\mathcal{F}_0) + \frac{\nu^2}{2} \mathfrak{D}_2(\mathcal{F}_0) + \dots = 0, \quad (2.51)$$

where  $\mathfrak{D}_0(\mathcal{F}_0) = D_{\text{med}}^{(\nu)}(\mathcal{F}_0)$  by the definition and  $\mathfrak{D}_{k \geq 1}$  terms encode the entire resurgence structure in an organized manner. If we set  $\nu = \mp \frac{1}{2}$ , however, we return back to the QCs in (2.38), i.e.,  $D_{\theta_{\hbar}^{\pm}} = D_{\text{med}}^{(\pm 1/2)} = 0$ .

To reveal the spectrum along with the associated resurgence spectrum, (2.51) should be solved recursively for  $\mathcal{F}_k$  in (2.48). Then, incorporating (2.45) and (2.48), at the first two orders, we obtain

$$D_0(\mathcal{F}_0) = 0, \quad (2.52)$$

and

$$D_1(\mathcal{F}_0) + \mathcal{F}_1 \left. \frac{\partial D_0}{\partial \mathcal{F}} \right|_{\mathcal{F}=\mathcal{F}_0} = 0, \quad (2.53)$$

where we used (2.47) to re-write the final expressions in terms of  $D_k$ , which we can compute via (2.46) at the quantization level.

The equation in (2.52) is the median QC in (2.40), as expected. The one in (2.53), on the other hand, can be re-expressed as

$$\mathcal{F}_1(\mathcal{F}_0) = \dot{\Delta}_{\theta_{\hbar}}[\mathcal{F}_0] = D_1(\mathcal{F}_0) \left( \left. \frac{\partial D_0}{\partial \mathcal{F}} \right|_{\mathcal{F}=\mathcal{F}_0} \right)^{-1}. \quad (2.54)$$

The higher-order terms in (2.48) can be obtained in the same manner. Then, finally, in this language, we express the general trans-series solution as

$$\begin{aligned} E^{(\nu)}(\mathcal{F}, \hbar) &= E^{(0)}(\mathcal{F}_0) + \nu \mathcal{F}_1 \left. \frac{\partial E^{(0)}}{\partial \mathcal{F}} \right|_{\mathcal{F}=\mathcal{F}_0} \\ &+ \frac{\nu}{2} \left( 2\mathcal{F}_2 \left( \left. \frac{\partial E^{(0)}}{\partial \mathcal{F}} \right|_{\mathcal{F}=\mathcal{F}_0} \right)^2 + \mathcal{F}_1^2 \left. \frac{\partial^2 E^{(0)}}{\partial \mathcal{F}^2} \right|_{\mathcal{F}=\mathcal{F}_0} \right) + O(\nu^3). \end{aligned} \quad (2.55)$$

Note that in (2.55), each expression depends on the median summed action  $\mathcal{F}_0 = \mathcal{S}_{\theta_{\hbar}^{\pm}}[\mathcal{F}]$ . To return back to the trans-series solution in (2.43), it is necessary to remove the Borel summations  $\mathcal{S}_{\theta_{\hbar}^{\pm}}$  and reduce  $\mathcal{F}_0$  back to a collection of the asymptotic solutions. Then, for  $\nu = \pm \frac{1}{2}$ , (2.43) is recovered by setting  $\mathcal{F}_0 = \mathcal{F}_{\text{P}} + \delta_{\text{NP}}$  and expanding around  $\mathcal{F}_{\text{P}}$  for  $\delta_{\text{NP}}$ .

Despite its abstractness, in comparison to the direct solutions to  $D_{\theta_{\hbar}^{\pm}} = 0$ , which leads to (2.43), the use of the median QC and Alien calculus yields a concrete separation of the median-summed and resurgence-structure parts. Since the latter never appears in the spectrum, this separation is very significant. In Section 5, we utilize this approach to construct exact non-perturbative solutions directly. It is also very useful to figure out how the resurgence cancellations take place when we do not have enough quantitative power to reveal them numerically. This last point helps us to understand the semi-classical quantization picture, which will be reviewed in Section 3.2 and thoroughly discussed in Section 4 for non-Hermitian inverted triple-well potential.

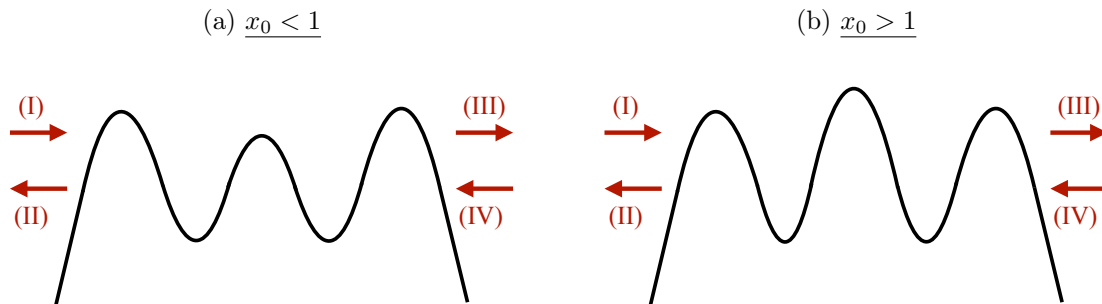


**Figure 7:** Inverted triple-well potential for two different values of parameter  $x_0$ . The incoming and outgoing waves are labeled as (I)–(IV) and their pairing is used to define the PT-symmetric, resonance, and anti-resonance boundary conditions.

### 3 Quantum mechanics of inverted triple-well

#### 3.1 Setup and numerical solutions

Let us introduce the inverted triple-well (ITW) potential of the form

$$V = -\frac{1}{2}(x^2 - 2^2)(x^2 - x_0^2)^2, \quad (3.1)$$

such that  $x_0 \in (-2, 2)$ . This potential, illustrated in Fig. 7, has a parity symmetry at the classical level and keeps the shape of an inverted triple-well for all  $x_0$  in the given interval. Since the classical potential is unbounded, ITW is a quintessential example of non-Hermitian quantum mechanics. In some sense, it can be considered as an idealized version of an open quantum system. Then, the system-environment interaction results in outward and inward probability flows, which are enumerated by (I)–(IV) in Fig. 7, and the relationship between these fluxes determines whether the quantized system has equilibrium or non-equilibrium character.

When ITW is tackled via the Schrödinger equation, a choice of the flow direction is made when the boundary conditions are set by requiring which solutions survive at  $x = \pm\infty$ . This amounts to imposing boundary conditions that select two of the waves (I)–(IV) in Fig. 7 and set the others to zero. When the waves (I) and (III), or equivalently (II) and (IV), are chosen to be non-vanishing and the others are set to zero, the quantized system can be in equilibrium if the inward and outward fluxes balance each other. These choices define a PT-symmetric system.

When the waves (II) and (III) are chosen as the surviving solutions at  $x = \pm\infty$ , there is an outward flow that is not compensated by an inward one, indicating that any state located originally in a finite region would eventually decay to  $x = \pm\infty$ . Such systems have resonance characters. On the other hand, if (I) and (IV) waves are chosen to non-zero, the flow is inward and the probability of finding a quantum state around the center increases in time. Such systems are called anti-resonance, since they have the opposite characters to the

resonance ones. In fact, the resonance and anti-resonance systems are time-reversal to each other, and, in exactly solvable settings, it has been shown that picking forward and backward time-evolution directions favor resonance and anti-resonance systems, respectively [132].

The PT-symmetric case is more subtle. The corresponding boundary conditions reflect the time-symmetric nature of the system, since the two PT-symmetric choices are mapped into each other under time reversal, i.e., the right-moving waves (I)-(III) are exchanged with the left-moving waves (II)-(IV). This suggests the equilibrium character of the PT-symmetric system when the inward and outward probability fluxes balance each other. In such a regime, the spectrum can remain real, which is one of the crucial characteristics of PT-symmetric quantum mechanics. However, there is no guarantee that this balance survives after quantization, and the quantized system may acquire complex eigenvalues in some parameter regions. These regions are called a *broken* PT-symmetric phase, in contrast to the *unbroken* phase with real eigenvalues.

Since the main criterion for the PT-symmetry breaking is the emergence of complex eigenvalues, it is natural to examine the spectrum numerically in different parameter regimes. For the ITW potential (3.1), we observe that when  $x_0$  exceeds a critical value  $x_{\text{cr}}$ , namely the exceptional point, complex eigenvalues begin to appear in the spectrum, signaling the PT-symmetry breaking. We illustrate this transition in Fig. 8. At  $x_0 = x_{\text{cr}}$ , the real parts of a pair of eigenvalues coalesce, and for  $x_0 > x_{\text{cr}}$  they develop complex-conjugate imaginary parts. This pattern, namely the coalescence of the real parts and the emergence of the imaginary parts in eigenvalues, is also familiar from other quantum-mechanical examples of PT-symmetry breaking; see, e.g., [12, 133].

### 3.2 Semi-classical picture

Having the numerical solutions for the eigenvalues, we turn to the main purpose of this paper, i.e., the analytic quantization of non-Hermitian quantum mechanics of ITW. As we stated before, our main approach is the EWKB framework, which is particularly helpful in determining the PT-symmetry breaking analytically. In doing so, we provide a concrete link to the semi-classical quantization in the path-integral formalism and describe physical properties in this language. For this reason, before analyzing the ITW potential using the EWKB formalism, we first introduce the basic building blocks for the semi-classical analysis of the ITW potential.

We first observe that, since (3.1) has two symmetric wells for any  $x_0 \in (-2, 2)$ , the perturbative spectra localized in these wells are degenerated to all orders. Note also that the perturbative series is real, meaning that when  $x_0 > x_{\text{cr}}$  the PT-symmetry breaking should be induced by non-perturbative effects. Another important feature of the perturbative sector of ITW is that the series diverges factorially at large orders, which is non-Borel summable. This is a general characteristic of perturbative sectors when the corresponding potentials have minima at the same level. In our particular case, we infer the perturbation expansion has the following form:

$$E_{\text{P}}(\hbar) = \sum_{k=0}^{\infty} \alpha_k^{(1)} \hbar^k + \sum_{k=0}^{\infty} \alpha_k^{(2)} \hbar^k, \quad \alpha_k^{(i)} \sim \mathcal{A}_i^{-k-\gamma_i} \Gamma(k + \eta_i + 1), \quad (3.2)$$

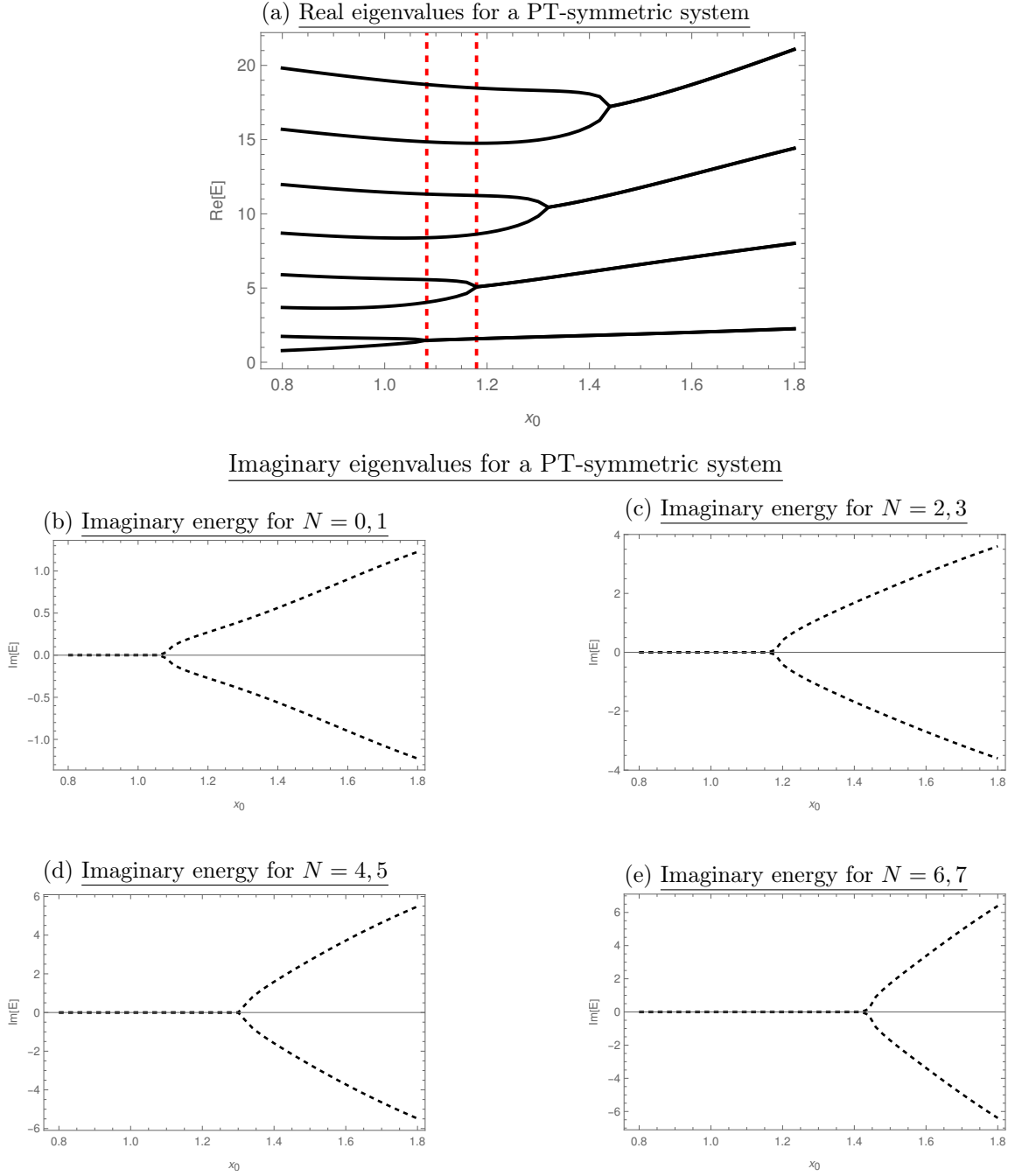


**Figure 8:** Numerical eigenvalues of the PT-symmetric inverted triple-well system as functions of  $x_0$  for energy levels  $N = 0, 1, \dots, 7$ . (a) Real parts of the low-lying eigenvalues; the dashed vertical lines mark the first two exceptional points. (b)–(e) Imaginary parts for each pair that coalesce at the exceptional points, showing the onset of complex-conjugate branches beyond the respective critical values.

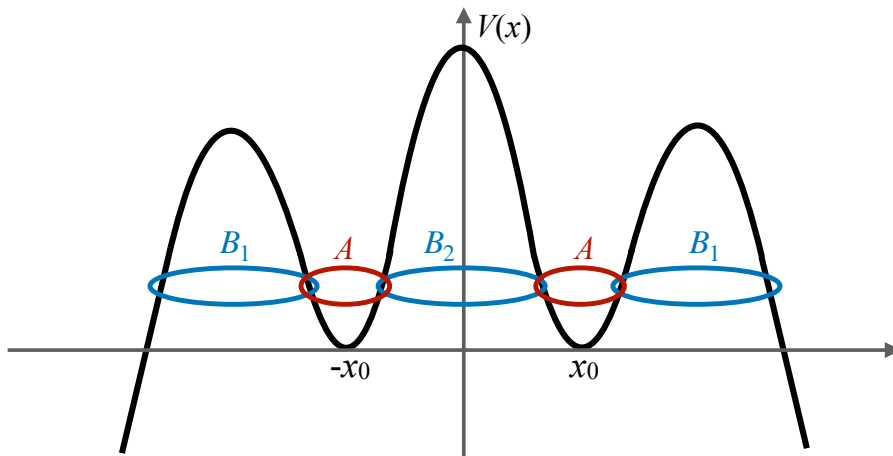


**Figure 9:** The WKB-cycle structure of the inverted triple-well potential. The outer  $B_1$  cycles are associated with bounce configurations, while the central  $B_2$  cycle between the two inner wells is related to the bion configuration. The red  $A$ -cycles are the perturbative cycles around the wells.

where  $\gamma_i$  and  $\eta_i$  will be determined later. Note that the perturbation series can be organized in a single sum, but separating it into two parts as in (3.2) will help us for our purpose.

We also note that the perturbation series in (3.2) leads to non-perturbative ambiguities upon the Borel-summation procedure. These ambiguities must participate in the so-called large- and low-orders resurgence cancellation, since the physical observables should be single-valued. Therefore, regardless of other physical properties, there should be compensating (ambiguous) imaginary non-perturbative contributions, to which we now turn our focus.

The non-perturbative sector of ITW is governed by two types of configurations. One of them is linked to the *bounce* solution, which is originally formulated to describe the vacuum decay in quantum mechanics and quantum field theory [134, 135]. In our setting, the bounce appears in the  $E = 0$  limit of the  $B_1$ -cycle depicted in Fig. 9. We label a bounce event contributing to the trans-series as  $[\mathcal{B}]$ . For the ITW in (3.1) and at the leading order in the non-perturbative sector, it reads

$$[\mathcal{B}]_{\pm} \simeq \mp i \frac{e^{-\frac{S_1}{\hbar}}}{2\sqrt{2\pi N!}} \left(\frac{\mathcal{C}}{\hbar}\right)^{N+\frac{1}{2}}, \quad (3.3)$$

where  $N$  corresponds to the energy levels,

$$S_1 = 2 \int_{x_0}^2 dx \sqrt{E - V(x)} = \frac{1}{2} x_0 (x_0^2 + 2) \sqrt{4 - x_0^2} + 8 (1 - x_0^2) \operatorname{arccot} \left[ \sqrt{\frac{2 - x_0}{2 + x_0}} \right], \quad (3.4)$$

is the classical action for a bounce and

$$\mathcal{C} = x_0^3 (4 - x_0^2)^{5/2}, \quad (3.5)$$

is the one-loop determinant term. The expression in (3.3) is sometimes called fugacity [136] in multi-instanton expansions (or the multi-bounce expansion in the present case) in the



dilute-gas treatment [19, 20, 47, 129, 135]. Although we do not delve into the dilute-gas picture, we will keep the language in this paper.

We note that bounce solutions in quantum mechanics and quantum field theory were originally introduced long ago in the context of the vacuum decay [134, 135]. In the exact quantization, however, a bounce does not necessarily signal a complex spectrum nor an instability. These are intrinsic characteristics of a quantum system and are mainly determined by the boundary conditions in our setting. Then, to uncover the precise role of the bounce solution in the non-perturbative spectrum, one should address the exact quantization techniques, which we discuss in Section 4 (see also [81] for a recent discussion).

The other types of non-perturbative configurations in the ITW system are linked to the *bion* solution. In our setting, a bion is associated with the  $E = 0$  limit of the  $B_2$ -cycle in Fig. 9. We find its classical action as

$$\begin{aligned} S_2 &= 2 \int_{-x_0}^{x_0} dx \sqrt{E - V(x)} \\ &= 4\pi (1 - x_0^2) + x_0 (x_0^2 + 2) \sqrt{4 - x_0^2} + 16 (1 - x_0^2) \operatorname{arccot} \left[ \sqrt{\frac{2 + x_0}{2 - x_0}} \right]. \end{aligned} \quad (3.6)$$

Unlike the bounce, a bion has a topological character, since it consists of a combination of instanton and anti-instanton events. Therefore, in this paper, we represent one-bion event as  $[\mathcal{I}\bar{\mathcal{I}}]$ , emphasizing the non-trivial inner structure that is in contrast to the one-bounce event  $[\mathcal{B}]$ .

At the leading order, a single instanton (or anti-instanton) event contribution is

$$[\mathcal{I}] = [\bar{\mathcal{I}}] \simeq \frac{e^{-\frac{S_2}{2\hbar}}}{\sqrt{2\pi N!}} \left( \frac{\mathcal{C}}{\hbar} \right)^{N+\frac{1}{2}}, \quad (3.7)$$

where  $\mathcal{C}$  is the same as in (3.5) and (3.7) can be considered as the fugacity of the instanton molecules in the dilute-gas system. It is well-known that in Hermitian quantum mechanics,  $[\mathcal{I}]$  (and  $[\bar{\mathcal{I}}]$ ) is responsible for the real splitting of the perturbative degeneracy in a double-well system. As we discuss later, for ITW, the role of  $[\mathcal{I}]$  stays the same if they appear in the trans-series solutions. Contrary to the Hermitian double-well case, this is not guaranteed, and we will show in Section 4.1 that in the broken PT-symmetric phase, no  $[\mathcal{I}]$  (nor  $[\bar{\mathcal{I}}]$ ) event contributes to the spectrum.

Another known fact in Hermitian systems is that when instanton and anti-instanton events are combined to form bions, it leads to an imaginary ambiguity. At the leading order, this ambiguous contribution becomes

$$[\mathcal{I}\bar{\mathcal{I}}]_{\pm} \simeq \mp i \frac{e^{-\frac{S_2}{\hbar}}}{2N!} \left( \frac{\mathcal{C}}{\hbar} \right)^{2N+1} + \operatorname{Re}([\mathcal{I}\bar{\mathcal{I}}]). \quad (3.8)$$

Note that the real part in (3.8) is single-valued, which we elaborate later. Finally, we would like to emphasize that the expressions (3.3), (3.7), and (3.8) are on an equal footing with their counterparts in the semi-classical analysis of Hermitian settings (see, e.g., [20, 129, 134, 135] for classical papers and [25, 28–36, 38, 39, 45–50, 137] more modern examples).

Having introduced the basic building blocks, let us return to the semi-classical quantization of the ITW system. Since the perturbation series is divergent and non-Borel summable and there are various non-perturbative configurations, it is natural to turn to the resurgence theory and examine the intricate relationships between different parts contributing to the spectrum. Before discussing the trans-series structures of PT-symmetric and (anti-)resonance systems in the next section, we now elaborate the resurgence cancellations between the Borel-summed perturbation series and ambiguous non-perturbative configurations.

As we mentioned in Section 2.2, this cancellation procedure is called the Bogomolny-Zinn-Justin (BZJ) mechanism [19, 20, 128, 129] and has been discussed intensively in Hermitian setups [21, 22, 26–42, 44–50, 61, 81, 137] (see also [16, 81] for related discussions in PT-symmetric systems without referencing to the PT-symmetry breaking). The BZJ mechanism is needed for the spectrum to be unambiguous. As we mentioned before, this should also be the case in non-Hermitian systems, where the final spectrum must be single-valued. This means that the Borel ambiguity of the perturbation series in (3.2) or the other non-perturbative ambiguities arising from configurations such as  $[\mathcal{B}]_{\pm}$  in (3.3) or  $[\mathcal{IT}]_{\pm}$  in (3.8) should vanish in the final spectrum.

When the spectrum is complex, some part of the imaginary contributions should remain. In this paper, we will encounter two possible ways leading to a complex spectrum:

1. First possibility is that the imaginary contributions from the Borel summation and non-perturbative configurations do not agree. Then, the cancellation takes place partially and results in an imaginary contribution in the Borel-summed trans-series. In our discussion, we observe such an emergence of complex spectra in the resonance and anti-resonance cases, as well as in the broken PT-symmetric phase.

A crucial point in such cases is that different analytic continuations, which originally lead to ambiguities, must lead to a single unambiguous result. Therefore, even if they do not coincide exactly, the imaginary parts of the Borel-summed perturbation series and non-perturbative configurations should still act in harmony.

2. Another possibility is that the imaginary non-perturbative contributions are not related to any perturbative series in the pre-Borel-summed trans-series. In this case, as there is no counterpart to this imaginary contribution, it directly leads to a complex spectrum. We encounter such non-perturbative configurations in the case of the broken PT-symmetry.

We emphasize that in all cases, the resurgence cancellations take place to some extent. In fact, as we will discuss in Section 4 and Section 5, there is a subpart in the full trans-series which is the same for all of the cases regardless of the other physical properties. It can be called a *minimal* trans-series, in comparison to the full trans-series [131]. The leading-order non-perturbative configurations of this subpart are  $[\mathcal{B}]_{\pm}$  and  $\text{Im}([\mathcal{IT}]_{\pm})$ , along with the perturbative expansion (3.2). For all choices of the boundary conditions, they participate in the resurgence cancellations in the same way. In fact, as we discussed above,

this is necessary since the perturbation series is non-Borel summable, which leads to a non-perturbative ambiguity and needs non-perturbative counterparts to fix it. Moreover, since it is in the same form for all the cases, this non-perturbative counterpart should be the same.

Let us finally numerically verify  $[\mathcal{B}]_{\pm}$  in (3.3) and  $\text{Im}([\mathcal{I}\bar{\mathcal{T}}]_{\pm})$  in (3.8) are indeed the events that take part in this cancellation. Being imaginary exponentially-suppressed contributions, they are intimately related to a divergent series via the dispersion relation [138, 139]. For this reason, we express the divergent series associated with the bounce ( $i = 1$ ) and bion ( $i = 2$ ) configurations as

$$\mathcal{E}^{(i)} = \sum_{k=0}^{\infty} \beta_k^{(i)} \hbar^k, \quad (3.9)$$

For  $[\mathcal{B}]_{\pm}$  in (3.3), we obtain the associated large-order behavior of the coefficients as

$$\beta_k^{(1)} \sim \frac{\mathcal{C}^{N+\frac{1}{2}}}{2\pi\sqrt{2\pi}N!} \frac{\Gamma(k+N+\frac{1}{2})}{S_1^{k+N+\frac{1}{2}}}, \quad (3.10)$$

and for  $\text{Im}([\mathcal{I}\bar{\mathcal{T}}]_{\pm})$ , we get

$$\beta_k^{(2)} \sim \frac{\mathcal{C}^{2N+1}}{2\pi N!} \frac{\Gamma(k+2N+1)}{S_2^{k+2N+1}}. \quad (3.11)$$

In Fig. 10, we compare (3.10) and (3.11) with the exact perturbation series, which is obtained using the Bender-Wu package [140], for several values of the parameter  $x_0$ . We note that in the parameter regions where  $[\mathcal{I}\bar{\mathcal{T}}]$  and  $[\mathcal{B}]$  events dominate, the behaviors of the exact perturbation series agree with (3.11) and (3.10), respectively. This can be seen in Fig. 10a for  $x_0 = \frac{1}{2}$  where the bion configuration dominates, and Fig. 10b for  $x_0 = 1.15$  where the bounce does. When  $[\mathcal{B}] \simeq [\mathcal{I}\bar{\mathcal{T}}]$ , we observe that both contributions should be taken into account to recover the behavior of the exact perturbation series. This is depicted in Fig. 10c, where we demonstrate that the individual contribution from  $[\mathcal{B}]$  or  $[\mathcal{I}\bar{\mathcal{T}}]$  does not reproduce the behavior of the exact perturbation series.

Note that despite these apparent differences in its non-perturbative counterpart for different values of  $x_0$ , the perturbation series is the same in any parameter region. This is simply because the properties of the well of  $V_{\text{ITW}}(x)$  in (3.1) do not change their characters for  $x_0 \in (-2, 2)$ . Then, the differences in Fig. 10 are only quantitative, and the large-order behavior of the exact perturbation series should be controlled by both bion and bounce configurations. In fact, a closer look at the large-order estimations from bounce and bion in  $x_0 = \frac{1}{2}$  and  $x_0 = 1.15$ , we observe that the subdominant contribution is numerically negligible, which we show in Fig. 10a and Fig. 10b by comparing the dominant contribution with the combined contributions of bion and bounce.

As a result, we conclude that, in general, the large-order perturbation theory is controlled by both  $[\mathcal{B}]$  and  $[\mathcal{I}\bar{\mathcal{T}}]$ , which also validates our separation of the perturbation series in (3.9) into two parts. Finally, for completeness, let us fix the constants  $\delta_i$  and  $\eta_i$  in (3.2) by comparing (3.10) and (3.11). We find  $\delta_1 = \eta_1 = N - \frac{1}{2}$  and  $\delta_2 = \eta_2 = 2N$ .

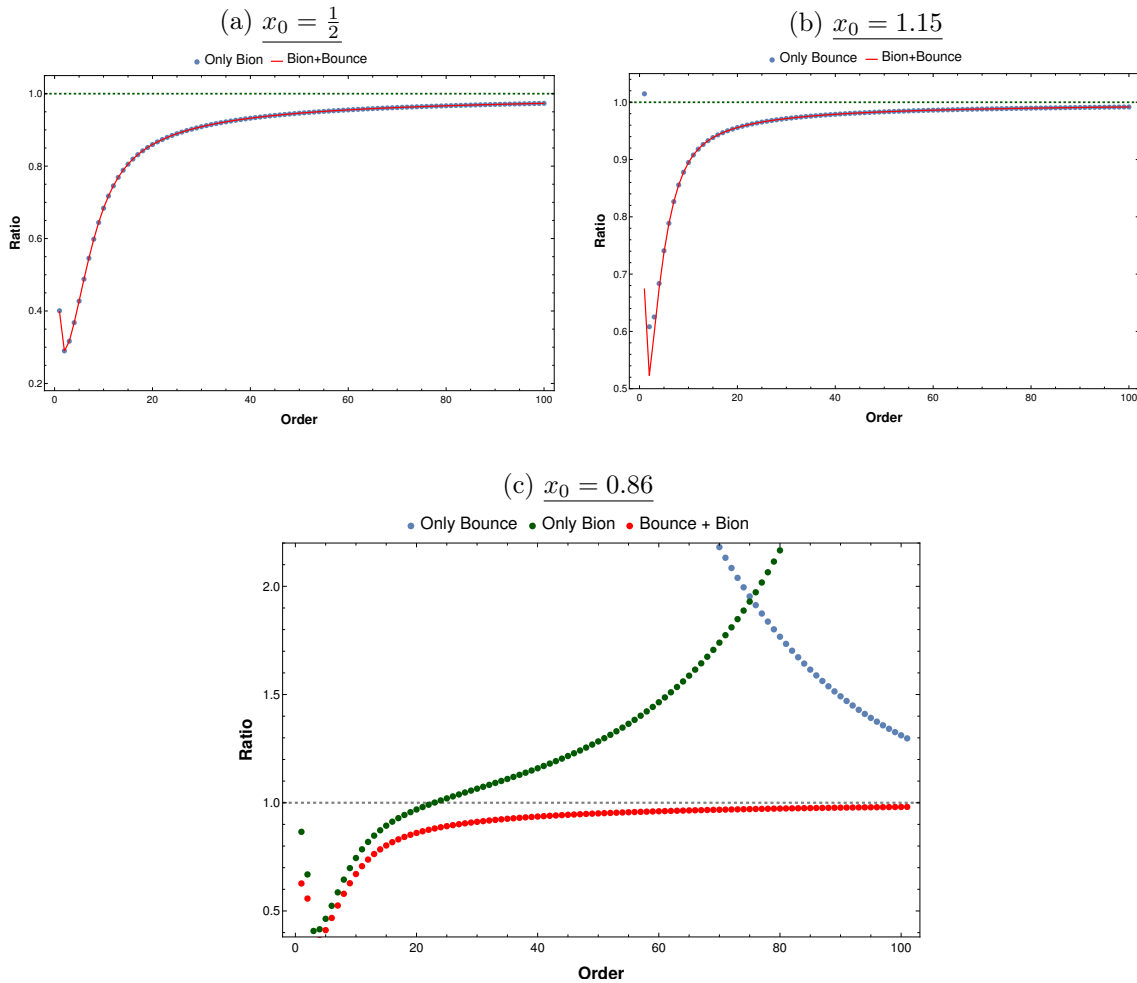


**Figure 10:** Large-order test of the perturbative coefficients against the semi-classical estimates from the bounce and bion contributions. The ratio plotted compares the exact Bender-Wu coefficients with the asymptotic formulas in three parametric regions. **(a)** For  $x_0 = \frac{1}{2}$ , the bion configuration dominates. **(b)** For  $x_0 = 1.15$ , the bounce configuration dominates. **(c)** For  $x_0 = 0.86$ , no configuration dominates. In **(a)** and **(b)**, the dominant bion or bounce contribution is shown by **blue dots**, while the combination of both bounce and bion is represented by **red line**. In **(c)**, the ratios involving only bounce (**blue dots**) and bion (**green dots**) do not reproduce the exact result. Instead, the combination of bounce and bion (**red dots**) captures the correct large-order behavior.

Despite their fundamental roles in the semi-classical dynamics, as we mentioned above, the bion and bounce configurations need to be supported by more comprehensive quantization schemes to obtain accurate information about the non-perturbative spectrum. At this point, the EWKB framework comes to our aid. In Section 4, we will solve the exact QCs to obtain the trans-series structure (up to a finite order) for PT-symmetric and (anti-)resonance cases independently. In addition to that, with the help of the Alien calculus, the EWKB formalism leads to truly *exact* non-perturbative corrections, which we discuss

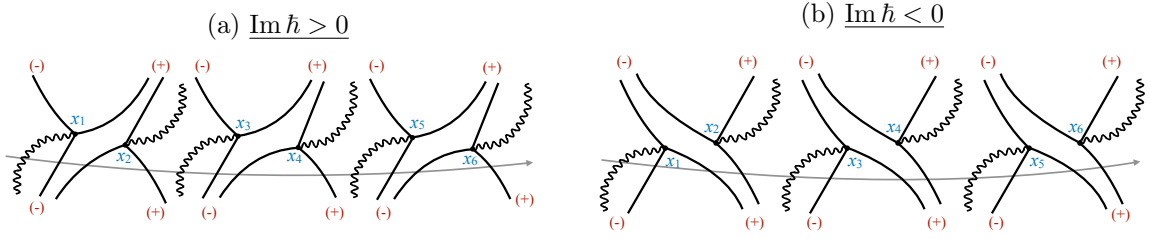


**Figure 11:** Analytic continuations of the inverted triple-well Stokes diagram for  $\text{Im } \hbar = 0^\pm$ . The two diagrams for  $\text{Im } \hbar > 0$  and  $\text{Im } \hbar < 0$  define the transition matrices  $T^{(+)}$  and  $T^{(-)}$  connecting the asymptotic solutions between  $x = -\infty$  and  $+\infty$ .

in Section 5. In the PT-symmetric case, this allows us to find the exact analytical semi-classical condition for the PT-symmetry breaking and to determine the exceptional points. Before addressing these solutions, we now return to the connection problem and describe PT-symmetric and (anti-)resonance problems in view of the EWKB framework.

### 3.3 Exact WKB of inverted triple-well

We start with  $\text{Im } \hbar = 0^\pm$  analytic continuations of the Stokes diagrams for the ITW potential, which are depicted in Fig. 11. For  $\text{Im } \hbar > 0$  and  $\text{Im } \hbar < 0$ , we define the transition matrices connecting  $x = \pm\infty$ , respectively, as

$$T^{(+)} = \begin{pmatrix} T_{1,1}^{(+)} & T_{1,2}^{(+)} \\ T_{2,1}^{(+)} & T_{2,2}^{(+)} \end{pmatrix}, \quad T^{(-)} = \begin{pmatrix} T_{1,1}^{(-)} & T_{1,2}^{(-)} \\ T_{2,1}^{(-)} & T_{2,2}^{(-)} \end{pmatrix}. \quad (3.12)$$

In terms of  $T^{(\pm)}$ , the connection problem is formulated as

$$\Psi_\infty^{(\pm)} = T^{(\pm)} \Psi_{-\infty}^{(\pm)}, \quad (3.13)$$

where

$$\Psi^{(\pm)} = \begin{pmatrix} \psi^{(1,\pm)} \\ \psi^{(2,\pm)} \end{pmatrix}$$

are the vector of WKB solutions for  $\text{Im } \hbar = 0^\pm$  and the subscripts indicate the solutions at  $x = \pm\infty$ , respectively. Then, the following conditions determine whether the system is (anti-)resonance or PT-symmetric:

- $T_{1,2}^{(\pm)} = 0$  and  $T_{2,1}^{(\pm)} = 0$  are for the PT-symmetric case.
- $T_{2,2}^{(\pm)} = 0$  for the resonance case and  $T_{1,1}^{(\pm)} = 0$  for the anti-resonance case.

The exact QCs for all possible cases are summarized in Table 1.

**Table 1:** Exact quantization conditions for the inverted triple-well.

<b>Im <math>\hbar &gt; 0</math></b>	
PT-symmetric 1	$T_{1,2}^{(+)} = i\Omega \{(1+A)^2 + B_1(1+A) + B_2(1+B_1)\} = 0$
PT-symmetric 2	$T_{2,1}^{(+)} = -i\Omega \{(1+A)^2 + B_1(1+A) + B_2(1+B_1)\} = 0$
Anti-resonance	$T_{1,1}^{(+)} = \Omega \{(1+A)^2 + B_2\} = 0$
Resonance	$T_{2,2}^{(+)} = \Omega \{(1+A+B_1)^2 + B_2(1+B_1)^2\} = 0$
<b>Im <math>\hbar &lt; 0</math></b>	
PT-symmetric 1	$T_{1,2}^{(-)} = i\Omega \{(1+A)^2 + AB_1(1+A) + A^2B_2(1+B_1)\} = 0$
PT-symmetric 2	$T_{2,1}^{(-)} = -i\Omega \{(1+A)^2 + AB_1(1+A) + A^2B_2(1+B_1)\} = 0$
Anti-resonance	$T_{1,1}^{(-)} = \Omega \{(1+A+AB_1)^2 + A^2B_2(1+B_1)^2\} = 0$
Resonance	$T_{2,2}^{(-)} = \Omega \{(1+A)^2 + A^2B_2\} = 0$

In all equations, we defined

$$\Omega = (A^{-2}B_1^{-2}B_2^{-1})^{1/2} \quad (3.14)$$

for convenience. In this way, until the QCs are solved to get the spectrum, all the computations are carried out exactly and the relationship among  $T_{i,j}^{(\pm)}$  becomes manifest.

Given all these terms, we first observe that

$$CT_{1,2}^{(\pm)} = T_{2,1}^{(\mp)}, \quad CT_{1,1}^{(\pm)} = T_{2,2}^{(\mp)}, \quad (3.15)$$

where  $C$  is the complex-conjugation operator. As expected,  $C$  acts as a time-reversal operator, mapping resonance to anti-resonance and also PT-symmetric to PT-symmetric with waves moving in the opposite directions. Note that one may be confused with the roles of the time-reversal operator  $C$  and the Stokes automorphism, as both map the QCs for  $\text{Im } \hbar > 0$  to the ones for  $\text{Im } \hbar < 0$  and vice versa. We will revisit the issue of time-reversal and elaborate its role at the end of this subsection.

Next, we show how the entire connection problem transforms under the Stokes automorphism. We know that the physics for  $\text{Im } \hbar > 0$  and  $\text{Im } \hbar < 0$  are mapped to each other via a Stokes automorphism, which should reveal itself in the connection problem in (3.13). To observe the one-to-one map precisely, in addition to the transition matrices  $T_{i,j}^{(\pm)}$ , we apply the Stokes automorphism to the solutions  $\Psi_{\mp\infty}^{(\pm)}$ . Applying the Stokes automorphism onto the transition matrices is the standard treatment, which we discussed in Section 2.3. The transformation of  $\Psi_{\mp\infty}^{(\pm)}$ , on the other hand, is not widely discussed in the literature. In our discussion, we follow the construction in [112].

The Stokes automorphism for ITW (3.1) is given by

$$\mathfrak{S}_A^\nu : A \mapsto A(1+B_1)^\nu(1+B_2)^\nu. \quad (3.16)$$

For the PT-symmetric parts, the action is straightforward:

$$\mathfrak{S}_A T_{1,2}^{(+)} = T_{1,2}^{(-)}, \quad \mathfrak{S} T_{2,1}^{(+)} = T_{2,1}^{(-)}. \quad (3.17)$$

For resonance and anti-resonance cases, on the other hand, we have

$$\begin{aligned} \mathfrak{S}_A T_{1,1}^{(+)} &= \Omega(1+B_1)^{-1} \{(1+A)^2 + A^2 B_1^2 (1+B_2) + 2AB_1(1+A+AB_2)\} \\ &= (1+B_1)^{-1} T_{1,1}^{(-)}, \end{aligned} \quad (3.18)$$

and

$$\begin{aligned} \mathfrak{S}_A T_{2,2}^{(+)} &= \Omega(1+B_1) \{(1+A)^2 + A^2 B_2\} \\ &= (1+B_1) T_{2,2}^{(-)}. \end{aligned} \quad (3.19)$$

The remaining factors are cancelled, once the Stokes automorphism is applied to the vector of the WKB solutions (wave-functions), which are given as

$$\Psi_{\infty}^{(+)} = \Sigma \Psi_{\infty}^{(-)}, \quad \Psi_{-\infty}^{(+)} = \Sigma^{-1} \Psi_{-\infty}^{(-)}, \quad (3.20)$$

where

$$\Sigma = \begin{pmatrix} (1+B_1)^{-1/2} & 0 \\ 0 & (1+B_1)^{1/2} \end{pmatrix}. \quad (3.21)$$

Then, in view of (3.17)-(3.19) and (3.21), the entire connection problem transforms under the Stokes automorphism as

$$\Psi_{\infty}^{(+)} = T_+ \Psi_{-\infty}^{(+)} \xrightarrow{\tilde{\mathfrak{S}}} \Sigma \Psi_{\infty}^{(-)} = \begin{pmatrix} (1+B_1)^{-1} T_{1,1}^{(-)} & T_{1,2}^{(-)} \\ T_{2,1}^{(-)} & (1+B_1) T_{2,2}^{(-)} \end{pmatrix} \Sigma^{-1} \Psi_{-\infty}^{(-)}, \quad (3.22)$$

where the right-hand side can be arranged as

$$\Psi_{\infty}^{(-)} = T_- \Psi_{-\infty}^{(-)}. \quad (3.23)$$

Having the entire system being mapped between  $\arg(\text{Im } \hbar) = 0^{\pm}$  cases, we make the following observations:

- A complex conjugation and a Stokes automorphism are equivalent, only if there is time-reversal symmetry at the quantum level. Note that this is always the case for Hermitian systems. However, the equivalence is not generalized to the resonance and anti-resonance cases, where the time-reversal symmetry is broken. We expect that this observation also holds for more general potentials as well.

We also note that recently, in the case of IDW [16], the PT-symmetric case was linked to the resonance system by a one-parameter Stokes automorphism (more precisely, half-Stokes automorphism  $S^{-1/2}$ ). It was shown that this link can be understood as a new formulation of the ABS conjecture [122]. Our analysis above, however, shows that this relationship does not generalize to the ITW system.

- Recalling the relations in (3.15), the forms of the exact QCs for the resonance and anti-resonance cases are exchanged by the Stokes automorphism up to a complex conjugation. Note that the complex conjugation has a crucial role here, as it does not alter the signs of the imaginary part of the resonance spectrum, i.e.,  $\text{Im } E < 0$  for  $\text{Im } \hbar > 0$  and  $\text{Im } \hbar < 0$ . This means that resonance solutions stay as resonance solutions for both  $\text{Im } \hbar = 0^\pm$ . Same arguments apply to the anti-resonance solutions with  $\text{Im } E > 0$  for both  $\text{Im } \hbar = 0^\pm$ . Note that this is in complete agreement with the previous point that the Stokes automorphism and complex conjugation (time reversal) are different operations.

- Fixing boundary conditions is basically equivalent to choosing the direction of the time evolution. This becomes evident in the spectra of resonance and anti-resonance cases via the imaginary signs of their respective eigenvalues. In the PT-symmetric case, however, the direction of time is lost due to the time-reversal symmetry; but as we showed in (3.15), the PT-symmetric choices are time-reversed partners of each other. Note that all these are consistent with the  $i\varepsilon$  prescription: the complex part is introduced to the energy parameter, which is equivalent to picking a boundary condition for the Green function.

Then, the role of the Stokes automorphism becomes mapping the analytic continuation around  $\text{Im } \hbar = 0$ , which is its original purpose. This is, in fact, crucial for the completeness of our setting, since the physical quantities lie on the Stokes ray corresponding to  $\text{Im } \hbar = 0$ , which is reached by the action of half-Stokes automorphism, i.e.,  $\mathfrak{S}_A^{\pm 1/2}$ . As the time direction should not be affected by the direction of the  $\text{Im } \hbar \rightarrow 0^\pm$  limits, the Stokes automorphism must not be related to the time-reversal.

## 4 Trans-series from exact WKB

### 4.1 PT-symmetric case

Let us consider the QCs,  $T_{1,2}^{(\pm)} = 0$ , in Table 1. The solution isolating the perturbative part on the left-hand side can be written as

$$2e^{\mp i\pi\mathcal{F}} \cos \pi\mathcal{F} = -\frac{\Pi_{B_1}}{2} + \varepsilon \left[ \text{Disc}_{\text{PT}} (\Pi_{B_1} \Pi_{B_2}) \right]^{1/2}, \quad (4.1)$$

where  $\varepsilon = \pm 1$ , indicating a non-perturbative splitting, and

$$\text{Disc}_{\text{PT}} = \frac{\Pi_{B_1}^2}{4} - \Pi_{B_2} (1 + \Pi_{B_1}) \quad (4.2)$$

is the re-scaled discriminant of the quadratic equation. The reason behind this rescaling will be clear, when we specify the terms associated with the bounce and bion contributions to the quantized system.

In Section 2.3, we discussed the construction of the trans-series solution around a perturbative saddle. Accordingly, we define

$$\mathcal{F} = N + \frac{1}{2} + \delta_{\text{PT}}. \quad (4.3)$$



Then, we can solve (4.1) for  $\delta_{\text{PT}}$  after expanding it for  $\delta_{\text{PT}} \ll 1$ . In our case, this approach is applicable in the below-barrier-top region where both  $\Pi_{B_1}$  and  $\Pi_{B_2}$  are exponentially suppressed<sup>5</sup>.

Note that the quantitative relationship between  $\Pi_{B_1}$  and  $\Pi_{B_2}$  depends on the size of the corresponding barriers and their dominance changes as the parameter  $x_0$  is altered. In the following, we will examine (4.1) in two asymptotic regimes corresponding to  $\Pi_{B_1}^2 \ll \Pi_{B_2}$  and  $\Pi_{B_2} \ll \Pi_{B_1}^2$ . By uncovering the corresponding trans-series, we will show that these limits correspond to the unbroken and broken phases of the PT-symmetric theory, which was shown numerically in Fig. 8.

The relationship between  $\Pi_{B_1}^2$  and  $\Pi_{B_2}$  becomes important when one deals with the square-root term in (4.1). It is straightforward to see that assuming  $\Pi_{B_1}^2 \ll \Pi_{B_2}$  or  $\Pi_{B_2} \ll \Pi_{B_1}^2$  leads to two distinct expansions, indicating different physical features in these asymptotic limits. Expanding directly in terms of  $\Pi_{B_1}$  and  $\Pi_{B_2}$ , however, could be tricky and possibly misleading, particularly when the higher order non-perturbative corrections to the trans-series is considered. This is because the actual small parameter  $\delta_{\text{PT}}$  appears also in  $\Pi_{B_1}$  and  $\Pi_{B_2}$ , and a second expansion in  $\delta_{\text{PT}}$  would be needed if the square-root term is expanded directly for  $\Pi_{B_1}^2 \ll \Pi_{B_2}$  or  $\Pi_{B_2} \ll \Pi_{B_1}^2$ .

Instead, we utilize the EWKB dictionary in (2.18) and (2.19) directly and re-arrange (4.1) as

$$\frac{1}{\pi} \cos(\pi\mathcal{F}) = -\tilde{\Pi}_{B_1} - \varepsilon \left[ \tilde{\Pi}_{B_1}^2 - \tilde{\Pi}_{B_2}^2 (1 + \Pi_{B_1}) \right]^{1/2}, \quad (4.4)$$

where we re-defined the actions on the right-hand side as

$$\tilde{\Pi}_{B_1} = \frac{e^{\pm i\pi\mathcal{F}}}{2 \cdot 2\pi} \Pi_{B_1} = \frac{e^{-\mathcal{G}^{(1)}}}{2\sqrt{2\pi}} \frac{e^{\pm i\pi\mathcal{F}}}{\Gamma(\frac{1}{2} + \mathcal{F})} \left( \frac{\mathcal{C}}{\hbar} \right)^{\mathcal{F}}, \quad (4.5)$$

$$\tilde{\Pi}_{B_2} = \frac{e^{\pm i\pi\mathcal{F}}}{2\pi} \Pi_{B_2}^{1/2} = \frac{e^{-\frac{1}{2}\mathcal{G}^{(2)}}}{\sqrt{2\pi}} \frac{e^{\pm i\pi\mathcal{F}}}{\Gamma(\frac{1}{2} + \mathcal{F})} \left( \frac{\mathcal{C}}{\hbar} \right)^{\mathcal{F}}. \quad (4.6)$$

The main reason behind this re-definition is being able to treat the contributions from the  $B_1$ - and  $B_2$ -cycles on an equal footing in (4.4). In order to see its benefit clearly, let us express  $\mathcal{F} = N + \frac{1}{2} + \delta_{\text{PT}}$  and expand  $\tilde{\Pi}_{B_{1,2}}$  and  $\Pi_{B_1}$  in  $\delta_{\text{PT}} \ll 1$ . The corresponding

---

<sup>5</sup>More precisely,  $\Pi_{B_1}(\mathcal{F}, \hbar)$  and  $\Pi_{B_2}(\mathcal{F}, \hbar)$  are considered as series expansions in  $\hbar \ll 1$  and their exponentially suppressed characters gradually disappear while approaching to barrier top region as they begin to be order  $O(\hbar^0)$  rather than  $O(e^{-1/\hbar})$ . This means that the (multi-)bounce or (multi-)bion configurations are no more suppressed, indicating more and more terms should be taken into account for good approximations as one approaches to the barrier top region. This continuous quantitative change, however, does not play an important role in our general discussion except when we discuss the barrier-top region in the PT-symmetric case in Section 5.1. Therefore, we keep treating  $\Pi_{B_{1,2}}$  as exponentially suppressed, unless it is stated otherwise.

series-expansions are

$$\tilde{\Pi}_{B_1} = \pm i(-1)^N \mathcal{K}_1 \sum_{k=0}^{\infty} H_k^{(1)} \delta_{\text{PT}}^k, \quad (4.7)$$

$$\tilde{\Pi}_{B_2} = \pm i(-1)^N \mathcal{K}_2 \sum_{k=0}^{\infty} H_k^{(2)} \delta_{\text{PT}}^k, \quad (4.8)$$

$$\Pi_{B_1} = 4\pi \mathcal{K}_1 \sum_{k=0}^{\infty} P_k^{(1)} \delta_{\text{PT}}^k, \quad (4.9)$$

where

$$\mathcal{K}_1 = \frac{e^{-\frac{S_1}{\hbar}}}{2\sqrt{2\pi} N!} \left(\frac{\mathcal{C}}{\hbar}\right)^{N+\frac{1}{2}}, \quad \mathcal{K}_2 = \frac{e^{-\frac{S_2}{2\hbar}}}{\sqrt{2\pi} N!} \left(\frac{\mathcal{C}}{\hbar}\right)^{N+\frac{1}{2}}, \quad (4.10)$$

and the constants  $S_{1,2}$  and  $\mathcal{C}$  are written in (3.4), (3.6) and (3.5). Note that we also recover the leading order approximation of bounce and half-bion (i.e., instanton or anti-instanton) events in (3.3) and (3.7) with  $\mathcal{K}_{1,2}$  being fugacities in respective dilute gas systems.

Another important addition to the original definitions of  $\Pi_{B_{1,2}}$  in (2.19) is the phase  $e^{\pm i\pi\mathcal{F}} = \pm i(-1)^N e^{\pm i\pi\delta_{\text{PT}}}$ . The expansion of the non-perturbative phase  $e^{\pm i\pi\delta_{\text{PT}}}$  in  $\delta_{\text{PT}} \ll 1$  produces imaginary contributions at each term  $O(\delta_{\text{PT}}^k)$  for  $k \geq 1$ , indicating that  $H_k^{(1,2)}$  have imaginary parts in addition to the real ones, i.e.,  $P_k^{(1,2)}$ , except  $H_0^{(1,2)}$ . To see the explicit connection to the original real expansion of  $\Pi_{B_{1,2}}$ , let us consider the series expansion

$$e^{\pm i\pi\delta_{\text{PT}}} = \sum_{n=0}^{\infty} \frac{(\pm i\pi)^n}{n!} \delta_{\text{PT}}^n$$

separately and express each term in (4.7) and (4.8) as

$$H_k^{(1,2)} = \sum_{n=0}^k \frac{(\pm i\pi)^n}{n!} P_{k-n}^{(1,2)}. \quad (4.11)$$

Later, this relation helps us to identify the ambiguous and non-ambiguous non-perturbative corrections to the spectrum.

With the rearrangements that we discussed above, the link to the semi-classical quantization in the path-integral formalism becomes manifest. More importantly, using (4.7)-(4.9), we can now understand the competition between the  $B_1$ - and  $B_2$ -cycles in terms of  $\mathcal{K}_1$  and  $\mathcal{K}_2$ , rather than the formal and intricate quantities  $\Pi_{B_1}$  and  $\Pi_{B_2}$ . This is possible, since the fugacities  $\mathcal{K}_1$  and  $\mathcal{K}_2$  are same order to each other and also to the leading-order non-perturbative correction  $\delta_{\text{PT}}$ . Then, the series in (4.7)-(4.9) are suppressed with respect to  $\mathcal{K}_1$  and  $\mathcal{K}_2$ , and the competition between bion and bounce is now reduced to a simple quantitative relationship between  $\mathcal{K}_1$  and  $\mathcal{K}_2$ .

We can now expand (4.4) in  $\delta_{\text{PT}} \ll 1$ . For example, the second-order expression reads

$$\begin{aligned}
& -\tilde{\Pi}_{B_1} - \varepsilon \left[ \tilde{\Pi}_{B_1}^2 - \tilde{\Pi}_{B_2}^2 (1 + \Pi_{B_1}) \right]^{1/2} \\
&= -\mathcal{K}_1 H_0^{(1)} - \varepsilon \sqrt{\mathcal{K}_1^2 \left( H_0^{(1)} \right)^2 - \mathcal{K}_2^2 \left( H_0^{(2)} \right)^2 - 4\pi \mathcal{K}_1 \mathcal{K}_2^2 P_0^{(1)} \left( H_0^{(2)} \right)^2} \\
& - \delta_{\text{PT}} \left( \mathcal{K}_1 H_1^{(1)} + \varepsilon \frac{\mathcal{K}_1^2 H_0^{(1)} H_1^{(1)} - \mathcal{K}_2^2 H_0^{(2)} H_1^{(2)} - 4\pi \mathcal{K}_1 \mathcal{K}_2^2 \left( H_0^{(2)} H_1^{(2)} P_0^{(1)} + \frac{1}{2} P_1^{(1)} \left( H_0^{(2)} \right)^2 \right)}{\sqrt{\mathcal{K}_1^2 \left( H_0^{(1)} \right)^2 - \mathcal{K}_2^2 \left( H_0^{(2)} \right)^2 - 4\pi \mathcal{K}_1 \mathcal{K}_2^2 P_0^{(1)} \left( H_0^{(2)} \right)^2}} \right). \tag{4.12}
\end{aligned}$$

Note that the square-root factors are independent of  $\delta_{\text{PT}}$ . Therefore, it is finally safe to choose a dominant non-perturbative saddle and expand the square-root terms for  $\mathcal{K}_1 \ll \mathcal{K}_2$  or  $\mathcal{K}_2 \ll \mathcal{K}_1$ .

On the left-hand side of (4.4), the expansion of the  $\Gamma$  functions leads to another expansion in  $\delta_{\text{PT}}$ :

$$-\frac{1}{\pi} \cos(\pi \mathcal{F}) = \frac{(-1)^N}{\pi} \sin(\pi \delta_{\text{PT}}) = (-1)^N \sum_{k=1}^{\infty} b_k \delta_{\text{PT}}^k, \tag{4.13}$$

where  $b_1 = 1$ ,  $b_2 = 0$ , and so on. Then, finally, solving the QC (4.4) order by order in  $\delta_{\text{PT}}$ , we can obtain the trans-series solutions to the non-perturbative corrections in the asymptotic limits up to  $O(\mathcal{K}_1^2)$  and  $O(\mathcal{K}_2^2)$ :

•  $\mathcal{K}_1 \ll \mathcal{K}_2$ : We first consider the case when the half-bion is the dominant configuration. In this limit, we found the solution to (4.4) as

$$\begin{aligned}
\delta_{\text{PT}}^{\text{UBr}} &\simeq -\varepsilon \mathcal{K}_2 H_0^{(2)} + \varepsilon \frac{\mathcal{K}_1^2 \left( H_0^{(1)} \right)^2}{2\mathcal{K}_2 H_0^{(2)}} \mp i\mathcal{K}_1 H_0^{(1)} + \mathcal{K}_2^2 H_0^{(2)} H_1^{(2)} \\
& - 2\mathcal{K}_1^2 H_0^{(1)} H_1^{(1)} + \varepsilon \mathcal{K}_1 \mathcal{K}_2 \left( \pm i H_1^{(1)} H_0^{(2)} \pm i H_0^{(1)} H_1^{(2)} - 2\pi P_0^{(1)} H_0^{(2)} \right), \tag{4.14}
\end{aligned}$$

where we kept  $H_k^{(1,2)}$  to show they are originating from  $\tilde{\Pi}_{B_{1,2}}$  in (4.4). In this sense, we observe that the action  $\Pi_{B_1}$  in (4.4) contributes only to the last term of  $O(\mathcal{K}_1 \mathcal{K}_2)$  in (4.14). We will elaborate its role shortly.

If we use (4.11) to reveal the ambiguous parts in (4.14), it becomes

$$\begin{aligned}
\delta_{\text{PT}}^{\text{UBr}} &\simeq -\varepsilon \mathcal{K}_2 P_0^{(2)} + \varepsilon \frac{\mathcal{K}_1^2 \left( P_0^{(1)} \right)^2}{\mathcal{K}_2 2P_0^{(2)}} \mp i\mathcal{K}_1 P_0^{(1)} + \mathcal{K}_2^2 \left( P_0^{(2)} P_1^{(2)} \mp i\pi \left( P_0^{(2)} \right)^2 \right) \\
& - 2\mathcal{K}_1^2 \left( P_0^{(1)} P_1^{(1)} \mp i\pi \left( P_0^{(1)} \right)^2 \right) \pm \varepsilon i\mathcal{K}_1 \mathcal{K}_2 \left( P_0^{(1)} P_1^{(2)} + P_1^{(1)} P_0^{(2)} \right). \tag{4.15}
\end{aligned}$$

Then, we observe that the leading order contribution is a single instanton effect, i.e.,  $[\mathcal{I}]$  or  $[\overline{\mathcal{I}}]$ . As expected, it leads to the level splitting of the perturbatively degenerate states and is in accordance with the standard picture in Hermitian quantum theories.

The one-instanton effect is accompanied by  $O(\mathcal{K}_1^2\mathcal{K}_2^{-1})$  term, which also comes with  $\varepsilon = \pm 1$  factor but with the opposite sign. Then, we express the first non-perturbative corrections in the trans-series as

$$\text{LO : } [\mathcal{I}] + [\mathcal{B}^2\mathcal{I}^{-1}] = [\overline{\mathcal{I}}] + [\mathcal{B}^2\overline{\mathcal{I}}^{-1}] = \varepsilon \left( -\mathcal{K}_2 H_0^{(2)} + \frac{\mathcal{K}_1^2 (H_0^{(1)})^2}{2\mathcal{K}_2 H_0^{(2)}} \right). \quad (4.16)$$

Note that since we assumed  $\mathcal{K}_1 \ll \mathcal{K}_2$ , the effect of  $[\mathcal{I}]$  (or  $[\overline{\mathcal{I}}]$ ) is never canceled by  $[\mathcal{B}^2\mathcal{I}^{-1}]$  (or  $[\mathcal{B}^2\overline{\mathcal{I}}^{-1}]$ ). In fact, the dominance between these two terms interchanges when  $\Pi_{B_1}^2 > \Pi_{B_2}$ , which, as we will see shortly, leads to a different expansion due to the square-root term in (4.1).

We also note that the term  $[\mathcal{B}^2\mathcal{I}^{-1}]$  corresponds to a new type of combination between the bounce and half-bion configurations. As far as we are aware, there is no previous discussion on the origin of such contributions in the literature. In our setting, it stems from the discriminant in (4.1), which itself is linked to the quadratic nature of the QCs  $T_{1,2}^{(\pm)} = 0$  in Table 1.

The first ambiguous imaginary contribution in (4.15) arises at orders  $O(\mathcal{K}_2^2)$  and  $O(\mathcal{K}_1)$  as

$$\text{Im}[\mathcal{B}]_{\pm} + \text{Im}[\mathcal{I}\overline{\mathcal{I}}]_{\pm} = \mp \left( \mathcal{K}_1 P_0^{(1)} + \pi\mathcal{K}_2^2 \left( P_0^{(2)} \right)^2 \right) \quad (4.17)$$

$$\simeq \mp \frac{e^{-\frac{S_1}{\hbar}}}{2\sqrt{2\pi} N!} \left( \frac{\mathcal{C}}{\hbar} \right)^{N+\frac{1}{2}} \mp \frac{e^{-\frac{S_2}{\hbar}}}{2(N!)^2} \left( \frac{\mathcal{C}}{\hbar} \right)^{2N+1} + O(\hbar), \quad (4.18)$$

where we used the fact that  $P_0^{(l=1,2)} = 1 + O(\hbar)$  to write the final expression. Note that (4.17) is the sum of the exact contributions from one-bounce and one-bion events. Hence, we used the shorthand representation with the equality sign. The expression in (4.18), on the other hand, recovers the leading-order imaginary contributions from one-bounce and one-bion events, which we discussed in Section 3.2 [see (3.3) and (3.8)]. As we verified numerically,  $[\mathcal{B}]_{\pm} + \text{Im}[\mathcal{I}\overline{\mathcal{I}}]_{\pm}$  is canceled against the Borel ambiguity of the perturbative sector. This shows the PT-symmetry is unbroken in  $\mathcal{K}_1 \ll \mathcal{K}_2$  region at least at the leading order.

The remaining terms in (4.15) are higher-order non-perturbative corrections. Unfortunately, the quantitative analysis showing the reality of the spectrum is quite cumbersome; therefore, it will not be pursued here. Of course, even with the best possible numerical approach never proves the reality of the spectrum rigorously. This exactness problem will be addressed in Section 5, when we consider the median QC in view of the Alien calculus, which will also help us to uncover the resurgence structure more precisely.

Despite the lack of quantitative information, let us finally comment on the roles of remaining terms in (4.15). The real parts are simply the higher-order corrections contributing to the spectrum directly. They are all products of two successive events; namely, they are two-bounce and one-bion (i.e., one instanton plus one anti-instanton) events and

appear in the next-to-leading (NLO) order non-perturbative corrections to the spectrum. Schematically, their contribution can be represented as

$$\text{NLO : } \quad \text{Re} [\mathcal{B}^2] + \text{Re} [\mathcal{I}\overline{\mathcal{I}}] . \quad (4.19)$$

The imaginary ambiguous terms, on the other hand, are associated with a two-bounce event and the successive events of one-bounce and a half bion, i.e.,

$$\text{Im} [\mathcal{B}^2]_{\pm} + [\mathcal{B}\mathcal{I}]_{\pm} \quad \text{or} \quad \text{Im} [\mathcal{B}^2]_{\pm} + [\mathcal{B}\overline{\mathcal{I}}]_{\pm} . \quad (4.20)$$

The contribution from  $[\mathcal{B}\mathcal{I}]_{\pm} \sim [\mathcal{B}\overline{\mathcal{I}}]_{\pm} \sim i\varepsilon\mathcal{K}_1\mathcal{K}_2$  should be linked to a Borel ambiguity of a divergent series. We anticipate this series to be the fluctuations around  $[\mathcal{I}] \sim [\overline{\mathcal{I}}]$ , which govern the leading-order non-perturbative splitting. However, it is possible that there exist higher-order terms participating in the resurgence cancellations in a similar way that we observed for the cancellation between the perturbative sector and  $[\mathcal{B}]_{\pm}$  and  $[\mathcal{I}\overline{\mathcal{I}}]_{\pm}$  events. We do not examine this cancellation qualitatively here but, instead, verify the removal of  $[\mathcal{B}\mathcal{I}]$  (and  $[\mathcal{B}\overline{\mathcal{I}}]$ ) from the median-summed series in Section 5.

After all these cancellations, the median-summed non-perturbative contributions to the spectrum become

$$\mathcal{S}_0 [\delta_{\text{PT}}^{\text{UBr}}] \simeq \varepsilon \left( -\mathcal{K}_2 \mathcal{S}_0 [P_0^{(1)}] + \frac{\mathcal{K}_1^2}{\mathcal{K}_2} \mathcal{S}_0 [\mathcal{P}_{\mathcal{B}^2\mathcal{I}}] \right) + \mathcal{K}_2^2 \mathcal{S}_0 [P_0^{(2)} P_1^{(2)}] - 2\mathcal{K}_1^2 \mathcal{S}_0 [P_0^{(1)} P_1^{(1)}] , \quad (4.21)$$

where we introduced  $\mathcal{P}_{\mathcal{B}^2\mathcal{I}-1} = \frac{(P_0^{(1)})^2}{2P_0^{(2)}}$  as a shorthand notation and  $\mathcal{S}_0$  refers to the median summation at  $\theta_h = 0$ . This is a real and unambiguous expression and confirms that the  $\mathcal{K}_1 \ll \mathcal{K}_2$  limit falls into the unbroken PT-symmetric phase. In Section 5, we will verify this result using Alien calculus as a limit of the exact solution, which is valid across all parameter regimes.

**Remark:** Recalling the discussion in Section 2.2 and the definition in (2.29), we remind ourselves that the median summation corresponds  $\mathcal{S}_0 = \mathcal{S}_{0\pm} \circ \mathfrak{S}_h^{\mp 1/2}$ . However, during the resurgence cancellation procedure, as we explained above, we did not consider the Stokes automorphism in a direct way. Then, in this sense, this procedure is an equivalent but more practically accessible way to consider the removal of the Stokes automorphism and subsequent Borel summations, leading to the median summation  $\mathcal{S}_0 [\delta_{\text{PT}}^{\text{UBr}}]$ .

Finally, let us comment on the other ambiguous term, which is a two-bounce effect, i.e.,  $[\mathcal{B}^2]$ . This contribution is not directly related to the cancellation of a real divergent series at a lesser non-perturbative order. Instead, it turns out that  $[\mathcal{B}^2]$  is related to a part of the entire trans-series, which is linked to the original perturbative expansion. This part is also called as *minimal* trans-series in the literature [131]. In (4.15), it reads as

$$\delta_{\text{NP}}^{\text{minimal}} \simeq \mp i \left( \mathcal{K}_1 P_0^{(1)} + \pi \mathcal{K}_2^2 \left( P_0^{(2)} \right)^2 - 2\pi \mathcal{K}_1^2 \left( P_0^{(1)} \right)^2 \right) \quad (4.22)$$

For our discussion, it is important that the minimal series appears across all parameter regimes of the PT-symmetric and (anti-)resonance systems in *exactly* the same form. We will prove its link to the original perturbative sector in Section 5.1.3.

- $\mathcal{K}_2 \ll \mathcal{K}_1$ : Now, let us consider the limit when the bounce configuration is the dominant one. Again, first keeping the imaginary contributions of  $e^{\pm i\pi\mathcal{F}}$  hidden, we find the non-perturbative corrections as

$$\begin{aligned} \delta_{\text{PT}}^{\text{Br}} &\simeq \mp i(1 + \varepsilon)\mathcal{K}_1 H_0^{(1)} \pm i\varepsilon \frac{\mathcal{K}_2^2 \left(H_0^{(2)}\right)^2}{2\mathcal{K}_1 H_0^{(1)}} - 2(1 + \varepsilon)\mathcal{K}_1^2 H_0^{(1)} H_1^{(1)} \\ &\quad + \mathcal{K}_2^2 \left( (1 + \varepsilon)H_0^{(2)} H_1^{(2)} \pm \frac{2i\pi\varepsilon \left(H_0^{(2)}\right)^2 P_0^{(1)}}{H_0^{(1)}} \right). \end{aligned} \quad (4.23)$$

Then, separating the imaginary factors using (4.11), we got

$$\begin{aligned} \delta_{\text{PT}}^{\text{Br}} &\simeq \mp i(1 + \varepsilon)\mathcal{K}_1 P_0^{(1)} \pm i\varepsilon \frac{\mathcal{K}_2^2 \left(P_0^{(2)}\right)^2}{2\mathcal{K}_1 P_0^{(1)}} - 2(1 + \varepsilon)\mathcal{K}_1^2 \left( P_0^{(1)} P_1^{(1)} \pm i\pi P_0^{(1)} P_0^{(1)} \right) \\ &\quad + \mathcal{K}_2^2 \left( (1 + \varepsilon)P_0^{(2)} P_1^{(2)} \mp i\pi(1 - \varepsilon) \left(P_0^{(2)}\right)^2 \right) \end{aligned} \quad (4.24)$$

Contrary to the previous case, there is no real term to split the perturbative degeneracy. In fact, the events  $[\mathcal{I}]$  and  $[\mathcal{B}^2\mathcal{I}^{-1}]$  disappear from the trans-series completely. Instead, we observe that there is a new type of event, i.e.  $[\mathcal{I}\bar{\mathcal{I}}\mathcal{B}^{-1}]_{\pm} \sim \pm i\frac{\mathcal{K}_2^2}{\mathcal{K}_1}$ . Again, we note that to our knowledge, such combinations between non-perturbative saddles have not been observed in Hermitian settings.

The remaining parts are similar to the bion and bounce combinations from the previous case, but they arise with different pre-factors, which have crucial impacts on the physical properties of the quantized system. Let us investigate their structure in more details:

We first observe that the imaginary contributions of one-bounce and one-bion configurations appear as:

$$\begin{aligned} &\text{Im} \left( (1 + \varepsilon)[\mathcal{B}]_{\pm} + (1 - \varepsilon)[\mathcal{I}\bar{\mathcal{I}}]_{\pm} \right) \\ &\simeq \mp \left( (1 + \varepsilon)\mathcal{K}_1 P_0^{(1)} + \pi(1 - \varepsilon)\mathcal{K}_2^2 \left(P_0^{(2)}\right)^2 \right) \\ &= \mp \left( \mathcal{K}_1 P_0^{(1)} + \pi\mathcal{K}_2^2 \left(P_0^{(2)}\right)^2 \right) \mp \varepsilon \left( \mathcal{K}_1 P_0^{(1)} - \pi\mathcal{K}_2^2 \left(P_0^{(2)}\right)^2 \right). \end{aligned} \quad (4.25)$$

The first part of (4.25) is in the same form as (4.17). Since the perturbative expansion does not change its behavior in the parameter region corresponding to  $\mathcal{K}_2 \ll \mathcal{K}_1$ , this part links to the Borel ambiguity that participates in the resurgence cancellation, which we verified numerically in Fig. 10.

The existence of the latter part in (4.25), on the other hand, has a very significant physical consequence. Since there is no other imaginary ambiguous contribution to the trans-series at the orders  $\mathcal{K}_1$  and  $\mathcal{K}_2^2$ , it remains in the Borel-summed series and contributes to the spectrum. As a result, the eigenvalues of the system become complex. This means that the PT-symmetry is *broken* non-perturbatively.

A very important feature of the surviving part in (4.25) is that it comes with the factor  $\varepsilon = \pm 1$ , which induces the splitting of the perturbatively degenerate states. Contrary to the unbroken phase, the splitting is an imaginary one, as it was predicted by the numerical solutions. This is in accordance with the PT-symmetry breaking examples in the literature, which we also find via numerical methods and showed in Fig. 8. As we explained above, the splitting in (4.16) has a clear link to the bion and bounce configurations through the exact QC (4.1), making our approach a first successful example for an analytic explanation.

Finally, we also emphasize that the imaginary parts of both bion and bounce are originally ambiguous terms. However, since it is combined with the splitting factor  $\varepsilon$ , the total contribution has no ambiguity. More specifically, we remind ourselves that in (4.16), assigning  $\varepsilon = +1$  or  $\varepsilon = -1$  to the states originally localized around one of the wells is an arbitrary decision. This random choice has no effect on the physical properties of the quantum system. Then, the apparent ambiguity for  $\pm\varepsilon$  terms in (4.25) is compensated by this randomness, leading to an unambiguous result after the Borel summations.

The numerical solutions in Fig. 8 indicate that the other imaginary contributions to the Borel-summed spectrum are also accompanied with the  $\varepsilon = \pm 1$  factor, while the real contributions should have the same sign for both perturbative states. Therefore, the terms in (4.24) which do not fall into these categories should not contribute to the physical spectrum. In our discussion, the only way for this is the resurgence cancellations.

In light of these facts, the real parts of two-bounce and one-bion contributions should play a role in the resurgence cancellations. More specifically, we split their contributions as

$$\begin{aligned} \text{Re} \left( (1 + \varepsilon) [\overline{\mathcal{I}\mathcal{I}}]_{\pm} + (1 + \varepsilon) [\mathcal{B}^2]_{\pm} \right) &= -2\mathcal{K}_1^2 P_0^{(1)} P_1^{(1)} + \mathcal{K}_2^2 P_0^{(2)} P_1^{(2)} \\ &+ \varepsilon \left( -2\mathcal{K}_1^2 P_0^{(1)} P_1^{(1)} + \mathcal{K}_2^2 P_0^{(2)} P_1^{(2)} \right), \end{aligned} \quad (4.26)$$

where the expression in the second line should cancel out. Comparing with the lower-order terms, we infer that the perturbative side of these cancellations is the fluctuations of  $\varepsilon[\mathcal{B}]_{\pm}$  and  $\varepsilon[\overline{\mathcal{I}\mathcal{I}\mathcal{B}^{-1}}]_{\pm}$  events:

$$\text{Re} \left( \mp i\varepsilon \mathcal{K}_1 \mathcal{S}_{\pm} \left[ P_0^{(1)} \right] \right) \longleftrightarrow \text{Re} \left( \varepsilon [\mathcal{B}^2]_{\pm} \right), \quad (4.27)$$

$$\text{Re} \left( \pm i\varepsilon \frac{\mathcal{K}_2^2}{2\mathcal{K}_1} \mathcal{S}_{\pm} \left[ \mathcal{P}_{\overline{\mathcal{I}\mathcal{I}\mathcal{B}^{-1}}} \right] \right) \longleftrightarrow \text{Re} \left( \varepsilon [\overline{\mathcal{I}\mathcal{I}}]_{\pm} \right), \quad (4.28)$$

where we introduced  $\mathcal{P}_{\overline{\mathcal{I}\mathcal{I}\mathcal{B}^{-1}}} = \frac{(P_0^{(2)})^2}{P_0^{(1)}}$  to simplify the notation. However, as before, it is possible that more than one non-perturbative sector is involved in the cancellations, but numerical computations are too cumbersome to pursue here.

Note that although there is a lack of numerical capability to demonstrate, the roles of  $\text{Re}(\varepsilon[\mathcal{B}^2]_{\pm})$  and  $\text{Re}(\varepsilon[\mathcal{I}\bar{\mathcal{I}}])$  are quite unconventional and deserve further discussion. We first remark that (4.26) is free from ambiguities and such terms normally do not play a role in the cancellations of ambiguous Borel summations, when the re-summed spectrum is real.

However, we recall that the series expansions in (4.27) and (4.28) have a double sign in front of the  $\varepsilon$  factor. Originally, this double-valuedness stems from the analytic continuations  $\text{Im } \hbar > 0$  and  $\text{Im } \hbar < 0$ . Note that the  $\text{Im } \hbar = 0^{\pm}$  limits [upper/lower signs in (4.27) and (4.28)] are linked to  $\mathcal{S}_{\pm}$  Borel summations, respectively. Then, combining these fixed signs for each analytic continuation and respective Borel summations leads to a real and single-valued expression as

$$\mp i\mathcal{S}_{\pm} \left[ P_0^{(1)} \right] \sim (\mp i) (\pm i) (1 + O(\hbar)) = (+1) (1 + O(\hbar)) , \quad (4.29)$$

$$\pm i\mathcal{S}_{\pm} [\mathcal{P}_{\mathcal{I}\bar{\mathcal{I}}B^{-1}}] \sim (\pm i)(\pm i) (1 + \dots) = (-1)(1 + \dots) , \quad (4.30)$$

where we utilized  $P_0^{(l=1,2)} = 1 + O(\hbar)$ . Then, their non-perturbative counterparts are expected to be real and single-valued as in (4.26).

The remaining term in (4.24) is the ambiguous imaginary contribution at  $O(\mathcal{K}_1^2)$ . As in the unbroken phase, it is a part of the minimal trans-series, which remains in the form of (4.22) as we expected, and plays a role in the cancellation of the Borel ambiguity emanating from the perturbation series  $\mathcal{S}_{\pm}[E_P]$ .

As a conclusion of this discussion, let us present the Borel-summed non-perturbative corrections in the broken phase together:

$$\begin{aligned} \mathcal{S}_0[\delta_{\text{PT}}^{\text{Br}}] \simeq & -i\varepsilon \left( \mathcal{K}_1 \mathcal{S}_0 \left[ P_0^{(1)} \right] - \frac{\mathcal{K}_2^2}{\mathcal{K}_1} \mathcal{S}_0 \left[ \mathcal{P}_{\mathcal{I}\bar{\mathcal{I}}B^{-1}} \right] + 2\pi\mathcal{K}_1^2 \mathcal{S}_0 \left[ \left( P_0^{(1)} \right)^2 \right] + \pi\mathcal{K}_2^2 \left( P_0^{(2)} \right)^2 \right) \\ & - 2\mathcal{K}_1^2 \mathcal{S}_0 \left[ P_0^{(1)} P_1^{(1)} \right] + \mathcal{K}_2^2 \mathcal{S}_0 \left[ P_0^{(2)} P_1^{(2)} \right] . \end{aligned} \quad (4.31)$$

Although we cannot verify the resurgence cancellations numerically beyond the leading order, in Section 5, we will show (4.15) is indeed the non-perturbative contribution to the spectrum in  $\mathcal{K}_2 \ll \mathcal{K}_1$  limit, which falls into the broken PT-symmetric phase.

## 4.2 Resonance and anti-resonance cases

We now turn our attention to the resonance and anti-resonance cases. As we discussed above in Section 3.3, their exact QCs, and hence their dynamics, are related to each other by time reversal. Both cases induce complex spectra, implying their non-equilibrium nature under the interaction with the surrounding environment. In the following, we will uncover the corresponding trans-series structures on an equal footing with the PT-symmetric one in Section 4.1.

### 4.2.1 Resonance solutions

Let us start with the resonance case. Its exact QCs for  $\text{Im } \hbar = 0^{\pm}$  are given in terms of  $T_{2,2}^{(\pm)}$  elements of the transition matrices, and they are presented in Table 1.



For the  $\text{Im } \hbar < 0$  deformation, it is straightforward to bring  $T_{2,2}^{(-)} = 0$  in the following form:

$$e^{+i\pi\mathcal{F}} 2 \cos(\pi\mathcal{F}) = i\varepsilon\sqrt{\Pi_{B_2}}, \quad (4.32)$$

or equivalently,

$$\frac{1}{\pi} \sin\left(\pi\delta_{\text{R}}^{(-)}\right) = \sum_{k=0}^{\infty} b_k \left(\delta_{\text{R}}^{(-)}\right)^k = \varepsilon\mathcal{K}_2 \sum_{k=0}^{\infty} H_k^{(2)} \left(\delta_{\text{R}}^{(-)}\right)^k, \quad (4.33)$$

where we set  $\mathcal{F} = \frac{1}{2} + N + \delta_{\text{R}}^{(-)}$  and used the definition of  $\mathcal{K}_2$  in (4.10).

For  $\text{Im } \hbar > 0$ ,  $T_{2,2}^{(+)} = 0$  is also a quadratic equation, and we find its formal solution for  $(1 + \Pi_A)$  as

$$e^{-i\pi\mathcal{F}} 2 \cos(\pi\mathcal{F}) = -\Pi_{B_1} - i\varepsilon\sqrt{\Pi_{B_2}}(1 + \Pi_{B_1}). \quad (4.34)$$

Then, setting  $\mathcal{F} = \frac{1}{2} + N + \delta_{\text{R}}^{(+)}$  and using the definitions in (4.10) and (4.7)-(4.9), we obtain

$$\sum_{k=0}^{\infty} b_k \delta_{\text{R}}^{(+)} = -2i\mathcal{K}_1 \sum_{k=0}^{\infty} H_k^{(1)} \delta_{\text{R}}^{(+)} - \varepsilon\mathcal{K}_2 \left( \sum_{k=0}^{\infty} H_k^{(2)} \delta_{\text{R}}^{(+)} \right) \left[ 1 + 2\pi\mathcal{K}_1 \sum_{k=0}^{\infty} P_k^{(1)} \delta_{\text{R}}^{(+)} \right]. \quad (4.35)$$

Note that, as in the PT-symmetric case [see e.g., (4.4)], the last  $\Pi_{B_1}$  on the right-hand side of (4.34) is not affected by the  $\frac{1}{2\pi}$  re-scaling and  $e^{-i\pi\mathcal{F}}$ . Thus, its fluctuation terms are real, and we introduced  $2\pi$  factor by hand in the last term in (4.35).

Both (4.33) and (4.35) can be solved order by order in a similar manner as the PT-symmetric system. In the current case, since the square-root terms in (4.32) and (4.34) contain only the  $\Pi_{B_2}$  action, the order of expansion does not matter. Then, we continued in a straightforward manner and up to orders  $O(\mathcal{K}_1^2)$  and  $O(\mathcal{K}_2^2)$ , we find the non-perturbative corrections of the resonance case for  $\text{Im } \hbar > 0$  and  $\text{Im } \hbar < 0$  as

$$\begin{aligned} \delta_{\text{R}}^{(+)} = & -\varepsilon\mathcal{K}_2 H_0^{(2)} + \mathcal{K}_2^2 H_0^{(2)} H_1^{(2)} - 2i\mathcal{K}_1 H_0^{(1)} - 4\mathcal{K}_1^2 H_0^{(1)} H_1^{(1)} \\ & + 2\varepsilon\mathcal{K}_1 \mathcal{K}_2 \left( iH_1^{(1)} H_0^{(2)} + iH_0^{(1)} H_1^{(2)} - 2\pi H_0^{(2)} P_0^{(1)} \right), \end{aligned} \quad (4.36)$$

and

$$\delta_{\text{R}}^{(-)} \simeq -\varepsilon\mathcal{K}_2 H_0^{(2)} + \mathcal{K}_2^2 H_0^{(2)} H_1^{(2)}, \quad (4.37)$$

respectively. Using (4.11), the complex parts can be uncovered explicitly as

$$\begin{aligned} \delta_{\text{R}}^{(+)} \simeq & -\varepsilon\mathcal{K}_2 P_0^{(2)} - 2i\mathcal{K}_1 P_0^{(1)} + \mathcal{K}_2^2 \left( P_0^{(2)} P_1^{(2)} - i\pi \left( P_0^{(2)} \right)^2 \right) \\ & - 4\mathcal{K}_1^2 \left( P_0^{(1)} P_1^{(1)} - i\pi \left( P_0^{(1)} \right)^2 \right) - 2i\varepsilon\mathcal{K}_1 \mathcal{K}_2 \left( P_0^{(1)} P_1^{(2)} + P_1^{(1)} P_0^{(2)} \right), \end{aligned} \quad (4.38)$$

and

$$\delta_{\text{R}}^{(-)} \simeq -\varepsilon\mathcal{K}_2 P_0^{(2)} + \mathcal{K}_2^2 \left( P_0^{(2)} P_1^{(2)} + i\pi \left( P_0^{(2)} \right)^2 \right). \quad (4.39)$$

Note that we highlighted some of the signs with red for future comparison with the anti-resonance trans-series; see (4.49).

Interestingly,  $\delta_{\text{R}}^{(+)}$  and  $\delta_{\text{R}}^{(-)}$  lead to quite different trans-series solutions. Let us now discuss how they lead to a consistent picture when the (median) Borel summations are taken into account:

- We first observe that for both cases, the one-instanton  $[\mathcal{I}]$  and one-bion  $[\mathcal{I}\bar{\mathcal{I}}]_{\pm}$  contributions are the same up to the imaginary ambiguity. They are on an equal footing with the unbroken PT-symmetric system in Section 4.1. Therefore, their roles are the same as well. The real part contributes to the leading-order non-perturbative spectra as

$$\text{LO : } \quad \varepsilon[\mathcal{I}] + \text{Re}([\mathcal{I}\bar{\mathcal{I}}]_{\pm}) , \quad (4.40)$$

where  $\varepsilon = \pm 1$  indicates the real splitting of the perturbatively degenerate energies.

- The ambiguous part arising from the one-bion event, i.e.,  $\text{Im}[\mathcal{I}\bar{\mathcal{I}}]_{\pm}$ , participates in the resurgence cancellations. Recall that it is a term in the minimal trans-series emanating from the perturbative sector [see (4.22)]. Then,  $\text{Im}[\mathcal{I}\bar{\mathcal{I}}]_{\pm}$  disappears after the Borel summations. However, the case of bounce contributions is quite different. In the trans-series for  $\delta_{\text{R}}^{(-)}$ , no contribution from any bounce event appears. For  $\delta_{\text{R}}^{(+)}$ , on the other hand,  $[\mathcal{B}]_{+}$  event contributes, but its coefficient does not match the term in (4.17). Therefore, while  $[\mathcal{B}]_{+}$  contribution in (4.39) fixes the ambiguity issue of the Borel summation  $\text{S}_{+}[E_{\text{P}}]$ , there is still an imaginary part left, which makes the spectrum complex

More precisely, we observe that at the leading order, the Borel-summed spectra in the  $\text{Im } \hbar = 0^{\pm}$  limits become

$$\text{Im}(\text{S}_{+}[E_{\text{P}}]) + \text{Im}[\mathcal{I}\bar{\mathcal{I}}]_{+} + 2[\mathcal{B}]_{+} = -i\mathcal{K}_1 P_0^{(1)} , \quad (4.41)$$

$$\text{Im}(\text{S}_{-}[E_{\text{P}}]) + \text{Im}[\mathcal{I}\bar{\mathcal{I}}]_{-} = -i\mathcal{K}_1 P_0^{(1)} , \quad (4.42)$$

which represent the leading-order imaginary parts of the spectra. A crucial feature of these results is that there is no ambiguity left, as both results are exactly the same, including their overall imaginary sign. Note that the minus imaginary sign is also fully consistent with the decaying feature of the resonant system.

**Remark:** In the literature, the results in (4.41) and (4.42) are known as a bounce contribution that leads to the decay of a metastable state. However, as we discussed thoroughly in the PT-symmetric case, its existence does not always lead to an instability. Similarly, for the  $\text{Im } \hbar = 0^{-}$  limit, we observe in (4.41) that the bounce configuration does not contribute at all and that the spectrum is complex. This is solely due to the Borel summation of the perturbative sector, whose imaginary part is canceled only partially. For  $\text{Im } \hbar = 0^{+}$ , on the other hand, as we stated above,  $[\mathcal{B}]_{+}$  event cancels  $\text{Im}(\text{S}_{+}[E_{\text{P}}])$ , while leaving an imaginary contribution behind, which is exactly the same as  $\text{Im}(\text{S}_{-}[E_{\text{P}}])$ .

This analysis shows that, although the resulting contributions in (4.41) and (4.42) are equivalent to the usual decay analysis based solely on the bounce contribution, the true

picture is quite different. We also emphasize that a bounce configuration is naturally multi-valued. In the literature, the imaginary sign is chosen so that the result is consistent with the decaying behavior. In our analysis, the resulting sign is fixed for any choice of analytic continuation, showing full consistency with the physical properties of the quantum system without any ad-hoc manipulation. A detailed comparison between the exact quantization procedure that we discussed in this paper and the standard decay analysis revolving around the bounce event would be very interesting for mathematical completeness. It might also be enlightening for the decay process beyond the standard semi-classical analysis, which includes non-linearities dominating early- and late-time behaviors.

- Let us finally discuss the higher-order non-perturbative contributions. In the unbroken PT-symmetric case, we indicated a resurgence relationship between  $[\mathcal{BT}]_{\pm}$  event, i.e.,  $O(\mathcal{K}_1\mathcal{K}_2)$  term, and the fluctuations of the instanton contributions, i.e.,  $S_{\pm} [P_0^{(2)}]$ . In the current case, for  $\delta_R^{(+)}$ , the coefficients of these two events in (4.39) do not agree, which indicates additional imaginary contributions to the spectrum. For  $\delta_R^{(-)}$ , on the other hand, the same contribution arises via the Borel summation of the expansion around the instanton, i.e.,  $S_- [P_0^{(2)}]$ . In both cases, the resulting imaginary part becomes

$$i\varepsilon \text{Im}[\mathcal{BT}]_{\pm} = i\varepsilon \mathcal{K}_1 \mathcal{K}_2 \left( P_0^{(1)} P_1^{(2)} + P_1^{(1)} P_0^{(2)} \right), \quad (4.43)$$

which has no sign ambiguity as it should be. We note that for the  $\text{Im} \hbar = 0^+$  case, the exact resurgence cancellation for  $S_+ [P_0^{(2)}]$  may need extra higher-order non-perturbative counterparts. However, this does not change the picture we presented here, as  $i\varepsilon \text{Im}[\mathcal{BT}]_{\pm}$  factor appears in the Borel-summed spectrum in any case.

- The final cancellations takes place via  $[\mathcal{B}^2]_+ \sim \mathcal{K}_1^2$  event in (4.38). One of them is between the bounce fluctuations  $\text{Re} \left( S_+ [P_0^{(1)}] \right)$  and  $\text{Re}[\mathcal{B}^2]_+$  contributions. More precisely, the resurgence relationship between these two terms in (4.39) is given by

$$\text{Re} \left( -2i\mathcal{K}_1 S_+ [P_0^{(1)}] \right) \longleftrightarrow \text{Re}[\mathcal{B}^2]_- = -2\mathcal{K}_1^2 P_0^{(1)} P_1^{(1)}, \quad (4.44)$$

which we infer from (4.27) and (4.29). Comparing with the  $O(\mathcal{K}_1^2)$  term in (4.39), it is clear that the cancellation is not exact, and, consequently, there is a real contribution to the spectrum at the order of one-bounce event as

$$\text{Re}[\mathcal{B}]_{\pm} = -2\mathcal{K}_1^2 P_0^{(1)} P_1^{(1)}. \quad (4.45)$$

Again, the resurgence relation in (4.44) may need higher-order non-perturbative terms, which we do not consider here. However, this does not affect the contribution in (4.45). Moreover, as in the broken PT-symmetric phase, the above cancellation is between real parts as the series  $P_0^{(1)}$  is associated with the remainder of the leading-order resurgence cancellation in (4.41) and equivalently (4.42).

The remaining imaginary part  $\text{Im}[\mathcal{B}^2]_+ = +4\pi i \left( P_0^{(1)} \right)^2$ , on the other hand, is linked to the minimal trans-series, and it plays a role in the cancellation of  $\text{Im}S_+ [E_P]$ . However,

comparing with (4.22), we observe that the prefactor  $4\pi i$  is not in complete agreement and that it leads to an imaginary contribution to the spectrum as well.

As a result, we obtain the resulting median-summed non-perturbative contributions,

$$\begin{aligned} \mathcal{S}_0 \left[ \delta_{\text{R}}^{(\pm)} \right] &\simeq -\varepsilon \mathcal{K}_2 \mathcal{S}_0 \left[ P_0^{(2)} \right] + \mathcal{K}_2^2 \mathcal{S}_0 \left[ P_0^{(2)} P_1^{(2)} \right] - i \mathcal{K}_1 \mathcal{S}_0 \left[ P_0^{(1)} \right] \\ &\quad + 2\mathcal{K}_1^2 \mathcal{S}_0 \left[ -P_0^{(1)} P_1^{(1)} + \pi i \left( P_0^{(1)} \right)^2 \right] - i\varepsilon \mathcal{K}_1 \mathcal{K}_2 \mathcal{S}_0 \left[ P_0^{(1)} P_1^{(2)} + P_1^{(1)} P_0^{(2)} \right]. \end{aligned} \quad (4.46)$$

Note that the last term introduces an imaginary splitting in addition to the real one, which is induced by the  $\varepsilon[\mathcal{I}]$  term. This means that for  $\varepsilon = +1$ , the corresponding imaginary contribution has a positive sign for every other state in the spectrum. However, this cannot change the overall imaginary sign of the spectrum, as  $-i\mathcal{K}_1$  term dominates and the quantum system has resonance properties for all states.

## 4.2.2 Anti-resonance solutions

As the anti-resonance case is the time-reversal of the resonance one, its physical properties can be inferred by a complex conjugation. In Section 3.3, we have already shown that the associated elements in the  $T^{(\pm)}$  matrices are linked via the complex conjugation operator and that its effect is expected to appear in the spectrum.

To see how the complex conjugation with the resonance case arises, let us examine the solutions of  $T_{1,1}^{(\pm)} = 0$  in Table 1:

$$e^{-i\pi\mathcal{F}} 2 \cos(\pi\mathcal{F}) = i\varepsilon \sqrt{\Pi_{B_2}}, \quad (4.47)$$

$$e^{+i\pi\mathcal{F}} 2 \cos(\pi\mathcal{F}) = -\Pi_{B_1} + i\varepsilon \sqrt{\Pi_{B_2}} (1 + \Pi_{B_1}), \quad (4.48)$$

respectively. The effect of the time-reversal appears in the exponential terms in (4.47) and (4.48) on the left-hand side of both equations, which are complex conjugates of their counterparts in (4.32) and (4.34), respectively. Note that the structures of the QCs for  $\text{Im } \hbar > 0$  and  $\text{Im } \hbar < 0$  are also exchanged. This mainly stems from (3.15) and indicates the Borel ambiguities of the perturbative expansions resulting from (4.47) and (4.48) have the opposite signs relative to those in (4.32) and (4.34). Then, these two signs change and balance to each other, leading to the same resurgence cancellations and the Borel-summed spectrum with the resonance system up to the imaginary sign.

To get the non-perturbative spectrum and the associated resurgence structure for the anti-resonance case independently, we define  $\mathcal{F} = N + \frac{1}{2} + \delta_{\text{AR}}^{(\pm)}$ . Then, by solving (4.47) and (4.48) in the same way as the resonance case, we obtain

$$\delta_{\text{AR}}^{(+)} \simeq \varepsilon \mathcal{K}_2 P_0^{(2)} + \mathcal{K}_2^2 \left( P_0^{(2)} P_1^{(2)} - i\pi \left( P_0^{(2)} \right)^2 \right), \quad (4.49)$$

$$\begin{aligned} \delta_{\text{AR}}^{(-)} &\simeq -\varepsilon \mathcal{K}_2 P_0^{(2)} + \mathcal{K}_2^2 \left( P_0^{(2)} P_1^{(2)} + i\pi \left( P_0^{(2)} \right)^2 \right) + 2i\mathcal{K}_1 P_0^{(1)} \\ &\quad - 4\mathcal{K}_1^2 \left( P_0^{(1)} P_1^{(1)} + i\pi \left( P_0^{(1)} \right)^2 \right) + 2i\varepsilon \mathcal{K}_1 \mathcal{K}_2 \left( P_0^{(1)} P_1^{(2)} + P_1^{(1)} P_0^{(2)} \right), \end{aligned} \quad (4.50)$$

where the red-colored signs are different from those for  $\delta_{\text{R}}^{(+)}$  in (4.38).

The resurgence cancellations take place in the same manner as the resonance case, up to these sign differences and the ones arising from the Borel summations. For example, at the leading order in  $\text{Im } \hbar > 0$ , combining the Borel-summed perturbative series and  $[\mathcal{I}\bar{\mathcal{I}}]_{\pm}$  events leads to

$$\text{Im}(\mathcal{S}_+ [E_{\text{P}}]) + \text{Im}([\mathcal{I}\bar{\mathcal{I}}]_+) = i\mathcal{K}_1 P_0^{(1)}. \quad (4.51)$$

For  $\text{Im } \hbar < 0$ , we have  $2[\mathcal{B}]_-$  contributing to the trans-series, which leads to

$$\text{Im}(\mathcal{S}_- [E_{\text{P}}]) + \text{Im}([\mathcal{I}\bar{\mathcal{I}}]_-) + [\mathcal{B}]_+ = i\mathcal{K}_1 P_0^{(1)}. \quad (4.52)$$

Both results are the same, indicating that there are no ambiguities, and the imaginary sign is fully consistent with the anti-resonance behavior of the quantum system.

In the same manner as the resonance case, we can deduce the remaining contributions, which we do not discuss here because the procedure is the same as the one for the resonance case. As a result, the median-summed non-perturbative part of the anti-resonance case becomes

$$\begin{aligned} \mathcal{S}_0 [\delta_{\text{AR}}^{(\pm)}] &\simeq -\varepsilon\mathcal{K}_2\mathcal{S}_0 [P_0^{(2)}] + \mathcal{K}_2^2\mathcal{S}_0 [P_0^{(2)}P_1^{(2)}] + i\mathcal{K}_1\mathcal{S}_0 [P_0^{(1)}] \\ &\quad - 2\mathcal{K}_1^2\mathcal{S}_0 [P_0^{(1)}P_1^{(1)} + \pi i (P_0^{(1)})^2] + i\varepsilon\mathcal{K}_1\mathcal{K}_2\mathcal{S}_0 [P_0^{(1)}P_1^{(2)} + P_1^{(1)}P_0^{(2)}]. \end{aligned} \quad (4.53)$$

**Remark:** As expected, the median summed trans-series solutions for resonance and anti-resonance cases are complex conjugate of each other:

$$\mathcal{S}_0 [\delta_{\text{R}}^{(\pm)}] = \mathcal{C}\mathcal{S}_0 [\delta_{\text{AR}}^{(\pm)}]. \quad (4.54)$$

The trans-series before the summation, on the other hand, are related via complex conjugation as

$$\mathcal{C}\delta_{\text{R}}^{(\pm)} = \delta_{\text{AR}}^{(\mp)}. \quad (4.55)$$

Since the Borel summation is single-valued, we also have

$$\mathfrak{S}_{\hbar}^{\pm 1}\delta_{\text{R}}^{(\pm)} = \delta_{\text{R}}^{(\mp)}, \quad \mathfrak{S}_{\hbar}^{\pm 1}\delta_{\text{AR}}^{(\pm)} = \delta_{\text{AR}}^{(\mp)}. \quad (4.56)$$

Then, we simply deduce that

$$\mathcal{C}\mathfrak{S}_{\hbar}\delta_{\text{R}}^{(\pm)} = \mathcal{C}\delta_{\text{R}}^{(\mp)} = \delta_{\text{AR}}^{(\pm)}. \quad (4.57)$$

This is equivalent to the relationship between the respective exact QCs in Table 1, which is

$$\mathcal{C}\tilde{\mathfrak{S}}T_{1,1}^{(\pm)} = \mathcal{C}T_{1,1}^{(\mp)} = T_{2,2}^{(\pm)}, \quad (4.58)$$

where  $\tilde{\mathfrak{S}}$  corresponds to the combined action of  $\mathfrak{S}_A$  and  $\Sigma$  in (3.21).

Finally, we note that in some cases, e.g., in unbroken PT-symmetric or other stable systems, the trans-series for  $\text{Im } \hbar > 0$  and  $\text{Im } \hbar < 0$  become complex conjugate to each other. This is not the case for (anti-)resonance systems, which is obvious from (4.55). Instead, the correct relationship between the two sides of the analytic continuation is given by the Stokes automorphism as in (4.56), which appears to be equivalent to  $\mathcal{C}$  if the system is stable. The last point is, in fact, an indication of the resurgence cancellations, which leads to real spectrum in such cases.

**Remark:** The fractional combinations of  $\mathcal{K}_1$  and  $\mathcal{K}_2$  in (4.14) and (4.23), on the other hand, do not exist in the resonance or anti-resonance spectrum. This indicates that such effects are closely related to the PT-symmetric boundary conditions, which may probably be understood better if complex boundary conditions are used.

## 5 Exact solutions from median quantization conditions

In this section, we focus on the median QCs for the PT-symmetric, resonance, and anti-resonance systems. This allows us to work directly on the ray that the Stokes discontinuities (for both  $A$ -cycle and  $\hbar$ -plane) lie, which is our main interest as the physical quantities are associated with them. At the level of the QCs, this is achieved by an action of half-Stokes automorphism on the QCs, which we obtained via Airy-type EWKB analysis.

Formally, these Stokes automorphisms are represented by

$$D_{i,j}^{\text{med}} = \mathfrak{S}_A^{\pm 1/2} T_{i,j}^{(\pm)}, \quad (5.1)$$

which are the QCs that the Stokes discontinuities are removed from the original version  $T_{i,j}^{(\pm)}$ . Note that this removal is ensured via the relations<sup>6</sup> (3.17), (3.18) and (3.19). Then, the solutions to  $D_{i,j}^{\text{med}} = 0$  contain no direct information about the resurgence cancellations, and they yield the Borel-summed trans-series for the systems under consideration.

Compared to the analysis in Section 4, considering the median QC provides us a direct route to the *exact* non-perturbative corrections to the spectrum. In this way, we can uncover the physical properties of the ITW system across all parameter regimes, including the fugacities (or actions) of the bounce and bion configurations. This is especially crucial for the PT-symmetric case, as there is an exceptional point. In the following, using the median QC, we will determine the exact transition point and the physical properties at the exceptional point and its immediate proximity in the language of semi-classical building blocks, i.e., a bounce and a (half-)bion. We also provide an equivalent analysis for the resonance and anti-resonance cases.

In addition to that, we will also revisit the resurgence cancellation using the Alien calculus techniques. In this way, we will be able to specify the resurgence cancellation from the first principles and improve the analysis in Section 3.2 and Section 4, where we deduce the cancellations using the numerical analysis and consistency relationships based on it. Finally, since the Alien calculus does not need quantitative output of the perturbative expansions, we will also extend confirmation of the resurgence cancellations beyond the leading order.

---

<sup>6</sup>To be more precise, we should also consider the Stokes automorphism  $\Sigma$  in (3.21). However, since we are mainly interested in the QCs of the form  $T_{i,j}^{(\pm)} = 0$ , the contributions of  $\Sigma$ , which affect only the pre-factors, do not alter the general picture. Therefore, we omit them from our discussion for simplifications.

### 5.1 PT-symmetric case

In the PT-symmetric case, we consider the median QC  $D_{\text{PT}} = D_{1,2}^{\text{med}} = \mathfrak{S}_A^{\pm 1/2} T_{1,2}^{(\pm)}$  and express it as<sup>7</sup>

$$D_{\text{PT}} = \Omega \left\{ \sqrt{1 + \Pi_{B_1}} \sqrt{1 + \Pi_{B_2}} (1 + \Pi_A^2) + \Pi_A (2 + \Pi_{B_1}) \right\} = 0. \quad (5.2)$$

Then, we find the solution of the quadratic equation for  $\Pi_A$  as

$$\Pi_A = -\frac{1 + \frac{1}{2}\Pi_{B_1} + \varepsilon\sqrt{\text{Disc}_{\text{PT}}}}{\sqrt{1 + \Pi_{B_1}}\sqrt{1 + \Pi_{B_2}}}, \quad (5.3)$$

where  $\varepsilon = \pm 1$  indicates the breaking of the degenerate perturbative states as before, and

$$\text{Disc}_{\text{PT}} = \frac{\Pi_{B_1}^2}{4} - \Pi_{B_2} (1 + \Pi_{B_1}),$$

which was originally defined in (4.2).

To relate (5.3), we utilize the Weber-type expressions as before. We first start by identifying the perturbative action as

$$\Pi_A = e^{-iJ_0}, \quad (5.4)$$

where  $J_0$  in the exponent is related to the standard Weber-type perturbative action as

$$J_0 = 2\pi\mathcal{F}_0, \quad (5.5)$$

where  $\mathcal{F}_0 = \mathfrak{S}_{\pm} \left[ \mathfrak{S}_h^{\pm 1/2} \mathcal{F} \right]$  as introduced in Section 2.3. This means that the action  $J_0$  is also a quantity without a Stokes discontinuity. The associated resurgence terms are related by the Alien calculus. Then, separating  $J_0$  into perturbative and non-perturbative parts as  $J_0 = J_{\text{P}} + J_{\text{NP}}$ , we re-write (5.3) as

$$e^{-iJ_{\text{NP}}} = \frac{1 + \frac{1}{2}\Pi_{B_1} + \varepsilon\sqrt{\text{Disc}_{\text{PT}}}}{\sqrt{1 + \Pi_{B_1}}\sqrt{1 + \Pi_{B_2}}}, \quad (5.6)$$

where we use  $J_{\text{P}} = 2\pi \left( N + \frac{1}{2} \right)$  via the perturbative quantization.

A more convenient way to express the solution is

$$J_{\text{NP}} = i \log \mathcal{Y} \left[ \Pi_{B_1}(J), \Pi_{B_2}(J) \right], \quad (5.7)$$

with

$$\mathcal{Y}(\Pi_{B_1}, \Pi_{B_2}) = \frac{1 + \frac{1}{2}\Pi_{B_1} + \varepsilon\sqrt{\text{Disc}_{\text{PT}}}}{\sqrt{1 + \Pi_{B_1}}\sqrt{1 + \Pi_{B_2}}}. \quad (5.8)$$

The compact expression in (5.7) involves the *entire* information about the non-perturbative spectrum after the Borel summations throughout the trans-series and associated resurgence

<sup>7</sup>Throughout this Section, the actions  $\Pi_{A,B}$  are in fact different from their original definitions in (2.18) and (2.19) by a half-Stokes automorphism, and they should be written as  $\mathfrak{S}_{\pm} \left[ \mathfrak{S}_A^{\pm 1/2} \Pi_A \right]$  and  $\mathfrak{S} \left[ \Pi_{B_{1,2}} \right]$ . However, to simplify the expressions, we continue to use the notation introduced in Section 2.1.

cancellations. This is a very strong statement that demonstrates the capacity of the current approach with respect to the asymptotic version in Section 4. If one wants to obtain the semi-classical structure<sup>8</sup> in the asymptotic limits, it is possible to tackle (5.7) in the same way we explain in Section 4. Then, the result would correspond to the Borel-summed spectrum of the PT-symmetric system, and we would recover the expressions (4.21) and (4.31).

Later in this subsection, we will revisit the asymptotic limits of the median summed spectrum and the corresponding resurgence structure. Before that, we will unlock the full capability of the solution (5.7) by analyzing the PT-symmetry breaking without any approximation and proving the exact conditions for the broken and unbroken phases. Then, having the exact conditions will allow us to probe the spectrum at the exceptional points, again without any approximation.

### 5.1.1 Exact conditions for broken and unbroken phases

To investigate the transition point, we first recall that the median-summed trans-series of the spectrum (2.55) at  $\nu = 0$ . Then, after setting  $2\pi\mathcal{F}_0 = J_0 = J_P + J_{NP}$ , we can introduce a Taylor expansion to  $E^{(0)}(J_0)$  as

$$E^{(0)}(J_0) = E^{(0)}(J_P) + \sum_{k=1}^{\infty} \frac{J_{NP}^k}{k!} \left( \frac{d^k E^{(0)}}{dJ^k} \right)_{J=J_P}, \quad (5.9)$$

where the first term corresponds to  $\mathcal{S}_0[E_P]$ . In some sense, this is a remainder of the Borel-summation process after the resurgence cancellations. This is a manifestly real quantity, as the original asymptotic series is real. The same also holds for the derivative terms when they are evaluated at  $J = J_P$ . Then, the exact spectrum  $E^{(0)}(J_0)$  can only acquire imaginary contributions from the  $J_{NP}$  term.

Recall that our analysis in Section 4 showed that the breaking of the PT-symmetry is controlled by the fugacity of bounce and bion configurations, which we defined in (4.10). Comparing them with the discriminant (4.2) at the leading order, we observe that

$$\text{Disc}_{\text{PT}} < 0, \quad \text{if } \mathcal{K}_1 < \mathcal{K}_2, \quad (5.10)$$

$$\text{Disc}_{\text{PT}} > 0, \quad \text{if } \mathcal{K}_2 > \mathcal{K}_1, \quad (5.11)$$

where we used  $\frac{\Pi_{B_1}^2}{4} \sim \mathcal{K}_1^2$  and  $\Pi_{B_2} \sim \mathcal{K}_2^2$ . Although the analysis in Section 4.1 is valid only when  $\mathcal{K}_1 \ll \mathcal{K}_2$  or  $\mathcal{K}_2 \ll \mathcal{K}_1$ , we observe that the same conditions control the imaginary part of the right-hand side of the solution in (5.6), which is valid for all parameter regions including  $\mathcal{K}_1 \sim \mathcal{K}_2$  and even  $\mathcal{K}_1 = \mathcal{K}_2$ .

In the following, to uncover the necessary conditions for the reality of the spectrum, we analyze (5.6) for three cases:  $\text{Disc}_{\text{PT}} < 0$ ,  $\text{Disc}_{\text{PT}} > 0$ , and  $\text{Disc}_{\text{PT}} = 0$ . We prove that

---

<sup>8</sup>We note that the connection to the semi-classical structure in the language of bounce and bion events is more apparent in Section 4 as the ambiguities arise in the same manner as a corresponding path integral analysis. This explicit link becomes obscure in the median QC and its Alien derivatives. However, the semi-classical information is traded with the manifestation of median summed spectrum and the resurgence structure.



the sign of  $\text{Disc}_{\text{PT}}$  indeed determines if the PT-symmetry is broken and that its zero gives the condition for the exceptional point.

•  $\text{Disc}_{\text{PT}} < 0$  (*Unbroken phase*): In this case, since the square-root in (5.6) produces an imaginary term. Then, assuming  $J_{\text{NP}}$  is real, we split the real and imaginary parts of the equation as

$$\cos(J_{\text{NP}}) = \frac{1 + \frac{\Pi_{B_1}}{2}}{\sqrt{1 + \Pi_{B_1}}\sqrt{1 + \Pi_{B_2}}}, \quad (5.12)$$

$$\sin(J_{\text{NP}}) = \varepsilon \frac{\sqrt{\Pi_{B_2}(1 + \Pi_{B_1}) - \frac{\Pi_{B_1}^2}{4}}}{\sqrt{1 + \Pi_{B_1}}\sqrt{1 + \Pi_{B_2}}}. \quad (5.13)$$

The first equation simply implies

$$J_{\text{NP}} = \arccos \left[ \frac{1 + \frac{\Pi_{B_1}}{2}}{\sqrt{1 + \Pi_{B_1}}\sqrt{1 + \Pi_{B_2}}} \right]. \quad (5.14)$$

In return, using this solution in (5.13), we obtain

$$\sin[\arccos(\mathcal{X})] = \sqrt{1 - \mathcal{X}^2} = \varepsilon \frac{\sqrt{\Pi_{B_2}(1 + \Pi_{B_1}) - \frac{\Pi_{B_1}^2}{4}}}{\sqrt{1 + \Pi_{B_1}}\sqrt{1 + \Pi_{B_2}}}, \quad (5.15)$$

where we set

$$\mathcal{X} = \frac{1 + \frac{\Pi_{B_1}}{2}}{\sqrt{1 + \Pi_{B_1}}\sqrt{1 + \Pi_{B_2}}}.$$

This shows (5.12) and (5.13) are consistent with each other. Note that even if we allow  $J_{\text{NP}}$  to be complex such that  $e^{-iJ_{\text{NP}}} = e^{-i\text{Re}(J_{\text{NP}})}e^{\text{Im}(J_{\text{NP}})}$ , the same procedure yields

$$\sin \left[ \arccos \left( e^{\text{Im}(J_{\text{NP}})} \mathcal{X} \right) \right] = \sqrt{1 - e^{2\text{Im}(J_{\text{NP}})} \mathcal{X}^2} = \varepsilon e^{2\text{Im}(J_{\text{NP}})} \frac{\sqrt{\Pi_{B_2}(1 + \Pi_{B_1}) - \frac{\Pi_{B_1}^2}{4}}}{\sqrt{1 + \Pi_{B_1}}\sqrt{1 + \Pi_{B_2}}}, \quad (5.16)$$

which forces us to set  $\text{Im}(J_{\text{NP}}) = 0$  for consistency. As a result, we conclude that when  $\text{Disc}_{\text{PT}} < 0$ , the *exact* spectrum is real and the quantum system still has *unbroken* PT-symmetry.

•  $\text{Disc}_{\text{PT}} > 0$  (*Broken phase*): Let us follow the same procedure when the square-root term in (5.6) is real. Then, for  $J_{\text{NP}} \in \mathbb{R}$ , the real and imaginary parts become

$$\cos(J_{\text{NP}}) = \mathcal{Y}(\Pi_{B_1}, \Pi_{B_2}), \quad (5.17)$$

$$\sin(J_{\text{NP}}) = 0. \quad (5.18)$$

The first equation gives

$$J_{\text{NP}} = \arccos \left[ \mathcal{Y}(\Pi_{B_1}, \Pi_{B_2}) \right], \quad (5.19)$$

and inserting it into the second one leads to

$$\sin [\arccos (\mathcal{Y})] = \sqrt{1 - \mathcal{Y}^2} = \sqrt{2} \sqrt{\frac{\sqrt{\text{Disc}_{\text{PT}}}}{\varepsilon \left(1 + \frac{\Pi_{B_1}}{2}\right) + \sqrt{\text{Disc}_{\text{PT}}}}}. \quad (5.20)$$

This is manifestly a non-zero quantity except when  $\text{Disc}_{\text{PT}} = 0$ . Therefore, we conclude that  $\text{Disc}_{\text{PT}} > 0$  corresponds to a *broken* PT-symmetric phase of the quantum theory and  $\text{Disc}_{\text{PT}} = 0$  gives the *exact* condition for the exceptional point of the PT-symmetric system, which we analyze now.

• Disc<sub>PT</sub> = 0 (Exceptional point): In order to uncover the reality of the spectrum for  $\text{Disc}_{\text{PT}} = 0$ , we follow the same prescription. In this case, the real and imaginary parts of (5.6) are written as

$$\cos (J_{\text{NP}}) = \frac{1 + \frac{\Pi_{B_1}}{2}}{\sqrt{1 + \Pi_{B_1}} \sqrt{1 + \Pi_{B_2}}} =: \mathcal{Z}, \quad (5.21)$$

$$\sin (J_{\text{NP}}) = 0. \quad (5.22)$$

Then, the same procedure yields

$$\sin [\arccos (\mathcal{Z})] = \sqrt{1 - \mathcal{Z}^2} = \frac{\sqrt{-\text{Disc}_{\text{PT}}}}{\sqrt{1 + \Pi_{B_1}} \sqrt{1 + \Pi_{B_2}}} = 0. \quad (5.23)$$

As a result, we observe that at the transition point, the spectrum is still real.

• Exceptional point condition: Note that  $\text{Disc}_{\text{PT}} = 0$  yields a simple relation between the actions of the  $B_1$ - and  $B_2$ -cycles:

$$\Pi_{B_2} = \frac{\Pi_{B_1}^2}{4(1 + \Pi_{B_1})}. \quad (5.24)$$

This is the exact condition for the *exceptional point*. Then, the exact conditions for unbroken and broken phases are written as

$$\underline{\text{Unbroken phase}} : \quad \Pi_{B_2} (1 + \Pi_{B_1}) > \Pi_{B_1}^2, \quad (5.25)$$

$$\underline{\text{Broken phase}} : \quad \Pi_{B_1}^2 > \Pi_{B_2} (1 + \Pi_{B_1}), \quad (5.26)$$

which are perfectly aligned with our numerical and approximate analytic analysis in Section 4.

### 5.1.2 Borel-summed spectrum

As we discussed above, the exact solution in (5.7) is for any  $x_0$ . In the following, we first analyze the spectrum around the exceptional point and examine the transition. Then, we revisit the asymptotic limits and verify our analysis in Section 4.

- Around exceptional point: Using the condition (5.24), we simplify (5.8) at the exceptional point as

$$\mathcal{Y}(\Pi_{B_1}, \Pi_{B_2}) = 1. \quad (5.27)$$

This points out that the exact median-summed non-perturbative correction to the spectrum, i.e.,  $E^{(0)}$  in (5.9) vanishes exactly as

$$J_{\text{NP}}^{\text{EP}} = 0. \quad (5.28)$$

We emphasize that (5.28) should not be interpreted as the disappearance of resurgence itself. What vanishes at the exceptional point is the exact median-summed non-perturbative correction to the spectrum, not the non-perturbative sectors or the resurgent structure encoded in the exact WKB data. Indeed, (5.28) does not exclude the presence of bounce and bion configurations, as well as their combinations, which exist for any  $x_0$ . As we show shortly, the resurgence cancellations occur at all orders in the trans-series in the unbroken and broken phases, as well as at the exceptional point. As we discussed in Section 3.2, this is necessary since, for any  $x_0$ , the perturbative expansions around both wells are divergent and non-Borel summable, and therefore ambiguous unless their ambiguities are canceled by the non-perturbative sectors.

The vanishing  $J_{\text{NP}}^{\text{EP}}$  in (5.28), on the other hand, shows a remarkable fact: The entire non-perturbative part is organized in such a way that at the exceptional point, the parts that do not participate in the resurgence cancellations cancel each other exactly. We also emphasize that this result needs an exact treatment of the spectrum, and, to our knowledge, the current EWKB approach that utilizes the Alien calculus is the only way to access this information with absolute precision.

Let us also analyze the vicinity of the exceptional point, where we can re-write (5.24) as

$$\Pi_{B_2} = \frac{\Pi_{B_1}^2}{4(1 + \Pi_{B_1})} + \delta_{B_2}. \quad (5.29)$$

Then, expanding for small  $\delta_{B_2}$ , we get

$$J_{\text{NP}} \sim \pm \frac{2i\sqrt{1 + \Pi_{B_1}}}{2 + \Pi_{B_1}} \sqrt{\delta_{B_2}} + O\left(\delta_{B_2}^{3/2}\right). \quad (5.30)$$

This shows that the PT-symmetry is broken for  $\delta_{B_2} \gtrsim 0$ , while it is unbroken for  $\delta_{B_2} \lesssim 0$ . This is in line with our exact analysis using Disc<sub>PT</sub> above. Finally, note that (5.30) is analytical and hence the unbroken and broken phases can transit to each other smoothly.

Let us now focus on the below-barrier-top sector, and estimate the exceptional points when the PT-symmetric phase transition for an individual state occurs in this sector. Recall that in the below-barrier-top sector, the  $B_1$ - and  $B_2$ -cycles are represented by (2.19). Then, we rewrite (5.24) as

$$\frac{e^{-\frac{s_1}{\hbar}}}{4} = e^{-\frac{s_2}{\hbar}} \left[ 1 + \frac{\sqrt{2\pi}e^{-\frac{s_1}{\hbar}}}{\Gamma(1+N)} \left(\frac{C}{\hbar}\right)^{\frac{1}{2}+N} \right], \quad (5.31)$$

where  $S_{1,2}$  and  $\mathcal{C}$  are controlled by the parameter  $x_0$  and are given in (3.4), (3.6), and (3.5), respectively.

The first two numerical solutions of (5.31) are

$$x_0^{\text{cr}} = \{1.08213, 1.17943\} . \quad (5.32)$$

These are the exceptional points for the pairs which correspond to the perturbative ground states and perturbative first excited states around the two wells of the ITW potential (3.1). As we discussed in Section 4, the non-perturbative effects break this degeneracy in the unbroken phase. Then, these states coalesce at their respective critical points in (5.32) and the real parts of their eigenvalues become degenerate for  $x_0 > x_0^{\text{cr}}$  in the broken phase. This picture and the solutions in (5.32) perfectly match the numerical analysis depicted in Fig. 8.

For the remaining excited states for  $N \geq 2$ , their PT-symmetries are broken when they lie above the barrier top. Let us finally verify this is indeed the case by investigating the transition of each state through the barrier top region individually:

Since we are still at the exceptional point, (5.3) still simplifies to  $\Pi_A = -1$  via (5.24). However, around the barrier top, i.e.,  $u \simeq u^{\text{BT}}$ , both  $A$ - and  $B$ -cycles have perturbative characters, meaning that  $\Pi_A \sim \Pi_B \sim O(1)$ . At the leading order, the action of the  $A$ -cycle reads

$$a(u \sim u^{\text{BT}}) \simeq \frac{S_3}{\hbar} , \quad (5.33)$$

where

$$S_3(x_0) = \frac{(2 + x_0^2) \sqrt{(8 + x_0^2)(4 - x_0^2)}}{2\sqrt{3}} + 4(x_0^2 - 1) \log \left[ \frac{\sqrt{8 + x_0^2} - \sqrt{3}\sqrt{4 - x_0^2}}{2\sqrt{x_0^2 - 1}} \right] \quad (5.34)$$

is the bounce action<sup>9</sup> at the barrier top. As a result, the leading-order solution to (5.3) at  $u = u_{\text{BT}}$  becomes

$$S_3(x_0^*) \simeq N + \frac{1}{2} . \quad (5.35)$$

This is the approximate condition for the quantized states  $N = 0, 1, \dots$  to lie around the barrier top region.

Since at the exceptional point,  $\Pi_A = -1$  is the exact QC,  $a = N + \frac{1}{2}$  becomes an exact relation at  $x_0 = x_0^{\text{cr}}$ . Then, comparing  $x_0^{\text{cr}}$  satisfying (5.31) and  $x_0^*$  satisfying (5.35), we can determine which PT-symmetry-breaking transition takes place while the states lie below the barrier-top sector. More specifically, we compare the solutions to (5.31) with the curve of  $S_3(x_0)$  for various values of  $N$ . If a point  $(x_0^{\text{cr}}, N)$  lies below the curve, it means the transition occurs in the below barrier top sector. Otherwise, those solutions for (5.31) become invalid.

---

<sup>9</sup>Note that we still use the name bounce since the  $A$ -cycle at  $u = u_{\text{BT}}$  is intimately related to the bounce configuration for the tilted-double well potential, which is obtained via  $V_{\text{TTW}} = u_{\text{BT}} - V_{\text{ITW}}$ . This correspondence is simply due to the duality between two potentials and their WKB-cycles. We refer [80, 81] for detailed discussion and several other examples.

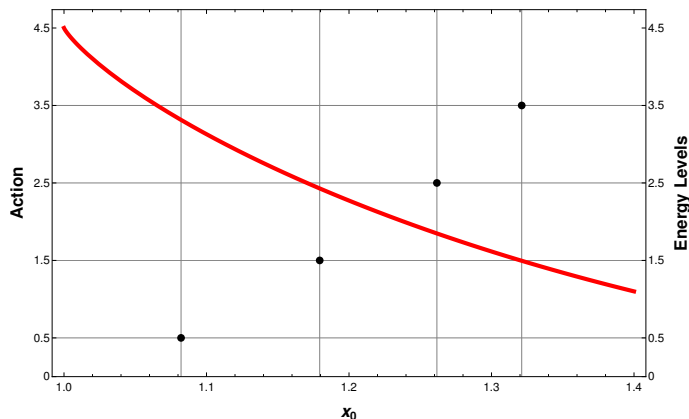


**Figure 12:** Comparison between the barrier-top condition  $S_3(x_0) = N + \frac{1}{2}$  and the exceptional-point condition obtained from (5.31). The red curve shows  $S_3(x_0)$ , the horizontal lines denote  $N + \frac{1}{2}$  for energy levels  $N = 0, 1, 2, 3$ , and the black dots mark the corresponding critical values  $x_0^{\text{cr}}$ . Only the first two intersections lie in the below-barrier regime where (5.31) can be applied.

In Fig. 12, we compare (5.34) with the critical points in (5.32) and next two solutions to (5.31), i.e.,  $\{1.26167, 1.32118\}$ . It shows only the first two PT-symmetry breakings occur below the barrier top, where (5.31) is applicable. Despite this limitation, (5.31) stands as a remarkably simple condition for the exceptional point in terms of the bion and bounce actions only.

**Remark 1:** Note that although the specific quantitative forms for  $\Pi_A$  and  $\Pi_{B_{1,2}}$  in  $\text{Disc}_{\text{PT}}$  changes around the barrier top region and above it, the conditions (5.25) and (5.26) are in fact valid for any parameter region and any classical energy values. This is because of the fact that the transition across a barrier top is a continuous one and that the median QC in both below and above barrier-top sectors is identical (see [81] for a similar discussion for triple-well potential). Therefore, the proof we provide in 5.1.1 valid for any  $x_0 \in (-2, 2)$  and  $E$  values.

**Remark 2:** Our analysis in this subsection and Section 5.1.1 provides an excellent display of the power of the EWKB analysis, particularly with the proper utilization of the median QC via Stokes automorphisms. On the other hand, it can also be interpreted as a possibly unreasonable power of the semi-classical analysis. After all, we showed that the exact exceptional point is simply given by the fugacities of the semi-classical bounce and bion configurations. Moreover, in both exact and semi-classical analysis, we presented that the imaginary contributions arising from the same square-root factor, i.e.  $\sqrt{\text{Disc}_{\text{PT}}}$ , which indicates that the PT-symmetry breaking for the ITW potential is due to the competition between the classical actions of bounce and half-bion configurations. This means that the higher-order corrections to the trans-series do not alter this picture at all.

A possible general reason behind this is the cluster expansion in the semi-classical picture, which was analyzed thoroughly in various setups [47, 59, 60] and briefly discussed

in the EWKB framework recently [81]. In a non-Hermitian setup, such as that we discuss in this paper, such a cluster expansion has never been investigated. It would be interesting to uncover if it exists or not and pursue its implications for the PT-symmetry breaking.

• *Asymptotic limits:* Let us now revisit the limiting cases of  $\Pi_{B_2} \ll \Pi_{B_1}^2$  and  $\Pi_{B_1}^2 \ll \Pi_{B_2}$  in comparison with the analysis in Section 4. Note that since we work on the Stokes rays, we can directly uncover the spectrum that survived after the Borel summation.

As in Section 4, we expanded around the perturbative states. Similarly, here we set  $J = J_P + J_{NP}$  and assume  $J_{NP} \ll 1$  due to the exponential suppressions. Since  $J_{NP}$  is the actual small parameter, we need to expand (5.7) in  $J_{NP}$  rather than  $\Pi_{B_{1,2}}$ , which depend on the parameter  $J$  themselves, as in Section 4. The Alien derivatives to the median-summed contributions (5.7) will involve the derivatives of  $\Pi_{B_{1,2}}$ . Therefore, foreseeing such contributions, which we will discuss in Section 5.1.3, we define the following expansions:

– For bounce configurations:

$$\frac{1}{2} \frac{d^m \Pi_{B_1}}{dJ^m} = 2\pi \mathcal{K}_1 \sum_{k=0}^{\infty} Q_{k,m}^{(1)}(J_P) J_{NP}^k. \quad (5.36)$$

– For half-bion configurations:

$$\frac{d^m (\Pi_{B_2})^{1/2}}{dJ^m} = 2\pi \mathcal{K}_2 \sum_{k=0}^{\infty} Q_{k,m}^{(2)}(J_P) J_{NP}^k. \quad (5.37)$$

where  $\mathcal{K}_1$  and  $\mathcal{K}_2$  are the fugacity terms defined in (4.10). Note that expansion terms  $Q_{k,m}^{(1,2)}$  are simply related to  $P_k^{(1,2)}$  by

$$Q_{k,m}^{1,2} = \frac{\Gamma(k+m+1)}{\Gamma(k+1)} Q_{k+m,0}^{(1,2)} = \frac{\Gamma(k+m+1)}{\Gamma(k+1)} P_{k+m}^{(1,2)}. \quad (5.38)$$

With these relations, it is manifest that  $Q_{k,m}^{(1,2)}$ , so that the series expansions (5.36) and (5.37) are related to unambiguous parts of the bounce and bion configurations in (4.7) and (4.8), as expected by construction.

Now, inserting the expansions (5.36) and (5.37) in (5.7) via (5.8), we can expand (5.7) for first  $J_{NP} \ll 1$  and then, for  $\mathcal{K}_1 \ll \mathcal{K}_2$  or  $\mathcal{K}_2 \ll \mathcal{K}_1$ , depending on the choice. Then, we can solve the resulting expansions order by order for  $J_{NP}$ . We point out that this procedure is similar to the solution scheme in Section 4. In the current version, however, the left-hand side involves only one term, i.e.  $J_{NP}$ , which simplifies the procedure significantly.

Following this procedure for  $\mathcal{K}_1 \ll \mathcal{K}_2$  and we obtain the solution up to  $O(\mathcal{K}_1^2)$  and  $O(\mathcal{K}_2^2)$  order as

$$\begin{aligned} \frac{1}{2\pi} J_{PT}^{\text{UBr}} &\simeq -\varepsilon \mathcal{K}_2 \mathcal{S}_0 [Q_{0,0}^{(2)}] + \varepsilon \frac{\mathcal{K}_1^2}{\mathcal{K}_2} \mathcal{S}_0 [\mathcal{Q}_{\mathcal{B}^2 \mathcal{I}^{-1}}] + \mathcal{K}_2^2 \mathcal{S}_0 [Q_{0,0}^{(2)} Q_{1,0}^{(2)}] - 2\mathcal{K}_1^2 \mathcal{S}_0 [Q_{0,0}^{(1)} Q_{1,0}^{(1)}] \\ &= -\varepsilon \mathcal{K}_2 \mathcal{S}_0 [P_0^{(2)}] + \varepsilon \frac{\mathcal{K}_1^2}{\mathcal{K}_2} \mathcal{S}_0 [\mathcal{P}_{\mathcal{B}^2 \mathcal{I}^{-1}}] + \mathcal{K}_2^2 \mathcal{S}_0 [P_0^{(2)} P_1^{(2)}] - 2\mathcal{K}_1^2 \mathcal{S}_0 [P_0^{(1)} P_1^{(1)}] \end{aligned} \quad (5.39)$$

for the unbroken phase. Similarly, same procedure for  $\mathcal{K}_2 \ll \mathcal{K}_1$  case, we obtain

$$\begin{aligned}
\frac{1}{2\pi} J_{\text{PT}}^{\text{Br}} &\simeq -i\varepsilon \mathcal{K}_1 \mathcal{S}_0 \left[ Q_{0,0}^{(1)} \right] + \frac{i\varepsilon \mathcal{K}_2^2}{2 \mathcal{K}_1} \mathcal{S}_0 \left[ \mathcal{Q}_{\mathcal{I}\bar{\mathcal{I}}B^{-1}} \right] - 2\mathcal{K}_1^2 \mathcal{S}_0 \left[ Q_{0,0}^{(1)} Q_{1,0}^{(1)} + i\pi\varepsilon \left( Q_{0,0}^{(1)} \right)^2 \right] \\
&\quad + \mathcal{K}_2^2 \mathcal{S}_0 \left[ Q_{0,0}^{(2)} Q_{1,0}^{(2)} - i\pi\varepsilon \left( Q_{0,0}^{(2)} \right)^2 \right] \\
&= i\varepsilon \mathcal{K}_1 \mathcal{S}_0 \left[ P_0^{(1)} \right] - \frac{i\varepsilon \mathcal{K}_2^2}{2\mathcal{K}_1} \mathcal{S}_0 \left[ \mathcal{P}_{\mathcal{I}\bar{\mathcal{I}}B^{-1}} \right] - 2\mathcal{K}_1^2 \mathcal{S}_0 \left[ P_0^{(1)} P_1^{(1)} + i\pi\varepsilon \left( P_0^{(1)} \right)^2 \right] \\
&\quad + \mathcal{K}_2^2 \mathcal{S}_0 \left[ P_0^{(2)} P_1^{(2)} - i\pi\varepsilon \left( P_0^{(2)} \right)^2 \right] \tag{5.40}
\end{aligned}$$

for the broken phase. Note that we defined  $\mathcal{Q}_{\mathcal{B}^2\mathcal{I}} = \frac{(Q_{0,0}^{(1)})^2}{Q_{0,0}^{(2)}}$  and  $\mathcal{Q}_{\mathcal{I}\bar{\mathcal{I}}B^{-1}} = \frac{(Q_{0,0}^{(2)})^2}{Q_{0,0}^{(1)}}$ . We also introduced  $\frac{1}{2\pi}$  factors as they appear in the final contribution to the spectrum via (5.9) and to make the comparison with the results in Section 4 directly. In this sense, the results in (5.39) and (5.40) recover the same Borel summed contributions in (4.21) and (4.31), and verify our semi-classical analysis in relation to the bion and bounce configurations.

### 5.1.3 Resurgence structure (revisited)

We now turn our focus to the resurgence structure of the spectrum. As discussed in Section 2, the Alien calculus encodes the ambiguous non-perturbative corrections, which are canceled against the Borel-summed series (both the perturbative sector and instanton fluctuations). For the median QC (5.2), using (2.46), we find the action of the Alien derivative,

$$D_{\text{PT}}^{(k \geq 1)}(J) = \tilde{\Omega}(J) \left( \Pi_A(J) + (-1)^k \Pi_A^{(-1)}(J) \right) L^k(J), \tag{5.41}$$

where

$$\tilde{\Omega}(J) = \frac{\sqrt{1 + \Pi_{B_1}(J)} \sqrt{1 + \Pi_{B_2}(J)}}{\sqrt{\Pi_{B_1}(J) \Pi_{B_2}(J)}}, \tag{5.42}$$

and

$$L(J) = \log \left[ (1 + \Pi_{B_1}(J)) (1 + \Pi_{B_2}(J)) \right]. \tag{5.43}$$

Let us also express the median QC (5.2) in this new notation as

$$D_{\text{PT}}^{(0)}(J) = \tilde{\Omega}(J) (2 \cos J + \Phi(J)), \tag{5.44}$$

where

$$\Phi(J) = \frac{2 + \Pi_{B_2}(J)}{\sqrt{1 + \Pi_{B_1}(J)} \sqrt{1 + \Pi_{B_2}(J)}}. \tag{5.45}$$

In the following, we will only compute the first correction, i.e.,  $J_1(J_0)$ , to the median-summed solution  $J_{\text{NP}}$ . Using (2.54) and the fact that  $D_{\text{PT}}^{(0)}(J_0) = 0$ , the one Alien derivative term is expressed as

$$J_1(J_0) \left[ -2 \sin(J_0) + \Phi'(J_0) \right] + 2i \sin(J_0) L(J_0) = 0, \tag{5.46}$$

where  $\overline{\Phi'(J_0)} = \left. \frac{d\Phi}{dJ} \right|_{J=J_0}$ . Then, the formal solution to  $J_1(J_0)$  becomes

$$J_1(J_0) = -i \frac{2 \sin(J_0) L(J_0)}{2 \sin(J_0) - \frac{d\Phi(J_0)}{dJ}}, \quad (5.47)$$

provided  $2 \sin(J_0) \neq \Phi'(J_0)$ .

To relate (5.46) to the semi-classical analysis, we expand (5.47) in  $J_{\text{NP}}$  and insert the median-summed non-perturbative corrections (5.39) or (5.40). Note that, since the right-hand side of (5.47) is independent of  $J_1$ , there is no need for an iterative solution procedure. Instead, we directly expand the entire expression for  $J = J_{\text{P}} + J_{\text{NP}}$  by using the solutions for  $J_{\text{NP}}^{\text{UBr}}$  and  $J_{\text{NP}}^{\text{Br}}$  at the respective limits.

Up to orders  $O(\mathcal{K}_1^2)$  and  $O(\mathcal{K}_2^2)$ , we obtained

$$\begin{aligned} \frac{1}{2 \cdot 2\pi} J_1^{\text{UBr}} &\simeq -i\mathcal{K}_1 Q_{0,0}^{(1)} - i\pi\mathcal{K}_2^2 \left(Q_{0,0}^{(2)}\right)^2 + 2\pi i\mathcal{K}_1^2 \left(Q_{0,0}^{(1)}\right)^2 - i\mathcal{K}_1\mathcal{K}_2 \left(Q_{1,0}^{(1)}Q_{0,0}^{(2)} + 2\pi Q_{0,0}^{(1)}Q_{0,1}^{(2)}\right) \\ &= -i\mathcal{K}_1 P_0^{(1)} - i\pi\mathcal{K}_2^2 \left(P_0^{(2)}\right)^2 + 2\pi i\mathcal{K}_1^2 \left(P_0^{(1)}\right)^2 - i\mathcal{K}_1\mathcal{K}_2 \left(P_1^{(1)}P_0^{(2)} + P_0^{(1)}P_1^{(2)}\right) \end{aligned} \quad (5.48)$$

for the unbroken phase and

$$\begin{aligned} \frac{1}{2 \cdot 2\pi} J_1^{\text{Br}} &\simeq 2\pi\mathcal{K}_1^2 \left(\varepsilon Q_{0,0}^{(1)}Q_{0,1}^{(1)} - i \left(Q_{0,0}^{(1)}\right)^2\right) - i\mathcal{K}_1 Q_{0,0}^{(1)} + \mathcal{K}_2^2 \left(2\pi\varepsilon Q_{0,1}^{(2)}Q_{0,0}^{(2)} + 3i\pi \left(Q_{0,0}^{(2)}\right)^2\right) \\ &\simeq 2\mathcal{K}_1^2 \left(\varepsilon P_0^{(1)}P_1^{(1)} - \pi i \left(P_0^{(1)}\right)^2\right) - i\mathcal{K}_1 P_0^{(1)} + \mathcal{K}_2^2 \left(\varepsilon P_1^{(2)}P_0^{(2)} + 3i\pi \left(P_0^{(2)}\right)^2\right) \end{aligned} \quad (5.49)$$

for the broken phase. Both expressions recover the parts that appear in the resurgence cancellation in the semi-classical analysis in Section 4.

Note that, as we mentioned before, although the general structures of  $J_1^{\text{UBr}}$  and  $J_1^{\text{Br}}$  are quite different, some of their subparts coincide. We have already uncovered this subpart in  $\mathcal{K}_1 \ll \mathcal{K}_2$  and  $\mathcal{K}_2 \ll \mathcal{K}_1$  limits and called it the minimal trans-series [see (4.22)]. Now, let us show its direct link to the perturbative sector.

In the language of Alien calculus, finding the minimal trans-series that emanates from the perturbative sector is quite straightforward. In general, we can turn off the non-perturbative corrections and take the perturbative QC, which is

$$D_{\text{Pert}}^{(0)}(J) = 1 + \Pi_A(J) = 0 \quad (5.50)$$

for both wells. Then, the  $k$ -th Alien derivative becomes

$$D_{\text{Pert}}^{(k \geq 1)}(J) = i\Pi_A L^k(J), \quad (5.51)$$

and setting  $J_0 = J_{\text{P}}$ , we obtained

$$J_1^{\text{minimal}}(J_{\text{P}}) = -iL(J_{\text{P}}) = -i \log \left[ (1 + \Pi_{B_1}(J_{\text{P}}))(1 + \Pi_{B_2}(J_{\text{P}})) \right]. \quad (5.52)$$



Note that the actions  $\Pi_{B_{1,2}}(J_P)$  still have non-perturbative characters, but since  $J_{\text{NP}} = 0$ , they are simply given by the respective fugacity terms,

$$\Pi_{B_i}(J_P) = \mathcal{K}_i. \quad (5.53)$$

Finally, expanding (5.52) for  $\mathcal{K}_1 \ll 1$  and  $\mathcal{K}_2 \ll 1$ , we obtained the corresponding minimal trans-series as

$$\frac{1}{2 \cdot 2\pi} J_1^{\text{minimal}} = -i \left( \mathcal{K}_1 P_0^{(1)} + \pi \mathcal{K}_2^2 \left( P_0^{(2)} \right)^2 - 2\pi \mathcal{K}_1^2 \left( P_0^{(1)} \right)^2 \right), \quad (5.54)$$

which recovers the expansion in (4.22). Note that the order of expansion in (5.52) is commutable, indicating that the resulting series (5.54) is independent of the quantitative dominance of  $\mathcal{K}_1$  or  $\mathcal{K}_2$  and that it is valid for all parameter regions.

Finally, we focus on the resurgence structure at the exceptional point. Since all the non-perturbative corrections vanish in the median-summed trans-series, it is straightforward to deduce that its resurgence structure only consists of the series in (5.54). For completeness, let us compute it as a limit of the general expression of  $J_1(J_0)$  for the ITW potential in (5.47):

At the exceptional point, the condition (5.24) leads to  $\Phi = 1$ . Note that this is independent of the quantization process, regardless of the fact that  $J_{\text{NP}}^{\text{EP}} = 0$ . Then, the derivative term in (5.47) vanishes at the exceptional point. Then, using the fact  $J_{\text{NP}}^{\text{EP}} = 0$ , (5.47) simplifies to

$$J_1^{\text{EP}}(J_0) = -iL(J_0), \quad (5.55)$$

which induces the minimal series after expanding for  $\mathcal{K}_1 \ll 1$  and  $\mathcal{K}_2 \ll 1$ .

## 5.2 Resonance and anti-resonance cases

Finally, considering the resonance and anti-resonance cases, we will solve them with the median QC exactly to obtain the median-summed spectrum. Then, we also revisit the semi-classical structure of the spectrum and the associated structure. Our discussion follows the same route as the previous analysis of the PT-symmetric system in Section 5.1. Therefore, in the following, we do not elaborate on the details, unless it is different from Section 5.1.

**Exact solutions:** As we discussed at the level of QCs in Section 3.3 and the trans-series solutions in Section 4.2, the resonance and anti-resonance systems are time-reversed partners of each other, which reveals itself via complex conjugation. The complex conjugation also appears for their median QCs, which are defined as

$$D_{\text{med}}^{(\text{R})} = \mathfrak{S}_A^{\pm 1/2} T_{2,2}^{(\pm)}, \quad D_{\text{med}}^{(\text{AR})} = \mathfrak{S}_A^{\pm 1/2} T_{1,1}^{(\text{R})}. \quad (5.56)$$

Using the expressions in Table 1, we obtain the median QCs as

$$D_{\text{med}}^{(\text{R})} = \Omega \left\{ (1 + \Pi_{B_1}) \sqrt{1 + \Pi_{B_2}} + \Pi_A^2 \sqrt{1 + \Pi_{B_2}} + 2\Pi_A \sqrt{1 + \Pi_{B_1}} \right\} = 0, \quad (5.57)$$

and

$$D_{\text{med}}^{(\text{AR})} = \Omega \left\{ \sqrt{1 + \Pi_{B_2}} + 2\Pi_A \sqrt{1 + \Pi_{B_1}} + \Pi_A^2 \sqrt{1 + \Pi_{B_2}} (1 + \Pi_{B_1}) \right\} = 0. \quad (5.58)$$

Then, it is manifest that  $D_{\text{med}}^{(\text{AR})} = \mathbf{C}D_{\text{med}}^{(\text{R})}$ .

To see how this relation is carried to the entire spectrum, let us rewrite (5.57) as

$$D_{\text{med}}^{(\text{R})} = \Omega \Pi_A^2 \sqrt{1 + \Pi_{B_2}} \left( 1 + \Pi_{B_1} + 2\Pi_A^{-1} \sqrt{1 + \Pi_{B_1}} + \left( \Pi_A^{-2} \sqrt{1 + \Pi_{B_2}} \right) \right). \quad (5.59)$$

Then, defining  $D_{\text{med}}^{(+)} = D_{\text{med}}^{(\text{R})}$  and  $D_{\text{med}}^{(-)} = D_{\text{med}}^{(\text{AR})}$ , we express both the median QCs in a compact form as

$$D_{\text{med}}^{(\pm)} = \Pi_A^{\mp 2} (1 + \Pi_{B_1}) \sqrt{1 + \Pi_{B_2}} + 2\Pi_A^{\mp 1} \sqrt{1 + \Pi_{B_1}} + \sqrt{1 + \Pi_{B_2}} = 0. \quad (5.60)$$

As in Section 5.1, these quadratic equations can be solved exactly, and we get

$$\Pi_A^{\mp 1} = \frac{-1 + i\varepsilon \sqrt{\Pi_{B_2}}}{\sqrt{1 + \Pi_{B_1}} \sqrt{1 + \Pi_{B_2}}}, \quad (5.61)$$

where the power  $\mp 1$  on the left-hand side refers to the solutions for  $D_{\text{med}}^{(\pm)} = 0$ , respectively. Finally, recalling the definition  $\Pi_A = e^{-iJ_0}$ , where  $J_0 = 2\pi\mathcal{F}_0 = 2\pi\mathbf{S}_{\pm} \left[ \mathfrak{G}_h^{\pm 1/2} \mathcal{F} \right]$ , we found

$$J_0^{(\pm)} = \mp i \log \left[ \frac{-1 + i\varepsilon \sqrt{\Pi_{B_2}}}{\sqrt{1 + \Pi_{B_1}} \sqrt{1 + \Pi_{B_2}}} \right], \quad (5.62)$$

which can be used to compute the exact trans-series via (2.55). Now, from (5.62), it is manifest that the entire median-summed spectra of the resonance and anti-resonance systems are complex conjugate to each other. We note that  $\varepsilon = \pm 1$  in (5.62) does not affect this property, as it leads to complex conjugate contributions to  $J_0^{(\pm)}$  in both cases.

Since the perturbative spectrum for any boundary condition for the ITW potential (3.1) is the same, the real difference takes place at the non-perturbative level. Therefore, it is also appropriate to uncover the exact non-perturbative solution by separating  $J_0 = J_{\text{P}} + J_{\text{NP}}$ . Then, using the perturbative QC, i.e.,  $e^{\pm iJ_{\text{P}}} = -1$ , we find the exact non-perturbative part as

$$J_{\text{NP}}^{(\pm)} = \pm i \log \left[ \frac{1 - i\varepsilon \sqrt{\Pi_{B_2}}}{\sqrt{1 + \Pi_{B_1}} \sqrt{1 + \Pi_{B_2}}} \right], \quad (5.63)$$

which, of course, preserves the complex conjugacy relationship.

As in the PT-symmetric case, we can use the exact solutions to check the reality of the spectrum. Again, let us assume  $J_{\text{NP}}^{(\pm)} \in \mathbb{R}$ . Then, (5.63) can be re-written into two parts as

$$\cos \left( J_{\text{NP}}^{(\pm)} \right) = \frac{1}{\sqrt{1 + \Pi_{B_1}} \sqrt{1 + \Pi_{B_2}}}, \quad (5.64)$$

$$\sin \left( J_{\text{NP}}^{(\pm)} \right) = \frac{\mp \varepsilon \sqrt{\Pi_{B_2}}}{\sqrt{1 + \Pi_{B_1}} \sqrt{1 + \Pi_{B_2}}}, \quad (5.65)$$

and setting  $\mathcal{X} = [(1 + \Pi_{B_1})(1 + \Pi_{B_2})]^{-\frac{1}{2}}$ , (5.64) becomes

$$J_{\text{NP}}^{(\pm)} = \arccos [\mathcal{X}]. \quad (5.66)$$

In turn, using this solution in (5.65), we obtain

$$\sin[\arccos(\mathcal{X})] = \sqrt{1 - \mathcal{X}^2} = \left(1 - \frac{1}{\sqrt{1 + \Pi_{B_1}}\sqrt{1 + \Pi_{B_2}}}\right), \quad (5.67)$$

which is not equal to (5.65). This concludes  $J_{\text{NP}}^{(\pm)} \notin \mathbb{R}$ . Therefore, the spectrum of both resonance and anti-resonance cases cannot be real.

We note that the above discussion is valid for all parameter regions and that there is no exceptional point for the (anti-)resonance sector for the ITW potential. This is actually manifest already in (5.61) as there is no competition between  $\Pi_{B_1}$  and  $\Pi_{B_2}$  actions, which would lead to different behavior of a square-root term as in the PT-symmetric case; see Section 5.1.

**Semi-classical expansion (revisited)** Finally, we conclude our discussion by revisiting the semi-classical resurgence structure that we analyzed in Section 4.2. Thanks to the elegance of the median QC approach and the exact non-perturbative solution in (5.63), obtaining the median summed trans-series is very straightforward:

Recalling the series definitions in (5.36) and (5.37), and expanding for  $J_{\text{NP}}$  for each case in (5.63), we obtained the median summed trans-series for both resonance and anti-resonance cases as

$$\begin{aligned} \frac{1}{2\pi} J_{\text{NP}}^{(\pm)} &\simeq \varepsilon \mathcal{K}_2 P_0^{(2)} + \mathcal{K}_2^2 P_0^{(2)} P_1^{(2)} - 2\mathcal{K}_1^2 P_0^{(1)} P_1^{(1)} \\ &\mp i \left( \mathcal{K}_1 P_0^{(1)} - 2\pi \mathcal{K}_1^2 \left(P_0^{(1)}\right)^2 + \varepsilon \mathcal{K}_1 \mathcal{K}_2 \left(P_1^{(1)} P_0^{(2)} + P_0^{(1)} P_1^{(2)}\right) \right), \end{aligned} \quad (5.68)$$

where we also used (5.38) in the last step. This recovers the median summed trans-series in (4.46) and (4.53). We also note that two solutions in (5.68) are complex conjugate to each other, i.e.,  $J_{\text{NP}}^{(+)} = \mathbb{C} J_{\text{NP}}^{(-)}$ . This is another manifestation of the time-reversal relationship between the resonance and anti-resonance systems.

Similarly, for the parts involving the resurgence cancellations, we utilize the Alien derivative construction in Section 2.3. For this reason, we first re-organize the median QC (5.60) as

$$D_{\text{med}}^{(\pm)} = \left(\Pi_A + \Pi_A^{(-1)}\right) + \Pi_A^{(\pm 1)} \frac{\Pi_{B_1}}{\sqrt{1 + \Pi_{B_2}}} + 2 \frac{\sqrt{1 + \Pi_{B_1}}}{\sqrt{1 + \Pi_{B_2}}}. \quad (5.69)$$

Then, recalling the notation that we introduced in the Alien-calculus discussion, we express the median QC as

$$D_{\pm}^{(0)} = 2 \cos(J) + e^{\pm iJ} \Phi_1(J) + \Phi_2(J), \quad (5.70)$$

where we put  $\pm$  in the subscript to refer to resonance and anti-resonance cases and also defined

$$\Phi_1(J) = \frac{\Pi_{B_1}(J)}{\sqrt{1 + \Pi_{B_2}(J)}}, \quad \Phi_2(J) = 2 \frac{\sqrt{1 + \Pi_{B_1}(J)}}{\sqrt{1 + \Pi_{B_2}(J)}}. \quad (5.71)$$

The first Alien derivative of the median QC in (5.70) can be computed via (2.46) as

$$D_{\pm}^{(1)} = (2i \sin J \pm e^{\pm iJ} \Phi_1(J)) J(J), \quad (5.72)$$

where  $L(J)$  is first defined in (5.43). Then, recalling (2.53), we obtain

$$J_1^{(\pm)}(J_0) = \frac{(2i \sin(J_0) \pm e^{\pm iJ_0} \Phi_1(J_0)) L(J_0)}{2 \sin(J_0) - e^{\pm iJ_0} (\pm i \Phi_1(J_0) + \Phi_1'(J_0)) - \Phi_2'(J_0)}. \quad (5.73)$$

In order to relate  $J_1^{(\pm)}$  to the semi-classical resurgence structure, we set  $J_0^{\pm} = J_P^{(\pm)} + J_{\text{NP}}^{(\pm)}$  and expanded (5.73) for  $\mathcal{K}_1 \ll 1$  and  $\mathcal{K}_2 \ll 1$  after inserting (5.68) in (5.73). As a result, we obtain

$$\begin{aligned} \frac{1}{2 \cdot 2\pi} J_1^{(\pm)} &\simeq \mp i \mathcal{K}_1 P_0^{(1)} - 2\mathcal{K}_1^2 \left( P_0^{(1)} P_1^{(1)} \mp \pi i (P_0^{(1)})^2 \right) - i\pi \mathcal{K}_2^2 \left( P_0^{(2)} \right)^2 \\ &\mp i\varepsilon \mathcal{K}_1 \mathcal{K}_2 \left( P_1^{(1)} P_0^{(2)} + P_0^{(1)} P_1^{(2)} \right), \end{aligned} \quad (5.74)$$

which enters the resurgence cancellations discussed in Section 4.2. We note that  $J_1^{(\pm)}$  are not complex conjugate of each other, as the  $O(\mathcal{K}_2^2)$  term has the same sign in both cases. This is because it emanates from the one-bion event  $[\mathcal{I}\bar{\mathcal{I}}]_{\pm}$  and is responsible for canceling the imaginary ambiguity arising from the perturbative sector, which is the same for both the resonance and anti-resonance systems.

Finally, combining the series in (5.68) and (5.74), we recover the semi-classical trans-series:

$$J^{(\pm)}(\nu) \simeq J_0^{(\pm)} + \nu \frac{1}{2\pi} J_1^{(\pm)}. \quad (5.75)$$

To prevent confusion, we emphasize that  $(\pm)$  in (5.74) and (5.75) does not refer to the non-perturbative ambiguities. More precisely,  $J^{(+)}$  in (5.75) is linked to the resonance-system trans-series (4.38) and (4.39), i.e.,  $\delta_{\text{R}}^{(+)} = J_{\text{med}}^{(+)}$ , and  $J^{(-)}$  is linked to the anti-resonance system, i.e.,  $\mathcal{S}_{\pm} \left[ \delta_{\text{AR}}^{(\pm)} \right] = J_{\text{med}}^{(-)}$  in (4.46). The non-perturbative ambiguities, on the other hand, are represented by  $\nu = \pm \frac{1}{2}$  in (5.75) as first introduced in Section 2.3.

## 6 Discussion and outlook

Despite its relatively simple definition, because of its rich structure, the inverted triple-well (ITW) potential provides a concrete example of the semi-classical and exact quantization of non-Hermitian quantum mechanics. Our analysis particularly highlights the effectiveness of resurgence methods in this setting and shows that the exact-WKB (EWKB) framework yields physically consistent and quantitatively precise results. Although it is primarily based on the technical capabilities of the EWKB framework, by a rigorous analysis of the resurgent structure of PT-symmetric and (anti-)resonance systems, this paper also presents possible exploitations for the resurgence theory of general non-Hermitian systems.

Our analysis shows that the semi-classical analysis of the PT-symmetric and (anti-)resonance systems based on the same building blocks, namely bion  $[\mathcal{I}\bar{\mathcal{I}}]$  and bounce  $[\mathcal{B}]$  configurations, simply stems from the underlying classical potential. At the quantum level,

however, these building blocks enter in different combinations depending on the systems (boundary conditions), and their physical roles change accordingly. For example, we have discovered novel fractional configurations such as  $[\mathcal{B}^2\mathcal{I}^{-1}]$  and  $[\mathcal{I}\bar{\mathcal{I}}\mathcal{B}^{-1}]$  in unbroken and broken PT-symmetric phases, respectively. These configurations have no direct analog in conventional Hermitian systems and do not appear in the resonance or anti-resonance ITW problem.

More interestingly, we have shown that a one-bounce configuration  $[\mathcal{B}]$  appears in qualitatively different ways in the unbroken and broken PT-symmetric phases, as well as in resonance and anti-resonance systems. In the unbroken PT-symmetric phase,  $[\mathcal{B}]$  participates in the resurgence cancellations and disappears from the exact spectrum. In the broken phase, in contrast, it appears with an extra factor of  $(1 + \varepsilon)[\mathcal{B}]$  and contributes to the imaginary splitting of the eigenvalues. In the resonance system, on the other hand,  $[\mathcal{B}]$  governs the leading instability but does not induce any splitting. This demonstrates that the role played by a given semi-classical configuration is determined primarily by the boundary conditions and the exact quantization procedure, rather than solely by the shape of the classical potential or by the existence of the bounce and bion saddles.

One of the highlights of our results is the exact characterization of the PT-symmetry breaking. We have proven that the unbroken and broken phases of the PT-symmetric system are determined directly by the signs of  $\text{Disc}_{\text{PT}}$ , i.e.,  $\text{Disc}_{\text{PT}} < 0$  and  $> 0$  indicate the unbroken and broken phases, respectively. The transition takes place at  $\text{Disc}_{\text{PT}} = 0$ , which yields the exact exceptional-point condition as a strikingly simple algebraic relation:  $\Pi_{B_2} = \Pi_{B_1}^2/4(1 + \Pi_{B_1})$ . Very interestingly, the Weber-type expression (2.19) reduces this equation to a simple relationship between the classical actions of the bion  $[\mathcal{I}\bar{\mathcal{I}}]$  and bounce ( $[\mathcal{B}]$ ) configurations, along with the one-loop-determinant prefactor of the latter [see (5.31)]. This implies that the non-Hermitian phase-transition can be probed exactly by semi-classical action data only.

Another particularly interesting characteristic of the exceptional point is the vanishing of the non-perturbative corrections. At the level of the exact median quantization condition (QC), we showed that this follows from the exact cancellations of the median-summed non-perturbative contributions. We also showed that, despite the vanishing of the net non-perturbative correction to the exact spectrum, the resurgent structure originating from the perturbative sector does not disappear. This strikingly beautiful resurgent structure at the exceptional point resembles the Cheshire cat resurgence observed in supersymmetric (SUSY) systems [40, 41, 43]. In the Cheshire cat resurgence, the perturbative contribution vanishes together with its associated resurgent structure, while the exact answer is maintained by non-perturbative contributions in a manner consistent with supersymmetry (see also [38, 39]). In the present ITW problem at the exceptional point, the situation is reversed: the perturbative series remains divergent and non-Borel summable, and the minimal resurgent structure survives, whereas the remaining non-perturbative spectral corrections cancel in the exact median-summed spectrum. We note that this structure also provides consistency with the coalescence of the real eigenvalues as in Fig. 8a. In the ITW system, such a coalescence of real eigenvalues is possible only if the real non-perturbative corrections vanish, since otherwise they would induce a level splitting, as in the unbroken

PT-symmetric phase.

Our analysis also highlights a distinctive feature of the non-perturbative structure of the symmetric inverted double-well (IDW) case. In the PT-symmetric boundary condition, the non-perturbative contribution drops out of the median-summed QC for IDW [16], whereas in the ITW case it still survives and leads to a much richer non-perturbative sector including the PT-symmetry breaking. This difference also precludes a direct ITW analog of the ABS conjecture, i.e., a relation between the PT-symmetric and (anti-)resonance QCs originally proposed for IDW in [122]. Unlike in the IDW case [16], PT-symmetric and (anti-)resonance systems are not connected by an analytic continuation. Accordingly, the PT-symmetric and (anti-)resonance QCs cannot be connected by a Stokes automorphism, which is mainly due to the presence of the inner-bion cycle in the ITW system.

There are several natural directions for future work. One immediate extension is to analyze systematically the barrier-top and above-barrier regions, where the hierarchy among non-perturbative contributions changes and the semi-classical structure becomes richer. It would also be interesting to clarify the relation between the present EWKB description and a complexified path-integral formulation in which bounce and bion sectors arise directly from complex saddles. A further question is how broadly the structures found here persist in more general non-Hermitian polynomial potentials, especially in systems with richer Stokes geometry or multiple exceptional points. In general, the present results suggest that EWKB and resurgence provide a powerful and flexible framework for the non-perturbative analysis of open quantum systems and non-Hermitian spectral problems beyond the specific ITW example studied here.

## Acknowledgments

This work is supported by the Japan Society for the Promotion of Science Grant-in-Aid for Scientific Research (JSPS KAKENHI) Grant Nos. 22H05118 and 25K07298 (S. K.), Grant Nos. 23K03425 and 22H05118 (T. M.), No. 24K17058 and the RIKEN TRIP initiative (RIKEN Quantum) (H. T.). C.P. thanks Keio University and the University of Tokyo for the hospitality, where the initial steps of the project took place.

## References

- [1] Y. Ashida, Z. Gong and M. Ueda, *Non-Hermitian physics*, *Adv. Phys.* **69** (2021) 249–435, [[2006.01837](#)].
- [2] N. Hatano and G. Ordonez, *Non-Hermitian Quantum Mechanics of Open Quantum Systems: Revisiting The One-Body Problem*, [2602.14105](#).
- [3] A. Bohm, M. Gadella and G. B. Mainland, *Gamow vectors and decaying states*, *American Journal of Physics* **57** (12, 1989) 1103–1108.
- [4] R. de la Madrid, *The rigged Hilbert space approach to the Gamow states*, *J. Math. Phys.* **53** (2012) 102113, [[1210.3570](#)].
- [5] Y. B. Zel’dovich, *On the theory of unstable states*, *Sov. Phys. JETP* **12** (1961) 542–548.
- [6] G. Gamow, *Zur Quantentheorie des Atomkernes*, *Z. Phys.* **51** (1928) 204–212.

- [7] A. Mostafazadeh, *PseudoHermiticity versus PT symmetry. The necessary condition for the reality of the spectrum*, *J. Math. Phys.* **43** (2002) 205–214, [[math-ph/0107001](#)].
- [8] A. Mostafazadeh, *Pseudo-Hermitian Representation of Quantum Mechanics*, *Int. J. Geom. Meth. Mod. Phys.* **7** (2010) 1191–1306, [[0810.5643](#)].
- [9] C. M. Bender, S. Boettcher and P. Meisinger, *PT symmetric quantum mechanics*, *J. Math. Phys.* **40** (1999) 2201–2229, [[quant-ph/9809072](#)].
- [10] C. M. Bender, D. C. Brody and H. F. Jones, *Complex extension of quantum mechanics*, *Phys. Rev. Lett.* **89** (2002) 270401, [[quant-ph/0208076](#)].
- [11] C. M. Bender, P. E. Dorey, C. Dunning, A. Fring, D. W. Hook, H. F. Jones et al., *PT Symmetry*. WSP, 2019, [10.1142/q0178](#).
- [12] C. M. Bender and D. W. Hook, *PT-symmetric quantum mechanics*, [2312.17386](#).
- [13] A. J. F. Siegert, *On the Derivation of the Dispersion Formula for Nuclear Reactions*, *Phys. Rev.* **56** (1939) 750–752.
- [14] C. M. Bender, *Making sense of non-Hermitian Hamiltonians*, *Rept. Prog. Phys.* **70** (2007) 947, [[hep-th/0703096](#)].
- [15] W.-Y. Ai, B. Garbrecht and C. Tamarit, *Functional methods for false vacuum decay in real time*, *JHEP* **12** (2019) 095, [[1905.04236](#)].
- [16] S. Kamata, *Exact WKB analysis for PT-symmetric quantum mechanics: Study of the Ai-Bender-Sarkar conjecture*, *Phys. Rev. D* **109** (2024) 085023, [[2401.00574](#)].
- [17] S. Kamata, *Exact Sum Rules and Zeta Generating Formulas from the ODE/IM correspondence*, [2508.06366](#).
- [18] B. Garbrecht and N. Wagner, *Path integral analysis of Schrödinger-type eigenvalue problems in the complex plane: Establishing the relation between instantons and resonant states*, [2507.23125](#).
- [19] J. Zinn-Justin, *Multi - Instanton Contributions in Quantum Mechanics*, *Nucl. Phys. B* **192** (1981) 125–140.
- [20] J. Zinn-Justin, *Instantons in Quantum Mechanics: Numerical Evidence for a Conjecture*, *J. Math. Phys.* **25** (1984) 549.
- [21] J. Zinn-Justin and U. D. Jentschura, *Multi-instantons and exact results I: Conjectures, WKB expansions, and instanton interactions*, *Annals Phys.* **313** (2004) 197–267, [[quant-ph/0501136](#)].
- [22] J. Zinn-Justin and U. D. Jentschura, *Multi-instantons and exact results II: Specific cases, higher-order effects, and numerical calculations*, *Annals Phys.* **313** (2004) 269–325, [[quant-ph/0501137](#)].
- [23] U. D. Jentschura and J. Zinn-Justin, *Instantons in quantum mechanics and resurgent expansions*, *Phys. Lett. B* **596** (2004) 138–144, [[hep-ph/0405279](#)].
- [24] U. D. Jentschura, A. Surzhykov and J. Zinn-Justin, *Multi-instantons and exact results. III: Unification of even and odd anharmonic oscillators*, *Annals Phys.* **325** (2010) 1135–1172, [[1001.3910](#)].
- [25] U. D. Jentschura and J. Zinn-Justin, *Multi-instantons and exact results. IV: Path integral formalism*, *Annals Phys.* **326** (2011) 2186–2242.

- [26] G. Basar, G. V. Dunne and M. Ünsal, *Resurgence theory, ghost-instantons, and analytic continuation of path integrals*, *JHEP* **10** (2013) 041, [[1308.1108](#)].
- [27] G. V. Dunne and M. Ünsal, *Generating nonperturbative physics from perturbation theory*, *Phys. Rev. D* **89** (2014) 041701, [[1306.4405](#)].
- [28] G. V. Dunne and M. Ünsal, *Uniform WKB, Multi-instantons, and Resurgent Trans-Series*, *Phys. Rev. D* **89** (2014) 105009, [[1401.5202](#)].
- [29] T. Misumi and T. Kanazawa, *Adjoint QCD on  $\mathbb{R}^3 \times S^1$  with twisted fermionic boundary conditions*, *JHEP* **06** (2014) 181, [[1405.3113](#)].
- [30] T. Misumi, M. Nitta and N. Sakai, *Neutral bions in the  $\mathbb{C}P^{N-1}$  model*, *JHEP* **06** (2014) 164, [[1404.7225](#)].
- [31] T. Misumi, M. Nitta and N. Sakai, *Neutral bions in the  $\mathbb{C}P^{N-1}$  model for resurgence*, *J. Phys. Conf. Ser.* **597** (2015) 012060, [[1412.0861](#)].
- [32] T. Misumi, M. Nitta and N. Sakai, *Classifying bions in Grassmann sigma models and non-Abelian gauge theories by D-branes*, *PTEP* **2015** (2015) 033B02, [[1409.3444](#)].
- [33] T. Misumi, M. Nitta and N. Sakai, *Non-BPS exact solutions and their relation to bions in  $\mathbb{C}P^{N-1}$  models*, *JHEP* **05** (2016) 057, [[1604.00839](#)].
- [34] T. Fujimori, S. Kamata, T. Misumi, M. Nitta and N. Sakai, *Bion non-perturbative contributions versus infrared renormalons in two-dimensional  $\mathbb{C}P^{N-1}$  models*, *JHEP* **02** (2019) 190, [[1810.03768](#)].
- [35] G. Başar and G. V. Dunne, *Resurgence and the Nekrasov-Shatashvili limit: connecting weak and strong coupling in the Mathieu and Lamé systems*, *JHEP* **02** (2015) 160, [[1501.05671](#)].
- [36] T. Misumi, M. Nitta and N. Sakai, *Resurgence in sine-Gordon quantum mechanics: Exact agreement between multi-instantons and uniform WKB*, *JHEP* **09** (2015) 157, [[1507.00408](#)].
- [37] G. V. Dunne and M. Ünsal, *WKB and Resurgence in the Mathieu Equation*, [[1603.04924](#)].
- [38] A. Behtash, G. V. Dunne, T. Schäfer, T. Sulejmanpasic and M. Ünsal, *Toward Picard–Lefschetz theory of path integrals, complex saddles and resurgence*, *Ann. Math. Sci. Appl.* **02** (2017) 95–212, [[1510.03435](#)].
- [39] A. Behtash, G. V. Dunne, T. Schäfer, T. Sulejmanpasic and M. Ünsal, *Complexified path integrals, exact saddles and supersymmetry*, *Phys. Rev. Lett.* **116** (2016) 011601, [[1510.00978](#)].
- [40] C. Kozçaz, T. Sulejmanpasic, Y. Tanizaki and M. Ünsal, *Cheshire Cat resurgence, Self-resurgence and Quasi-Exact Solvable Systems*, *Commun. Math. Phys.* **364** (2018) 835–878, [[1609.06198](#)].
- [41] G. V. Dunne and M. Ünsal, *Deconstructing zero: resurgence, supersymmetry and complex saddles*, *JHEP* **12** (2016) 002, [[1609.05770](#)].
- [42] T. Fujimori, S. Kamata, T. Misumi, M. Nitta and N. Sakai, *Nonperturbative contributions from complexified solutions in  $\mathbb{C}P^{N-1}$  models*, *Phys. Rev. D* **94** (2016) 105002, [[1607.04205](#)].
- [43] D. Dorigoni and P. Glass, *The grin of Cheshire cat resurgence from supersymmetric localization*, *SciPost Phys.* **4** (2018) 012, [[1711.04802](#)].



- [44] G. Basar, G. V. Dunne and M. Ünsal, *Quantum Geometry of Resurgent Perturbative/Nonperturbative Relations*, *JHEP* **05** (2017) 087, [[1701.06572](#)].
- [45] T. Fujimori, S. Kamata, T. Misumi, M. Nitta and N. Sakai, *Exact resurgent trans-series and multibion contributions to all orders*, *Phys. Rev. D* **95** (2017) 105001, [[1702.00589](#)].
- [46] T. Fujimori, S. Kamata, T. Misumi, M. Nitta and N. Sakai, *Resurgence Structure to All Orders of Multi-bions in Deformed SUSY Quantum Mechanics*, *PTEP* **2017** (2017) 083B02, [[1705.10483](#)].
- [47] A. Behtash, G. V. Dunne, T. Schaefer, T. Sulejmanpasic and M. Ünsal, *Critical Points at Infinity, Non-Gaussian Saddles, and Bions*, *JHEP* **06** (2018) 068, [[1803.11533](#)].
- [48] N. Sueishi, *1/ε problem in resurgence*, *PTEP* **2021** (2021) 013B01, [[1912.03518](#)].
- [49] G. V. Dunne, T. Sulejmanpasic and M. Ünsal, *Bions and Instantons in Triple-well and Multi-well Potentials*, [2001.10128](#).
- [50] T. Fujimori, S. Kamata, T. Misumi, M. Nitta and N. Sakai, *All-order resurgence from complexified path integral in a quantum mechanical system with integrability*, *Phys. Rev. D* **107** (2023) 105011, [[2205.07436](#)].
- [51] M. Hongo, T. Misumi and Y. Tanizaki, *Phase structure of the twisted SU(3)/U(1)<sup>2</sup> flag sigma model on  $\mathbb{R} \times S^1$* , *JHEP* **02** (2019) 070, [[1812.02259](#)].
- [52] T. Fujimori, M. Honda, S. Kamata, T. Misumi and N. Sakai, *Resurgence and Lefschetz thimble in three-dimensional  $\mathcal{N} = 2$  supersymmetric Chern–Simons matter theories*, *PTEP* **2018** (2018) 123B03, [[1805.12137](#)].
- [53] T. Fujimori, E. Itou, T. Misumi, M. Nitta and N. Sakai, *Confinement-deconfinement crossover in the lattice  $CP^{N-1}$  model*, *Phys. Rev. D* **100** (2019) 094506, [[1907.06925](#)].
- [54] T. Misumi, T. Fujimori, E. Itou, M. Nitta and N. Sakai, *Lattice study on the twisted  $CP^{N-1}$  models on  $\mathbb{R} \times S^1$* , *PoS LATTICE2019* (2019) 015, [[1911.07398](#)].
- [55] T. Fujimori, E. Itou, T. Misumi, M. Nitta and N. Sakai, *Lattice  $CP^{N-1}$  model with  $\mathbb{Z}_N$  twisted boundary condition: bions, adiabatic continuity and pseudo-entropy*, *JHEP* **08** (2020) 011, [[2006.05106](#)].
- [56] T. Fujimori, M. Honda, S. Kamata, T. Misumi, N. Sakai and T. Yoda, *Quantum phase transition and resurgence: Lessons from three-dimensional  $\mathcal{N} = 4$  supersymmetric quantum electrodynamics*, *PTEP* **2021** (2021) 103B04, [[2103.13654](#)].
- [57] M. Ünsal, *Strongly coupled QFT dynamics via TQFT coupling*, *JHEP* **11** (2021) 134, [[2007.03880](#)].
- [58] H. Nishimura, T. Fujimori, T. Misumi, M. Nitta and N. Sakai, *Resurgence and semiclassical expansion in two-dimensional large- $N$  sigma models*, *JHEP* **06** (2022) 151, [[2112.13999](#)].
- [59] C. Pazarbaşı and M. Ünsal, *Cluster Expansion and Resurgence in the Polyakov Model*, *Phys. Rev. Lett.* **128** (2022) 151601, [[2110.05612](#)].
- [60] C. Pazarbaşı and M. Ünsal, *Polyakov model in 't Hooft flux background: a quantum mechanical reduction with memory*, *JHEP* **08** (2022) 116, [[2112.02483](#)].
- [61] A. Çavuşoğlu, C. Kozçaz and K. Tezgin, *Unified genus-1 potential and a parametric perturbative/nonperturbative relation*, *Phys. Rev. D* **110** (2024) 125001, [[2311.17850](#)].
- [62] R. Balian, G. Parisi and A. Voros, *Discrepancies from asymptotic series and their relation to complex classical trajectories*, *Phys. Rev. Lett.* **41** (Oct, 1978) 1141–1144.

- [63] A. Voros, *The return of the quartic oscillator. the complex wkb method*, *Annales de l'I.H.P. Physique theorique* **39** (1983) 211–338.
- [64] H. J. Silverstone, *Jwkb connection-formula problem revisited via borel summation*, *Phys. Rev. Lett.* **55** (Dec, 1985) 2523–2526.
- [65] T. Aoki, T. Kawai and Y. Takei, *The bender-wu analysis and the voros theory*, in *ICM-90 Satellite Conference Proceedings* (M. Kashiwara and T. Miwa, eds.), (Tokyo), pp. 1–29, Springer Japan, 1991.
- [66] T. Aoki, T. Kawai and Y. Takei, *New turning points in the exact WKB analysis for higher-order ordinary differential equations*, *Analyse algebrique des perturbations singulieres. I*, *Hermann, Paris* (1994) 69–84.
- [67] Y. Takei, *On the connection formula for the first Painleve equation : from the viewpoint of the exact WKB analysis(Painleve Transcendents and Asymptotic Analysis)*, *Kyoto University Research Information Repository* **931** (1995) 70–99.
- [68] E. Delabaere, H. Dillinger and F. Pham, *Exact semiclassical expansions for one-dimensional quantum oscillators*, *J. Math. Phys.* **38** (1997) 6126–6184.
- [69] E. Delabaere and F. Pham, *Resurgent methods in semiclassical asymptotics*, *Ann. Inst. H. Poincare* **71** (1999) 1–94.
- [70] Y. Takei, *An explicit description of the connection formula for the first Painleve equation, Toward the Exact WKB Analysis of Differential Equations, Linear or Non-Linear*, *Kyoto Univ. Press* (2000) 271–296.
- [71] T. Kawai and Y. Takei, *Algebraic Analysis of Singular Perturbation Theory*. American Mathematical Society, 2005.
- [72] Y. Takei, *Sato's conjecture for the Weber equation and transformation theory for Schrödinger equations with a merging pair of turning points*, *RIMS Kokyuroku Bessatsu* **B10** (2008) 205–224.
- [73] T. Aoki, T. Kawai and Y. Takei, *Microlocal Analysis and Complex Fourier Analysis*, *World Scientific, Singapore, New Jersey, London, 2002*, pp. 1-22. 2002.
- [74] T. Aoki, T. Kawai and Y. Takei, *The Bender-Wu analysis and the Voros theory. II*, *Adv. Stud. Pure Math. (Math. Soc. Japan)* **54** (2009) 19–94.
- [75] A. Fruchard and R. Schäfke, *On the parametric resurgence for a certain singularly perturbed linear differential equation of second order*, in *Asymptotics in Dynamics, Geometry and PDEs; Generalized Borel Summation vol. II* (O. Costin, F. Fauvet, F. Menous and D. Sauzin, eds.), (Pisa), pp. 213–243, Edizioni della Normale, 2011.
- [76] K. Iwaki and T. Nakanishi, *Exact WKB analysis and cluster algebras*, *J. Phys. A: Math. Theor.* **47** (2014) 474009, [[1401.709](#)].
- [77] N. Sueishi, S. Kamata, T. Misumi and M. Ünsal, *On exact-WKB analysis, resurgent structure, and quantization conditions*, *JHEP* **12** (2020) 114, [[2008.00379](#)].
- [78] N. Sueishi, S. Kamata, T. Misumi and M. Ünsal, *Exact-WKB, complete resurgent structure, and mixed anomaly in quantum mechanics on  $S^1$* , *JHEP* **07** (2021) 096, [[2103.06586](#)].
- [79] S. Kamata, T. Misumi, N. Sueishi and M. Ünsal, *Exact WKB analysis for SUSY and quantum deformed potentials: Quantum mechanics with Grassmann fields and Wess-Zumino terms*, *Phys. Rev. D* **107** (2023) 045019, [[2111.05922](#)].

- [80] T. Misumi and C. Pazarbaşı, *Exact WKB in all sectors. Part I. Potentials with degenerate saddles*, *JHEP* **04** (2025) 100, [[2410.09511](#)].
- [81] T. Misumi and C. Pazarbaşı, *Exact WKB in all sectors II: Potentials with non-degenerate saddles*, [2511.20778](#).
- [82] N. A. Nekrasov and S. L. Shatashvili, *Quantization of Integrable Systems and Four Dimensional Gauge Theories*, in *16th International Congress on Mathematical Physics*, pp. 265–289, 8, 2009, [0908.4052](#), DOI.
- [83] A. Mironov and A. Morozov, *Nekrasov Functions and Exact Bohr-Zommerfeld Integrals*, *JHEP* **04** (2010) 040, [[0910.5670](#)].
- [84] A.-K. Kashani-Poor and J. Troost, *Pure  $\mathcal{N} = 2$  super Yang-Mills and exact WKB*, *JHEP* **08** (2015) 160, [[1504.08324](#)].
- [85] A.-K. Kashani-Poor, *Quantization condition from exact WKB for difference equations*, *JHEP* **06** (2016) 180, [[1604.01690](#)].
- [86] S. K. Ashok, D. P. Jatkar, R. R. John, M. Raman and J. Troost, *Exact WKB analysis of  $\mathcal{N} = 2$  gauge theories*, *JHEP* **07** (2016) 115, [[1604.05520](#)].
- [87] F. Yan, *Exact WKB and the quantum Seiberg-Witten curve for  $4d$   $N = 2$  pure  $SU(3)$  Yang-Mills. Abelianization*, *JHEP* **03** (2022) 164, [[2012.15658](#)].
- [88] D. Gaiotto, G. W. Moore and A. Neitzke, *Spectral networks*, *Annales Henri Poincaré* **14** (2013) 1643–1731, [[1204.4824](#)].
- [89] D. G. L. Allegretti, *On the Wall-Crossing Formula for Quadratic Differentials*, *Int. Math. Res. Not.* **2023** (2023) 8033–8077, [[2006.08059](#)].
- [90] P. Dorey, C. Dunning and R. Tateo, *Spectral equivalences, Bethe Ansatz equations, and reality properties in  $PT$ -symmetric quantum mechanics*, *J. Phys. A* **34** (2001) 5679–5704, [[hep-th/0103051](#)].
- [91] P. Dorey, C. Dunning and R. Tateo, *The ODE/IM Correspondence*, *J. Phys. A* **40** (2007) R205, [[hep-th/0703066](#)].
- [92] K. Ito, M. Mariño and H. Shu, *TBA equations and resurgent Quantum Mechanics*, *JHEP* **01** (2019) 228, [[1811.04812](#)].
- [93] K. Ito and H. Shu, *TBA equations for the Schrödinger equation with a regular singularity*, *J. Phys. A* **53** (2020) 335201, [[1910.09406](#)].
- [94] K. Imaizumi, *Exact WKB analysis and TBA equations for the Mathieu equation*, *Phys. Lett. B* **806** (2020) 135500, [[2002.06829](#)].
- [95] K. Ito and H. Shu, *ODE/IM Correspondence and Quantum Periods*, vol. 51 of *SpringerBriefs in Mathematical Physics*. Springer, 2025, [10.1007/978-981-96-0499-9](#).
- [96] Y. Emery, *TBA equations and quantization conditions*, *JHEP* **07** (2021) 171, [[2008.13680](#)].
- [97] K. Ito and H. Shu, *TBA equations and exact WKB analysis in deformed supersymmetric quantum mechanics*, *JHEP* **03** (2024) 122, [[2401.03766](#)].
- [98] K. Ito, H. Shu and J. Yang, *TBA and wall-crossing for deformed supersymmetric quantum mechanics*, [2510.06956](#).

- [99] A. Grassi, M. Marino and S. Zakany, *Resumming the string perturbation series*, *JHEP* **05** (2015) 038, [[1405.4214](#)].
- [100] A. Grassi, Y. Hatsuda and M. Marino, *Topological Strings from Quantum Mechanics*, *Annales Henri Poincare* **17** (2016) 3177–3235, [[1410.3382](#)].
- [101] S. Codesido and M. Marino, *Holomorphic Anomaly and Quantum Mechanics*, *J. Phys. A* **51** (2018) 055402, [[1612.07687](#)].
- [102] S. Codesido, M. Marino and R. Schiappa, *Non-Perturbative Quantum Mechanics from Non-Perturbative Strings*, *Annales Henri Poincare* **20** (2019) 543–603, [[1712.02603](#)].
- [103] L. Hollands and A. Neitzke, *Exact WKB and abelianization for the  $T_3$  equation*, *Commun. Math. Phys.* **380** (2020) 131–186, [[1906.04271](#)].
- [104] S. K. Ashok, P. N. Bala Subramanian, A. Bawane, D. Jain, D. P. Jatkar and A. Manna, *Exact WKB Analysis of  $\mathbb{CP}^1$  Holomorphic Blocks*, *JHEP* **10** (2019) 075, [[1907.05031](#)].
- [105] I. Coman, P. Longhi and J. Teschner, *From quantum curves to topological string partition functions II*, [2004.04585](#).
- [106] K. Iwaki and M. Marino, *Resurgent Structure of the Topological String and the First Painlevé Equation*, *SIGMA* **20** (2024) 028, [[2307.02080](#)].
- [107] S. Kamata, *Exact quantization conditions and full transseries structures for PT symmetric anharmonic oscillators*, *Phys. Rev. D* **110** (2024) 045022, [[2406.01230](#)].
- [108] H. Taya, T. Fujimori, T. Misumi, M. Nitta and N. Sakai, *Exact WKB analysis of the vacuum pair production by time-dependent electric fields*, *JHEP* **03** (2021) 082, [[2010.16080](#)].
- [109] S. Enomoto and T. Matsuda, *The exact WKB for cosmological particle production*, *JHEP* **03** (2021) 090, [[2010.14835](#)].
- [110] S. Enomoto and T. Matsuda, *The Exact WKB analysis and the Stokes phenomena of the Unruh effect and Hawking radiation*, *JHEP* **12** (2022) 037, [[2203.04501](#)].
- [111] R. Namba and M. Suzuki, *Exact WKB Formulation of Quantization and Particle Production in Time-Dependent Backgrounds*, [2509.19194](#).
- [112] T. Fujimori, S. Kamata, T. Misumi, N. Sueishi and H. Taya, *Exact-WKB Analysis of Two-level Floquet Systems*, [2504.12838](#).
- [113] T. Miyachi, R. Namba, H. Omiya and N. Oshita, *Path to an exact WKB analysis of black hole quasinormal modes*, *Phys. Rev. D* **111** (2025) 124045, [[2503.17245](#)].
- [114] T. Miyachi, R. Namba, H. Omiya and N. Oshita, *Instability of parametrized black hole quasinormal modes in the high-overtone limit via the exact WKB analysis*, [2512.18631](#).
- [115] K. Ito and J. Yang, *Exact WKB Analysis and TBA Equations for the Stark Effect*, *PTEP* **2024** (2024) 013A02, [[2307.03504](#)].
- [116] O. Morikawa and S. Ogawa, *Unified exact WKB framework for resonance — Zel’dovich/complex-scaling regularization and rigged Hilbert space —*, *JHEP* **10** (2025) 049, [[2505.02301](#)].
- [117] Z. Duan, J. Gu, Y. Hatsuda and T. Sulejmanpasic, *Instantons in the Hofstadter butterfly: difference equation, resurgence and quantum mirror curves*, *JHEP* **01** (2019) 079, [[1806.11092](#)].

- [118] K. Imaizumi, *Exact conditions for quasi-normal modes of extremal M5-branes and exact WKB analysis*, *Nucl. Phys. B* **992** (2023) 116221, [[2212.04738](#)].
- [119] A. van Spaendonck and M. Vonk, *Painlevé I and exact WKB: Stokes phenomenon for two-parameter transseries*, *J. Phys. A* **55** (2022) 454003, [[2204.09062](#)].
- [120] B. Bucciotti, T. Reis and M. Serone, *An anharmonic alliance: exact WKB meets EPT*, *JHEP* **11** (2023) 124, [[2309.02505](#)].
- [121] M. Türe and M. Ünsal, *Quantum Hamilton-Jacobi theory, spectral path integrals, and exact WKB analysis*, *Phys. Rev. D* **111** (2025) 105010, [[2406.07829](#)].
- [122] W.-Y. Ai, C. M. Bender and S. Sarkar, *PT-symmetric  $-g\varphi^4$  theory*, *Phys. Rev. D* **106** (2022) 125016, [[2209.07897](#)].
- [123] G. Alvarez and C. Casares, *Exponentially small corrections in the asymptotic expansion of the eigenvalues of the cubic anharmonic oscillator.*, *Journal of Physics A: Mathematical and General* **33.29** (2000) 5171.
- [124] G. Alvarez, *Langer-Cherry derivation of the multi-instanton expansion for the symmetric double well.*, *Journal of mathematical physics* **45.8** (2004) 3095.
- [125] I. Gahramanov and K. Tezgin, *Remark on the Dunne-Ünsal relation in exact semiclassics*, *Phys. Rev. D* **93** (2016) 065037, [[1512.08466](#)].
- [126] A. Gorsky and A. Milekhin, *RG-Whitham dynamics and complex Hamiltonian systems*, *Nucl. Phys. B* **895** (2015) 33–63, [[1408.0425](#)].
- [127] A. Çavuşoğlu, C. Kozçaz and K. Tezgin, *Resurgence of deformed genus-1 curves: A novel perturbative/nonperturbative relation*, *Phys. Rev. D* **111** (2025) 105007, [[2408.02628](#)].
- [128] E. Bogomolny and V. Fateyev, *Large order calculations in gauge theories*, *Physics Letters B* **71** (1977) 93–96.
- [129] E. Bogomolny, *Calculation of instanton-anti-instanton contributions in quantum mechanics*, *Physics Letters B* **91** (1980) 431–435.
- [130] D. Dorigoni, *An introduction to resurgence, trans-series and alien calculus*, *Annals of Physics* **409** (Oct, 2019) 167914.
- [131] A. van Spaendonck and M. Vonk, *Exact instanton transseries for quantum mechanics*, *SciPost Phys.* **16** (2024) 103, [[2309.05700](#)].
- [132] G. Ordonez and N. Hatano, *The arrow of time in open quantum systems and dynamical breaking of the resonance–anti-resonance symmetry*, *J. Phys. A* **50** (2017) 405304, [[1610.01548](#)].
- [133] C. M. Bender and D. J. Weir, *PT phase transition in multidimensional quantum systems*, *J. Phys. A* **45** (2012) 425303, [[1206.5100](#)].
- [134] S. R. Coleman, *The Fate of the False Vacuum. 1. Semiclassical Theory*, *Phys. Rev. D* **15** (1977) 2929–2936.
- [135] C. G. Callan, Jr. and S. R. Coleman, *The Fate of the False Vacuum. 2. First Quantum Corrections*, *Phys. Rev. D* **16** (1977) 1762–1768.
- [136] C. G. Callan, Jr., R. F. Dashen and D. J. Gross, *Toward a Theory of the Strong Interactions*, *Phys. Rev. D* **17** (1978) 2717.

- [137] A. Behtash, *More on Homological Supersymmetric Quantum Mechanics*, *Phys. Rev. D* **97** (2018) 065002, [[1703.00511](#)].
- [138] C. M. Bender and T. T. Wu, *Anharmonic oscillator. 2: A Study of perturbation theory in large order*, *Phys. Rev. D* **7** (1973) 1620–1636.
- [139] L. N. Lipatov, *Divergence of the Perturbation Theory Series and the Quasiclassical Theory*, *Sov. Phys. JETP [Zh. Eksp. Teor. Fiz.* 72,411(1977)] **45** (1977) 216–223.
- [140] T. Sulejmanpasic and M. Ünsal, *Aspects of perturbation theory in quantum mechanics: The BenderWu Mathematica  $\text{\textcircled{R}}$  package*, *Comput. Phys. Commun.* **228** (2018) 273–289, [[1608.08256](#)].